ANKARA YILDIRIM BEYAZIT UNIVERSITY

GRADUATE SCHOOL OF NATURAL AND APPLIED SCIENCES

DEVELOPMENT OF AN ELECTRODYNAMIC COOLING SYSTEM AND SIMULATOR TO IMPROVE THE PERFORMANCE OF A DOUBLE FACED PHOTOVOLTAIC SYSTEM

M.Sc. Thesis by

Muhammed Selman EREL

Department of Electrical and Electronics Engineering

December, 2021

ANKARA

DEVELOPMENT OF AN ELECTRODYNAMIC COOLING SYSTEM AND SIMULATOR TO IMPROVE THE PERFORMANCE OF A DOUBLE FACED PHOTOVOLTAIC SYSTEM

A Thesis Submitted to

The Graduate School of Natural and Applied Sciences of

Ankara Yıldırım Beyazıt University

In Partial Fulfillment of the Requirements for the Degree of Master of Science in Electrical and Electronics Engineering, Department of Electrical and Electronics Engineering

by

Muhammed Selman EREL

December, 2021

ANKARA

M.Sc. THESIS EXAMINATION RESULT FORM

We have read the thesis entitled **"DEVELOPMENT OF AN ELECTRODYNAMIC COOLING SYSTEM AND SIMULATOR TO IMPROVE THE PERFORMANCE OF A DOUBLE FACED PHOTOVOLTAIC SYSTEM"** completed by **MUHAMMED SELMAN EREL** under the supervision of **PROF. DR. ŞERAFETTİN EREL** and we certify that in our opinion it is fully adequate, in scope and in quality, as a thesis for the degree of Master of Science.

Prof. Dr. Şerafettin EREL

Supervisor

Prof. Dr. Hüseyin CANBOLAT

Jury Member

Doç. Dr. Mustafa Burak TÜRKÖZ

Jury Member

Prof. Dr. Sadettin ORHAN

Director

Graduate School of Natural and Applied Sciences

ETHICAL DECLARATION

I hereby declare that, in this thesis which has been prepared in accordance with the Thesis Writing Manual of Graduate School of Natural and Applied Sciences,

- All data, information and documents are obtained in the framework of academic and ethical rules,
- All information, documents and assessments are presented in accordance with scientific ethics and morals,
- All the materials that have been utilized are fully cited and referenced,
- No change has been made on the utilized materials,
- All the works presented are original,

and in any contrary case of above statements, I accept to renounce all my legal rights.

Date: 28.12.2021 **Signature:** ………………………………

Name & Surname: Muhammed Selman EREL

ACKNOWLEDGEMENTS

Firstly, I would like to express my gratefulness by heart to my supervisor, Prof. Dr. Şerafettin EREL for this support and motivation during my thesis study. He is not only my graduate study advisor but also my engineering advisor throughout my life. He sparked the first fire of electrical and electronics engineering in my life. He and his studies inspired me throughout my life. o His experience, wisdom, foresight and golden touches shaped my thesis study. It was an honor and pleasure to work with him. Also, special thanks for Mustafa Latif ÇOBANKAYA and Mamoun Lyes HENNACHE for their valuable studies. Their studies were rather helpful to improve my thesis study.

Later, I express my sincere love and special thanks to my mother and father, sisters, Meryem Sena and Ahsen, grandmothers and grandfather for their sincere prayers, support, courage and patience for me. Special thanks for my parents to support me economically, morally and motivate me when I was down.

2021, 28 December **Muhammed Selman EREL**

DEVELOPMENT OF AN ELECTRODYNAMIC COOLING SYSTEM AND SIMULATOR TO IMPROVE THE PERFORMANCE OF A DOUBLE FACED PHOTOVOLTAIC SYSTEM

ABSTRACT

Photovoltaic cooling is a way to improve electrical performance of photovoltaics against thermal effects. Based on this purpose, the thesis study is developed with three subsystems: Solar simulator system, dynamic control system and double faced photovoltaic system. Solar simulator system has two identical light sources, two identical photovoltaic panels back to back, cooler and heater. By activating heater, thermal effect on electrical performance of double faced system is observed. By activating cooler, cooling effect on electrical performance of double faced photovoltaic system is observed.

Dynamic control system has two temperature sensors those are inside the solar simulator and outside the solar simulator. Based on temperature difference between temperature sensors, cooling mechanism is activated electrodynamically. Temperature measurement is done in a real-time manner.

Double faced photovoltaic system is designed to improve electrical performance of photovoltaic systems. It is placed inside the solar simulator system to improve the output power.

It is concluded that designed solar simulator system eases the observation of thermal and cooling effect on electrical performance of photovoltaic systems. Thanks to its time-independent and weather-independent operation, it is possible to conduct experiments in every day time, every month and every weather.

Keywords: Solar cell, efficiency, double faced solar cell, cooling system

ÇİFT TARAFLI FOTOVOLTAİK SİSTEMİN PERFORMANSINI İYİLEŞTİRME AMAÇLI BİR ELEKTRODİNAMİK SOĞUTMA SİSTEMİ VE SİMÜLATÖRÜNÜN GELİŞTİRİLMESİ

ÖZ

Fotovoltaik soğutma, Fotovoltaiklerin sıcaklık etkisine karşı elektriksel performansını artırmanın bir yoludur. Bu amaca bağlı olarak, tez çalışması üç alt sistem ile geliştirilmiştir: Güneş simulatör sistemi, dinamik kontrol sistemi ve çift taraflı Fotovoltaik sistem.

Güneş simulatör sistemi iki özdeş ışık kaynağına, çift taraflı iki özdeş Fotovoltaik panele, soğutucuya ve ısıtıcıya sahiptir. Isıtıcıyı aktifleştirerek, sıcaklık etkisinin çift taraflı Fotovoltaik sistemin elektriksel performasına etkisi gözlemlenir. Soğutucuyu aktifleştirerek, soğutma etkisinin çift taraflı Fotovoltaik sistemin elektriksel performasına etkisi gözlemlenir.

Dinamik kontrol sistemi, biri güneş simulatör sisteminin içinde diğeri güneş simulatör sisteminin dışında iki adet sıcaklık sensörüne sahiptir. Sıcaklık sensörlerinin arasındaki sıcaklık farkına bağlı olarak soğutma mekanizması elektrodinamik olarak aktifleştirilir. Sıcaklık ölçümü gerçek zamanlı olarak yapılır.

Çift taraflı Fotovoltaik sistem, fotovoltaik sistemin elektriksel performansını artırmak için tasarlanmıştır. Çıkış gücünü artırmak için güneş simulatör sisteminin içine yerleştirilmiştir.

Bu çalışmadan şu çıkarılmaktadır ki tasarlanan güneş simulatör sistemi sıcaklık ve soğutma sisteminin Fotovoltaik sistemlerin elektriksel performansları üzerindeki etkisini gözlemlemeyi kolaylaştırmaktadır. Güneş simulatör sisteminin zamandan ve hava durumundan bağımsız çalışması sayesinde deneylerin günün her zamanında, her ayda ve her mevsimde yapılması mümkündür.

Anahtar Kelimeler: Güneş pili, verimlilik, çift taraflı güneş pili, soğutma sistemi

CONTENTS

NOMENCLATURE

Subscripts

D_N	Electron Diffusion Constant
D_P	Hole Diffusion Constant
I_{mp}	Current at maximum power
I_O	Saturation Current
I_{PH}	Photogenerated Current
I_S	Saturation Current
I_{SC}	Short Circuit Current
L_N	Electron Diffusion Length
L_P	Hole Diffusion Length
N_A	Acceptor Impurity Concentration
N_D	Donor Impurity Concentration
n_i	Intrinsic Concentration
R_S	Series Resistance
R_{Shunt}	Shunt Resistance
V_B	Barrier Voltage
V_{mp}	Voltage at maximum power
V_{OC}	Open Circuit Voltage
V_T	Thermal Voltage
β_{ref}	Reference Temperature Coefficient
η_{Tref}	Efficiency at Reference Temperature

Acronyms

AC	Alternating Current
ASTM	American Society for Testing and Materials
BJT	Bipolar Junction Transistor
BOM	Bill of Material
CCW	Counter-clockwise
CW	Clockwise
DC	Direct Current
DDM	Double Diode Model
DSSC	Dye-sensitized Solar Cell
ECT	Equivalent Cell Temperature
FF	Fill Factor
HOMO	Highest Occupied Molecular Orbital
KVL	Kirchhoffs Voltage Law
LCD	Liquid Crystal Display
LED	Light Emitting Diode
LUMO	Lowest Unoccupied Molecular Orbital
MOSFET	Metal Oxide Semiconductor Field Effect Transistor
MPPT	Maximum Power Point Tracking
NREL	National Renewable Energy Laboratory
NTC	Negative Temperature Coefficient
OPAMP	Operational Amplifier
PCM	Phase Change Material
PTC	Positive Temperature Coefficient
PV	Photovoltaic

PV/T	Photovoltaic Thermal
SDM	Single Diode Model
SSDM	Simplified Single Diode Model
TCO	Transparent Conducting Oxide

LIST OF TABLES

LIST OF FIGURES

CHAPTER 1

INTRODUCTION

Energy is the most important pillar of world life. It drives whole creatures in many aspects ranging from microscale creatures to macroscale creatures. It is essential for reproduction, movement and survival of each life in world. Humanity needs energy like other creatures. It utilizes this phenomena in order to satisfy it's daily life.

Need for energy is increased as the civilization is developed. At the beginning, energy is only needed to set a fire. However, later on, machines, vehicles need energy to work. As the technology progresses, people search for alternative energy sources due to easy-to-reach-energies and non-destructive energies. This demand directs people to renewable energy sources. Renewable energy sources are solar energies, wind power energies, tidal power energies and geothermal energies. Solar energies are the most important energy among renewable energy sources.

Solar energy is infinite and clean energy source for Photovoltaic and Photovoltaic Thermal (PV/T) panels. While solar thermal panels convert solar energy to thermal energy, photovoltaic panels convert solar energy to electrical energy. PV/T panels are utilized in remote rural areas. Thanks to PV/Ts, rural homemakers generate their hot water and electricity although they are rather far from grid connection. Moreover, solar energy is also used extensively in space technology. Satellites are orbiting the world in many years without any service interruption. These are energized by photovoltaics even while moving thanks to their sun tracker systems.

1.1 Definition of Photovoltaics

Dictionary definition of photovoltaics is given as “Relating to the production of electricity at the meeting point of two substances that have been exposed to light” or it can be explained in another way as “Photovoltaic effect, process in which two dissimilar materials in close contact produce an electrical voltage when struck by light or other radiant energy [1]”.

The first time photovoltaic effect seen in history is in 1839 by French Physicist Alexandre Edmond Becquerel [2]. Photovoltaic effect is called also as "Becquerel effect" in honor of its discoverer, Becquerel [3].

After Mr. Becquerel, Willoughby Smith discovered the photovoltaic effect in selenium in 1873. In 1876, Richard E. Day and William G. Adams discovered that illuminating a junction between selenium and platinum also has a photovoltaic effect. These discoveries are followed by the built of the first solar cell in 1883 by Charles Fritts. Mr. Fritts coated the semiconductor selenium with an extremely thin layer of gold to form the junctions. The built device was only about %1 efficient. However, these discoveries could not be able to be explained until 1905. In 1905, Albert Einstein explained the photoelectric effect such that he received the Nobel Prize in 1921 [4]. Working mechanism of photovoltaic cells aka. solar cell is based on photoelectric effect such that when a photon is exposed to a metal surface, electrons become free from metal surface. When the frequency is increased from visible light to ultraviolet, the more electrons are pulled from the metal surface. In 1918, Polish scientist Jan Czochralski opened the door to produce practical solar cells by introducing the method for monocrystalline silicon production.

The first practical solar cells are produced in 1954 in Bell Laboratories with %4.5 efficiency followed by %6 efficiency within a few months with Pearson, Chapin and Fuller patent. In 1957, they reached the %8 efficiency at Silicon Solar cells. They utilized designed solar cells in Satellites. The first solar powered Satellite is Vanguard I with 0.1W at 100 cm^2 solar panel. That invention was rather interested people that The New York Times forecasts that solar cells will eventually lead to a source of "limitless energy of the sun". This news attracted all people ranging from academia to industry, First Solar Energy Symposium is organized in 1955 in Arizona [5].

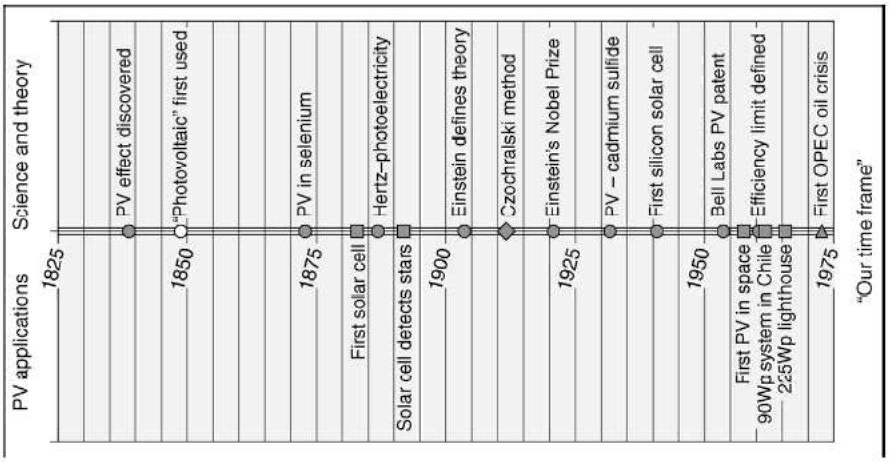

Figure 1.1 Simplified timeline of photovoltaics [6]

1.2 Photovoltaics Working Principles

Photovoltaic panels, in other words solar cells, are nothing but transducers. Indeed, when AT&T assignors (Gerald L. Pearson, Daryl M. Chapin and Calvin S. Fuller) receive US2780765 patent, they filed their patent as "Solar Energy Converting Apparatus". Also they refer to it as the "solar battery". Although converter was rather correct at that time battery term was not that much wrong definition by considering technological development race and level at that time.

1.2.1 Photovoltaic Anatomy

Photovoltaic panels are basically stack of layered structure and these structures are given below:

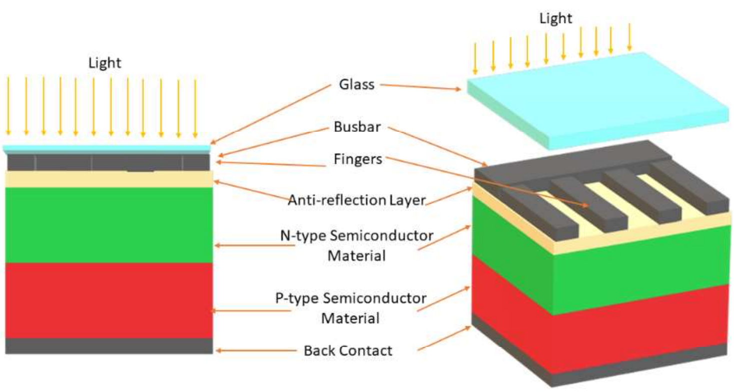

Figure 1.2 Structural representation of photovoltaic cell

Glass: This layer protects the solar cell from environmental effects. Although this layer is named as glass, it can be also plastic. However, transparency is essential for this layer. Any opacity leads to efficiency reduction for solar cell. In addition to protection, this layer provides the packaging of solar cell.

Busbar: This metallic structures are used to conduct electricity when solar cell is illuminated. This metallic roads are silver pasted roads having higher conductivity, lower resistivity located at the main line of the solar cell. Busbars are thicker than fingers because it conveys more current than fingers. In new generation solar cells, due to the fact that busbars shadow illumination, restrict the photons hit the semiconductor, TCO layers are introduced in new generation solar cells. TCO stands for Transparent Conducting Oxides. It allows the illumination to pass through it. This doped metal oxides used at other optoelectronic devices such as LCD displays. This structures are known as front contact provides the opportunity to take contact and connect to load/utility. Depending on the p and n type material structure order, it is named as cathode or anode. If p-type material is above then this layer is known as anode, otherwise it is named as cathode. As the number of busbars is increased, efficiency of the solar cell is also increased.

Fingers: This metallic structures are utilized to convey photoelectric current when photons hit the solar cell. This structures are thinner than busbars and they are located perpendicular to busbars. This metal grids collect the generated photoelectric current from photoelectric material and deliver it to busbars. Because they have significant resistance and shading effect on solar cell, this structure is replaced with TCO layers. As the Busbar/finger ratio increases, conduction efficiency increases. However, as a drawback, shading effect increases.

Anti-reflection Layer: When a photon beam is hit to an intersection of two optical media, it reflects naturally. In order to make as much as the photon inside possible, i.e., to trap the light, a special type of layer is introduced substrate material and front contact layers. The purpose of this layer is to reduce the reflection index. The reflection index of air is 1.00, water is 1.33 and glass is 1.52. Aim of this layer is, to make optical transition as smooth as possible. In addition to below front contact structure, above glass coating is also possible for anti-reflection coating. While substrate above coating eases the transition to semiconductor, glass-above coating eases the transition to glass, i.e. it eases the transition between air and glass optical transition.

N-type Semiconductor Material: N- type semiconductor material is a semiconductor material having more electrons compared to protons. Such materials are nothing but doped materials. Doped materials are named as impurity. In n-type semiconductors, impurities give free electrons to dope-accepted materials. The aim of such process is to increase charge carriers in the material. In conventional solar cell, silicon is used for photovoltaic material. In n-type region 5A group elements are doped into 4A group element silicon. By this way, extra 1 electron is gained to the lattice.

P-type Semiconductor Material: P-type semiconductor material is a semiconductor having more holes compared to electrons. Such materials are nothing but doped materials. Doped materials are named as impurity. In p-type semiconductors, impurities takes one electron from doping-accepting materials. The aim of such process is to increase charge carriers in the material. In conventional solar cell, silicon is used for photovoltaic material. In p-type region, 3A group elements are doped into 4A group element silicon. By this way, extra 1 hole is gained to the lattice. The region where p and n type intersects is named as pn-junction. This region has characteristic features itself.

Back Contact: This metallic layer is utilized to conduct electricity when solar cell is illuminated. Advantage of back contact over front contact is that illumination direction is towards front contact, i.e., back contact do not eliminate illumination. Therefore, there is not restriction for contact area. As the contact area covers the whole solar cell, resistivity of back contact is rather low. Therefore, efficiency improvement issues are not concerned compared to front contact. Although this contact metals are used to convey photoelectric current, as the work function increases efficiency decreases [7]. Though majority of the metals have lower work function, it is good to mention about work function of the back contact metals over solar cell efficiency.

Working Mechanism of photovoltaic cells is illustrated below:

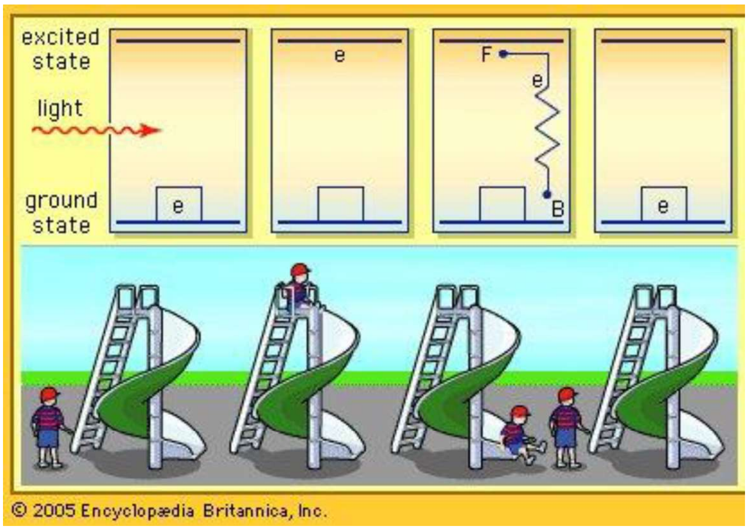

Figure 1.3 Photovoltaic Effect Illustration [1]

When an electron in ground state is excited by an incident photon, this electron, which is normally at the ground state, is elevated to excited state by consuming energy from photonic energy. Excess energy at excited state is consumed by a load connected. This load can be a simple resistor or a huge motor. Journey of the electron can be explained analogously with a child playing on a slide. As child moves up on slide, potential energy of child increases. Child slides down from the slide by consuming his/her potential energy. Interestingly, movement of child and electron is only one directional. It justifies that photoelectric effect generated DC-current [1].

1.2.2 Energy Levels and Band Gap

There are two possibility for electron in an atom: valence band, conduction band. As illustrated earlier, when situation is stable, electron sits on valence band. Valence electrons are the electrons which sit on outermost shell of the atom. These electrons are connected to the atom with a weak bond. These bonds are called covalent bond. These electrons are oriented in such a way that they form a perfect structure, lattice, called as crystal structure.

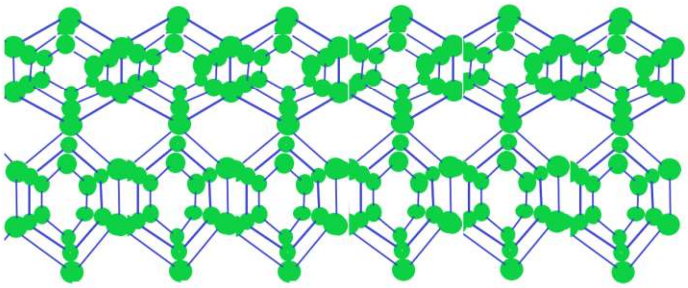

Figure 1.4 Structural representation of a material

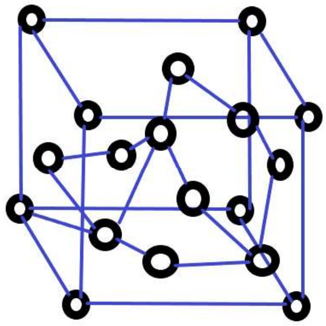

Figure 1.5 Cubic structural representation of a material

Valence electrons are key factor for grouping the material. Based on the valence electron number, group in periodical table is determined. Metal groups have lower valence band compared to ametal groups. Electrical conductivity is related to metallic property of the material. In conductor materials, valence electrons are elevated to conduction band with just a small amount of energy. On the other hand, isolators have more electrons compared to metals in outer shell of the atom and they are bound to the core with stronger bonds. Therefore, more energy is required to pull an electron from isolators compared to conductors. Semiconductors are sitting in between conductors and isolators. Energy required to pull an electron from semiconductor is less than isolator but more than conductors. This required energy is named as “Band Gap”. Band Gap determines the material whether it is conductor, insulator or semiconductor. Although there is not a consensus on Which Band Gap value stands for insulator or conductor, a semiconductor has band gap below than 3.0eV considering silicon having band gap about 1.0eV [8].

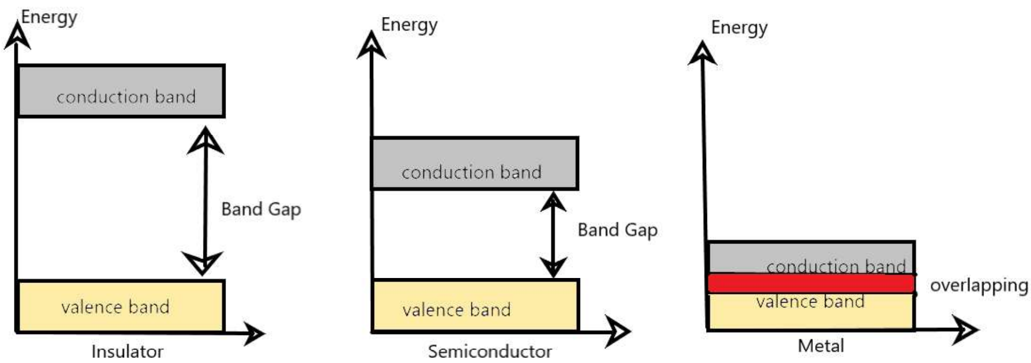

Figure 1.6 Energy bands of semiconductors in three states

If a beam of light is incident to an atom, there are possibly three cases to occur [9]:

- **Reflection:** If a photon is directed towards an atom and if frequency of the photon is not equal to resonance frequency of the atom then photon is reflected. This phenomena happens when the matter is opaque. If matter is opaque then photon hit to atom cannot vibrate other atoms and photon reemitted from same surface as reflected light.
- **Transmission :** If a photon is directed towards an atom and if frequency of the photon is not equal to resonance of the atom then photon is transmitted. The physics behind transmission and reflection is same but only difference is that in reflection case photon is received from same surface. On the other hand, in transmission case, photon is received from other surface of the material. If matter is transparent then photon hit to atom vibrates neighbouring atoms and photon reemitted from other surface of the matter.
- **Absorption:** If a photon is directed towards an atom and if frequency of the photon is equal to resonance freqeuncy of the electron then photon is absorbed. Resonance frequency of the electron is analogious to spring connected to an electron bound to atom. This spring vibrates at a specific frequency just like a single note in piano. If a photon hits an electron then that electron starts to vibrate. This vibration is conducted to other atoms and converted to heat energy. Eventually photon is energy is converted to heat energy and never given back as photonic energy.

1.2.3 PN-Junction

It is controversially not concluded whether it opens the door to solar cells or transistor, pn-juntion is one of the main pillar in electronics engineering. It is fundamental building block for transistor-based circuits, computer systems, singly diode. In history, the first time pn-junction invented is in 1940 by Russell Shoemaker Ohl. Mr. Ohl was an electrochemist in Bell's Laboratory. At the same time, this discovery is the beginning of modern electronics revolution and plays a vital role in bipolar junction transistors, aka. BJTs. [10].

Practically, pn-junction is nothing but a small diode. It allows the current in one direction only. P-type material is full of hole and n-type material is full of electron. If these two sections are connected contact layer between these two section is called as depletion layer. P-type side of depletion layer is full of eletron and n-type side of depletion layer is full of hole. This depletion layer is nonconductive layer contary to p-type and n-type regions. Term depletion comes from there and this nonconductivity is utilized as one-directional current device, aka. diode. If pn-junction is utilized as diode, p-type and n-type regions are named as anode and cathode, respectively. Holes in p-type and electrons in n-type regions are called as majority charge carrriers. However, electrons in p-type region and holes in n-type region are called as minority carriers. These majority and minority carriers from drift and diffusion currents in pn-junction. Anatomy and related charge movements in pn-junction are given below:

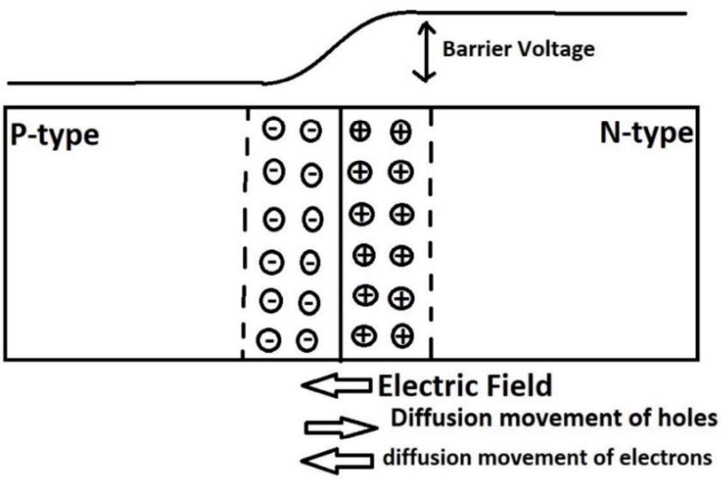

Figure 1.7 Atomic and energy level-based representation of pn-junction

Barrier Voltage across pn-junction when zero-bias applied is given below:

$$V_B = V_T \ln \frac{N_A N_D}{n_i^2}$$

Where V_T is thermal voltage which is $V_T = kT/q = 25$ mV at the room temperature. N_A and N_D are impurity concentrations and n_i is intrinsic concentration. When it is time to bias the pn-junction, there are two cases:

- Forward Bias
- Reverse Bias

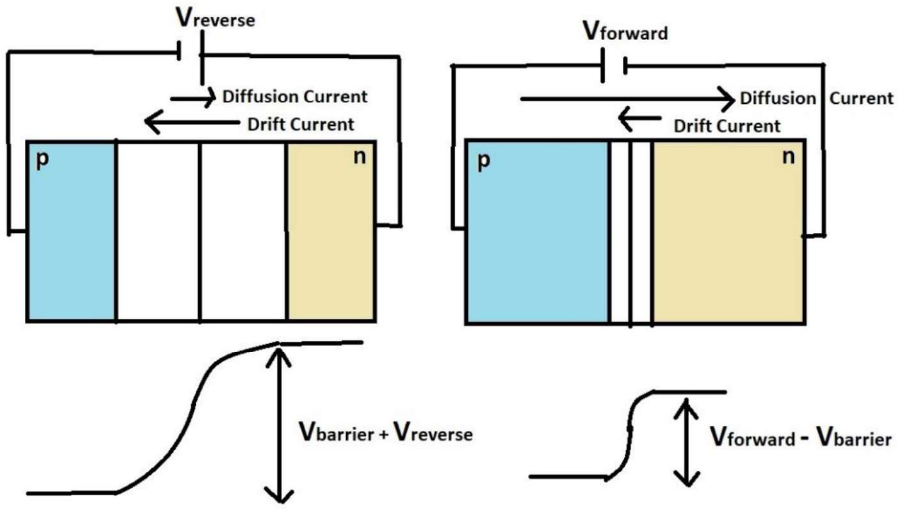

Figure 1.8 Forward bias and reverse bias representation of pn-junction

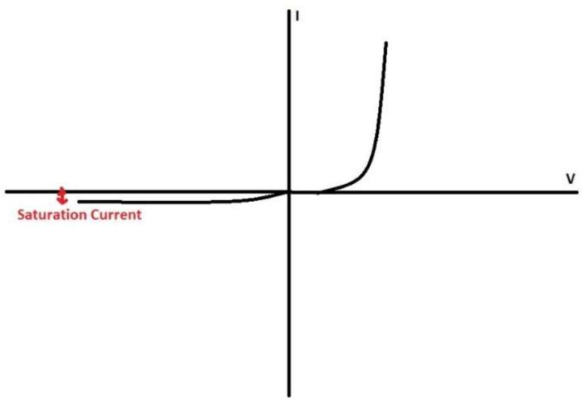

Figure 1.9 IV-characteristic of a PN junction

Forward biasing and reverse biasing of pn-junction and current-voltage characteristic of pn-junction are given above. When junction is biased reversely drift current dwarfs diffusion current because reverse bias voltage is constructive in this case. Interestingly, current cannot go beyond a value when reverse bias voltage is increased, i.e. current saturates. Because of this, this reverse bias current is named as saturation current. On the other hand, if junction is biased forward, diffusion current dominates drift current. Contary to reverse bias current, forward bias current increases as the forward bias voltage is increased. Forward and saturation currents are given below:

$$I_s = Aqn_i^2\left(\frac{D_p}{L_pN_D} + \frac{D_n}{L_nN_A}\right)$$

$$I = \ I_s\left(e^{\frac{V}{V_T}} - 1\right)$$

Where A is cross-sectional area of pn-junction, n_i is intrinsic concentration, N_A and N_D are impurity concentrations. D_P and D_N are electron and hole diffusion constants. L_p and L_n are hole diffusion length in n-type side and electron diffusion length in p-type side, respectively.

Interestingly as the biasing direction is reversed, depletion region depth increases, like forward bias shrinks depletion region. Depletion region vs. biased voltage is given below:

$$W = \sqrt{\frac{2\varepsilon_S}{q}\left(\frac{1}{N_A} + \frac{1}{N_D}\right)V_{barrier}} \text{ for forward bias}$$

$$W = \sqrt{\frac{2\varepsilon_S}{q}\left(\frac{1}{N_A} + \frac{1}{N_D}\right)(V_{barrier} + V_{reverse})} \text{ for reverse bias}$$

1.2.4 Solar Cell Types

On the earth crust, following oxygen, silicon is the most plenty element. It can be found as oxidized form as silicon dioxide in the shape of quartz or shore sand. In order to utilize silicon, it should be required to refine. In refinement process SiO_2 is heated at 1800°C with carbon. In semiconductor business, purity is one of the esential necessity for silicon. Silicon is %98 pure in nature. Therefore, it is required to further refinement process. To do so, it is tranferred to trichlorosilane ($SiHCl_3$) which is volatile liquid. This liquid is firstly distilled and then reduced by reacting with a hot surface of silicon. This process is named as Siemens process. These two refinement processes require considerable amount of energy [10].

Although many different types of photovoltaics are designed, it is not possible to strictly classify photovoltaics based on structure or material. Many authorities are classified photovoltaic cells differently. However, there is a consensus on that Photovoltaic cells are grouped based on technological development into three: First generation PV cells, Second Generation PV Cells and Third Generation PV Cells. Nikolay Belyakov grouped photovoltaic cells in his work [11], and it is depicted as below:

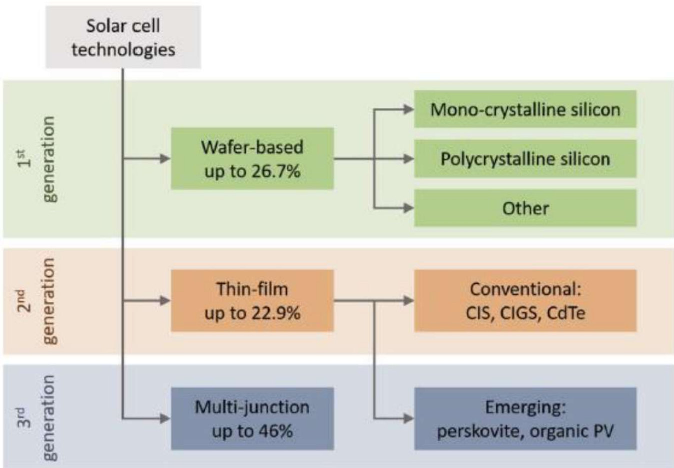

Figure 1.10 Photovoltaic technologies [11]

Nikolay Belyakov grouped solar cell by considering semiconductor material used. He stated that first group photovoltaics are wafer-based photovoltaics and they are silica based systems. It includes both monocrystalline and polycrystalline photovoltaics. Second Group solar cells are stated as thin-film cells. Thin-film structure absorbs solar radiation more efficiently than silica-based structure by allowing the use of extremely thin film structures. Thin-film technology can be split into two groups: Conventional thin-film Technologies and emerging thin-film technologies. Conventional thin-film Technology aka. Second generation of solar cell Technology, includes amorphous silicon (a-Si), cadmium Telluride (CdTe), copper indium diselenide (CIS) and its further development copper indium gallium selenide (CIGS). The third group thin-film technology is emerging thin-film technology. It includes perovskite and organic photovoltaics. Emerging thin-film Technologies are also grouped under emerging multi-junction solar cells. Emerging multi-junction solar cells utilizes several pn-junctions in order to increase efficiency. These Technologies are considered as third generation Technologies and emerging Technologies.

Table 1.1 Solar cell efficiency values for lab and modules as of 2017 [12]

Classification	Cell Efficiency(%)	Module Efficiency(%)
1st generation:Wafer-based Systems		
Monocrystalline Silicon	26.1	24.4
Polycrystalline Silicon	22.3	19.9
2nd Generation:thin-film Systems		
CIGS	22.9	19.2
CdTe	22.1	18.6
Amorphous Silicon	13.6	
3rd Generation:Emerging Technologies		
Multi-junction	46.0	
Perovskite	23.3	11.6
Organic PV	12.6	

Wafer-based Systems

At the begining of solar cell revolution, photovoltaic cells was being produced from crystalline silicon ingot, pure silicon. Growth ingot was cut into slices called as wafers. Resulted crystalline structure was named as monocrystalline structure because it was single-crystal structure from same ingot. Monocrystalline or single-crystal solar cells are rather highly-efficient. In 2014, Panasonic hits the efficiency of 25.6% with its monocrystalline PV cell [13]. However, production of single-crystal structure was rather dificult. Another option to produce solar cells from silicon was polycrystalline or multicrystalline structure. They have lower efficiency compared to monocrystalline solar cells but cost of them was rather lower and production of it was easier than former one. The most commercial systems in market utilizes multicrystalline solar cells due to its cost-efficient and easy-to-manufacture features though lower slightly lower efficiency, about %24.

Thin-film Systems

Idea of thin-film stucture dates back to 1970s. It was proposed that a thin-film noncrystalline structure, nothing but amorphous silicon, to deposit directly to a support material. Although light absorption characteristic was rather successful, amorphous silicon has 40 times higher rate of light absorption compared to monocrystalline solar cell [14], overall efficiency was lower compared to crystalline solar cells, 12.5% rather than 24%.

Deposition idea is evolved to different thin-film materials rather than silicon. Researchers proposed other materials having similiar optical properties but lower energy intensity and lower production cost. Such materials are $CuInSe_2$, CIS and CdTe. They have higher efficiency than silicon. Also they have higher light absorption than silicon. For example, 1mm thick CdTe can absorb 90% of solar spectrum whereas 100 mm or more silicon is required to absorb sunlight. In addition to high solar absorption, it is rather easy and cheap to manufacture. However, drawback of this kind of PV cell is that efficiency is low, similiar to a-Si PV cell. Not only efficiency but also other factors affect the reputation of CdTe. It is difficult to obtain low-resistance contact to p-type CdTe. It is difficult to dope p-type CdTe and there is a instability of cell and module performance in CdTe for PV applications [15]. CIGS and CIS materials are another material having high potential to be seen in market. Overall efficiency of 20% is achieved in laboratory environment [16]. CIGS is a compound formed of copper, indium, gallium and selenium. Due to high flexibility of the design of compounds, great technological jumps can be expected in future [15].

Emerging Technologies

Efficiency of single-junction structure hits to 31-33% in ideal case. This was the limit by Shockley-Queisser limit. To exceed this limit, different designs, production techniques are produced. Multi-junction cell was one such design techniques. This technique proposes several pn-junction of different semiconductors. Each junction structure responsible for a certain portion of spectrum such that at the end, whole spectrum was covered by pn-junctions. This idea was rather successful because efficiency hits to %46. Although this was a laboratory efficiency value, it has positive impact to lower production costs. In addition to multijunction structures, perovskite materials are other way to exceed this limit. Perovskite name comes from the perovskite material utilized in solar cells in order to harvest the light. Perovskite materials has same crystalline structure with calcium titanium oxide. Perovskite materials are rather cheap and easy to manufacture. As an advantage, like multi-junction cell structures, perovskite solar cells responsible for whole spectrum. Organic solar cells are another way to exceed SQ-limit. Organic Photovoltaic cells include one or several photoactive semiconducting layers. Organic solar cells include carbon to propose advantages. Carbon-based materials are easy and cheap to manufacture. However, still efficiency values are below %15, lower than wafer-based solar cells. On the other hand, researchers proceed their efforts to increase efficiency levels to comparable level. Organic material-based solar cells are divided into two categories: dye-sensitized solar cell (DSSC) and organic solar cell (OSC). DSSC solar cells are first invented by Oregan and Gratzel in 1991 with a efficiency of %7.1 [17]. Schematic below shows the structure of DSSC. On the other hand, organic semiconductor materials included in OSC form a single active layer as a single light absorber layer located between two electrodes with different energy band gap. Photovoltaic performance of OSC solar cells is rather low. Dr. Tang CW first annouced his bilayer OSC based on phythalocyanine copper as a p-type semiconductor with an efficiency of 1% [18].

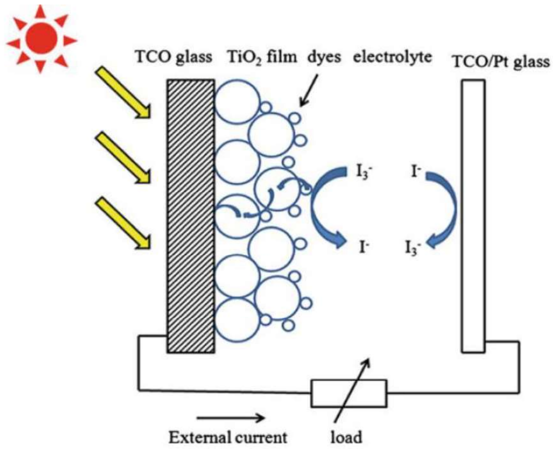

Figure 1.11 Dye-sensitized solar cell structure [19]

In addition to Nikolay Belyakov, other authorities also group photovoltaic cells. J.A. Luceno-Sanchez et. Al grouped solar cells into 4 main categories called as generations (GEN). Their grouping idea is given below:

First-Generation (1GEN)

a. Monocrystalline
b. Polycrystalline
c. Gallium Arsenide

Second-Generation (2GEN)

a. Amorphous Silicon (a-Si)
b. Microcrystalline silicon thin film solar cells
c. CdTe/CdS
d. CIGS

Third-Generation (3GEN)

a. Nanocrystalline films
b. Active Quantum Dots
c. Tandem/Stacked Multilayer Inorganics
d. Organic Polymer-based Solar cells
e. Dyed-Sensitized Solar Cells

Fourth Generation (4GEN)

a. Combination of Polymer Thin films with Novel Inorganic Structures

Efficiency and cost relation of the first three Generation is given below:

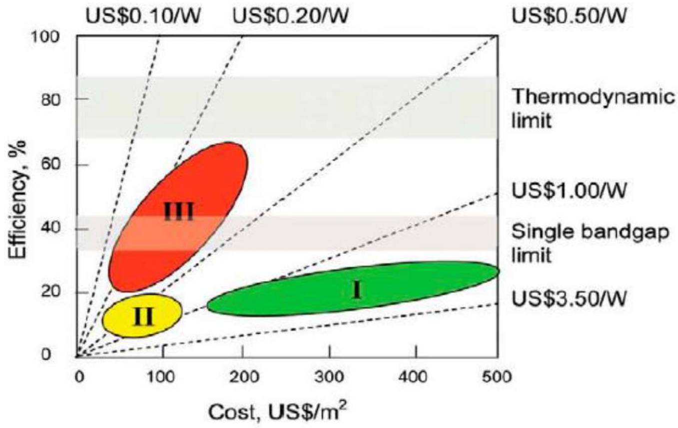

Figure 1.12 Efficiency vs. cost relation of GEN1, GEN2 and GEN3 pv technologies, taken from [20]

Efficiency and technology relation of four generations of PV cells are given below:

Table 1.2 PV technology summary, taken from [21]

GEN	Technology	Production Method	Characteristic	Efficiency(%)
1GE	m-Si	Czochralski	Expensive, stable	24.4
1GEN	p-Si	Siemens	Low cost, high defect	19.9
1GEN	GaAs	Expitaxial Growth	Expensive, good design	18.4-28.8
2GEN	a-Si	Large-area Deposition	Non-toxic, short life cycle	10.2-12.7
2GEN	μc-Si	Roll-to-roll	Low defect, good degradability	11.9-14.0
2GEN	CIGS	Deposition	Tuneable band gap	22.3
2GEN	CdTe	Deposition	High Temp tolerance,low fooling	21
3GEN	DSSC	Roll-to-roll	Work in low-light, robust	5.0-20.0
3GEN	QDs	Solution Casting	Efficient conductivity	11.0-17.0

3GEN	OPSCs	Solution Casting	High work fnctn, thermally stable	9.7-11.2
3GEN	PVSC	Sputtering	Cheap, simple	21.1-21.6
3GEN	MJ	Stacking	Wide range of design, challenging manufacture	35.8
3GEN	IMM	Monolithic Growth	Cheap, high band gap	40-44.4
4GEN	BHJ PSC	Solution Casting	Reproducible and stable	4.28
4GEN	PSC	Solution Casting	Good functionality	2.82-11.8
4GEN	PVSC	Spray Deposition	Stable, long life time	1.07-11.14
4GEN	PVSC	Solution Casting	Long life time, reduced electrn-hole recombtn	5.7-11.95
4GEN	PSC	Solution Casting	Improved electron transport	4.1-8.6

First-Generation Photovoltaic Solar Cells

1GEN solar cells are basically formed of thick crystalline films. These films are made up of Si. Silicon solar cells allocate 90% of PV cell market. Si is utilized in PV cell due some reasons. These are the fact that Si is the most second abundant material in earth’s crust, Si is stable and non-toxic material which does not contaminate the enviroment. Si PV cells can be easily manufactured by utilizing already-exist silicon microelectronics device manufacturing facilities.

1.Monocrystalline Silicon (m-Si)

m-Si Solar cells are produced by utilizing Czochralski process. This process is based on a silicon seed. Silicon is growth from this silicon seed and resulted ingot is sliced into wafers. Thanks to this technology, diameter of 10 to 300 mm and a length of 50 cm to 2 ingots can be obtained [22]. Czochralski method is difficult due to some reasons. These reasons are the fact that Si should have very high purity, this Si is named as solar grade silicon, high amount of energy is required and temperature should be controlled to maintain crystal growth.

2.Polycrystalline Silicon (p-Si)

p-Si cells are manufactured as a reply to Czochralsky method. There are some advantages for p-Si over Czochralsky method. These are the fact that it is required to consume less energy and release less greenhouse gases. However, efficiency of p-Si, 19.9%, is less than m-Si [23]. The underlying reasons for low efficiency is due to grain boundaries and higher concentration of impurities.

3. Gallium Arsenide (GaAs)

GaAs is utilized in PV cells instead of Silicon. GaAs has some advantages over Silicon. These are the fact that it has band gap of 1.43 eV, closer to ideal single-junction PVC, it has higher absorptivity hence only a few microns are required to absorb usable sunlight portion whereas silicon requires 100 micro meter or more to absorb same solar power. It allows customizable cell design being compatible with III-V group materials. They have lower temperature coefficient than silicon, therefore their performance is less temperature-dependent. GaAs is produced by combining Ga and As. Production is in 4 steps. In first step, a mixture of Ga and As are reacted under high temperature conditions to form crystalline ingots of GaAs. Then ingot is sliced into wafers. These thin wafers are used as substrate seed to growth very thin sheets. Then epitaxy process is performed. Finally, metallic contacts and antireflective layers are produced. GaAs is frequently utilized in multi-junction cells.

Second-Generation Photovoltaic Solar Cells

2GEN solar cells are basically focused on thin-film Technologies. The underlying idea behind this technique is to minimize the cost by reducing the amount of material used. 2GEN PV cells include a-Si, μc-Si, CIGS and CdTe. There are some advantages of Second Generation photovoltaic cells. These are the fact that cheaper process is carried out compared to Si-based PV cells, less amount of material is utilized in the process, less number of production stages compared to 1GEN PV solar cells. On the other hand, there are some disadvantages of 2GEN over 1GEN PV cells. These are the fact that lower efficiency is observed in 2GEN solar cells, 20.3%<24.4%, light-dependent degredation severely effects the 2GEN solar cells due to thinner film structure.

1. *Amorphous Silicon (a-Si) and Micro-Crystalline Silicon (μc-Si)*

a-Si is a transition type PV cell or it can be said hybrid Silicon and thin film structure solar cell. Amorphous silicon is utilized due to some advantages. These advantages are the fact that silicon material can be found easily in nature, manufacturing process needs lower energy than other solar cell types, a-Si has higher absorption rate and thinner, then less amount of material is utilized. On the other hand, a-Si has a disadvantage. It is the fact that non-crystalline, thinner structure is prone to be degraded by sunlight. In order to eliminate this drawback, H is doped to a-Si. Resulted a-Si:H is named as microcyrstalline Silicon. Efficiency in laboratory environment is 11.9% for single-junction and 14.0% for multijunction solar cells [23].

2. *Copper Indium Gallium Selenide(CIGS)*

CIGS solar cells are based on $Cu(In_xGa_{1-x})Se_2$ absorber material. Band-gap varies between 1.0eV to 1.7eV by varying the “x” value. Although CIGS is early-stage large scale commercialization, its manufacturing method decreases overall cost of manufacturing photovoltaic cells. Co-evaporation technique is utilized in CIGS production. Also, one-stage hot wall deposition technique is also considered to reduce overall cost of PV cells. On the other hand, by thinking hazards of cadmium extraction and use, CIGS solar cells release fewer health and evironmental concerns than CdTe solar cells. Maximum Laboratory efficiency hit by Stion is 23.2% [24]. Structure of CIGS solar cell is given below.

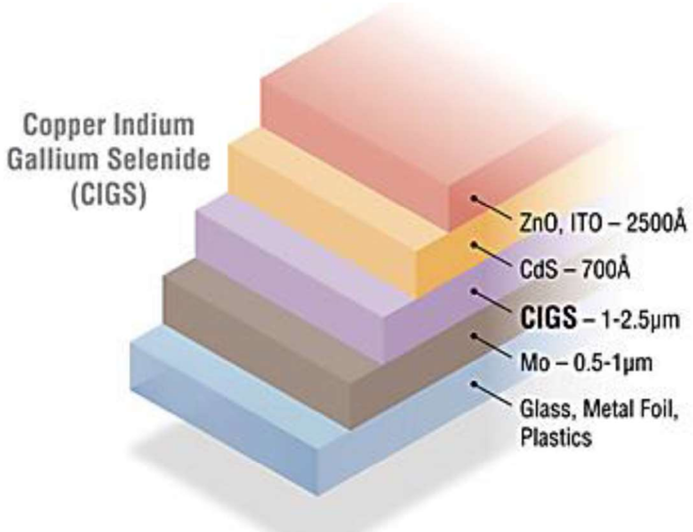

Figure 1.13 CIGS structure [25]

3. *Cadmium Telluride (CdTe)*

CdTe is also nice selection for solar energy absorber in solar cells. It is chosen for thin film structure because of its optimum band gap, high absorption coefficient and ease to be doped. A-Si solar cells was the first thin film technology. This technology had some problems: deposition of silicon onto substrate was time-consuming and costly and efficiency was low. To improve this technology, CdTe solar cells are introduced. CdTe Solar cells was 11% more efficient than a-Si and its energy band gap is 1.4eV which fits solar spectrum very well. CdTe is easy to produce because it is easy to deposit onto substrate. Each cell has CdS layer known as Window layer which decreases reflection of incoming rays. CdTe PV cells can operate at higher temperatures than silicon can operate at. Also, CdTe captures better in humid environments than silicon. However, CdTe is formed of materials potentially more toxic silicon. Because of this, usage of CdTe is limited in some environments. Cross-section view of CdTe-based solar cells is given below:

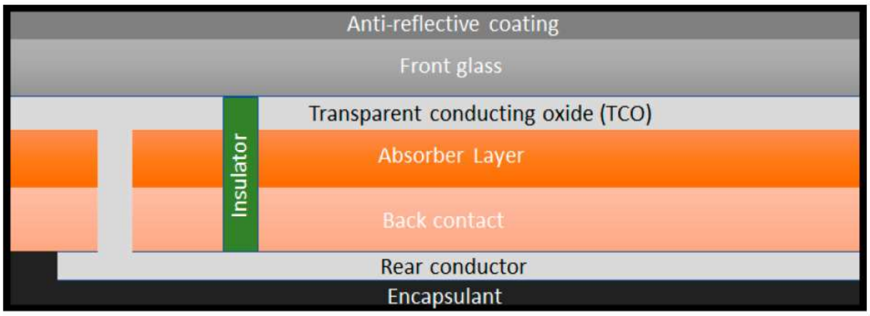

Figure 1.14 Cross-section view of CdTe-based pv cells, taken from [21]

Third-Generation Photovoltaic Solar Cells

Idea of 3GEN PV cell arises from to increase device efficiency and reduce the distance to the Carnot limit. Underlying method is to utilize thin film stuructures, new materials and new designs. Although, it seems to increase cost of unit area structure, idea of 3GEN will reduce the cost per watt. In addition, materials utilized in 3GEN PV cells are nontoxic like Silicon-based Solar cells and very abundant materials on earth crust. Also, it is possible to reach high efficiencies like 60% by using state-of-art methods like hot carrier collection, generation of multiple carriers. Main advantages of 3GEN PV cells are suitability for large-scale production, mechanical robustness and high efficiencies at high temperatures. However, challenge in 3GEN PV cells is to reduce cost/watt ratio. Basically, there are five type of technology in 3GEN PV cells: Dye-Sensitized solar cells, Organic and polymeric solar cells, perovskite cells, Quantum Dot cells and Multi-junction cells.

1. *Dye-Sensitized Solar Cells*

DSSC PV cells are basically low-cost solar cells belonging to the group of thin-film cells. It is formed of photo-sensitized anode and an electrolyte resulting a photoelectrochemical system. DSSCs are also known as Gratzel cell [26]. DSSC has five different layers [26]: Transparent anode glass sheet named as TCO glass, A layer of TiO_2 to improve electronic conduction, A monolayer of charge transfer dye to enhance the absorption of light, An electrolyte containing a redox mediator in an organic solvent to improve regeneration of dye and a cathode made with a crystal coated with a platinum to facilitate the collection of electrons. Working mechanism of DSSC is as follows: when DSSC is exposed to sunlight, dye is excited and an electron moves to conduction band of the TiO_2 film. Dye promotes to the diffusion of electrons towards the anode and then reused in the external charge before becoming part of the cathode [21]. With the invention of DSSCs, many artificial dye molecules are sensitized and launched to the market. Altough natural dyes show lower efficiency like 1.5% and 1.7% [27], theoretical limit is 20% for DSSC and efforts are to reach this limit [28]. Shematic view for DSSC is given below:

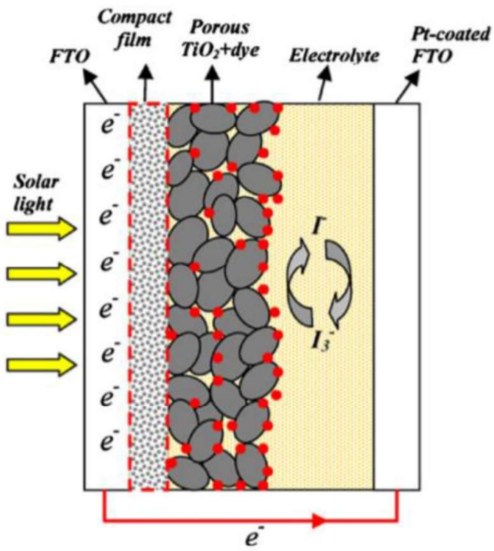

Figure 1.15 Schematic diagram for DSSC, taken from [19]

2. *Quantum Dot Solar Cells*

In recent researches, scientists try to find a way to increase power conversion efficiency of solar cells from sunlight. Shockley–Queissar limit says that when a single p-n junction is utilized maximum conversion efficiency of the junction is 31%. Many methods are studied to excess this limit. These methods are tandem cells, hot carrier solar cells, solar cells producing multiple electron-hole pairs per photon through impact ionization, multiband and impurity solar cells and thermophotonic solar cells. Hot carrier solar cells are one of such methods. Concept of “hot” comes from the following: solar spectrum includes photons with 0.5eV-3.5eV. Photons with lower energy than semiconductor band gap energy are not absorbed. On the other hand, photons with higher energy than semiconductor band gap energy are absorbed with an excess energy of "$photon\ energy - semiconductor\ bang\ gap\ energy$". This kinetic energy creates an effective temperature for carriers whose temperature is higher than lattice temperature. Effective temperature can be ten times higher than lattice temperature. Although one way to excess the Shockley–Queissar limit is to utilize cascaded multiple p-n junction, another way to increase conversion efficiency is to reduce loss caused by thermal relaxation of photogenerated hot electrons and holes. Due to the fact that effective masses of hole and electron are different, cooling time for hole and electron are different too. By utilizing quantum-dot structures in solar cells, efficiency of 66% is possible [29].

3. Organic and Polymer Solar Cells

Researchers conduct studies to find out new materials to replace inorganic materials in solar cells because mass production of silicon in first generation cells are difficult, gallium is rarely found in crust and Cadmium is a toxic. Therefore, organic materials are good replacement for inorganic photovoltaic materials. Mechanism of electricity generation in OPVCs are different than inorganic materials. Working mechanism of the OPVCs are as follows: Electron donor material absorbs the photons from the radiation and excited states are created. Excited state is a bound state of an electron and hole attracting each other with an electrostatic interaction. Acceptor material acquires electrons from dissociated electron-hole pair. Energy band gap in OPVC materials are defined as energy difference between HOMO and LUMO levels. Open circuit voltage is nothing but difference of HOMO of donor materials and LUMO of acceptor materials. Finally, each excited state generates a load-free carrier that can be collected by electrode of material with higher electron affinity and hole is acquired by the material with lower ionization potential. All of the mechanism is illustrated as below.

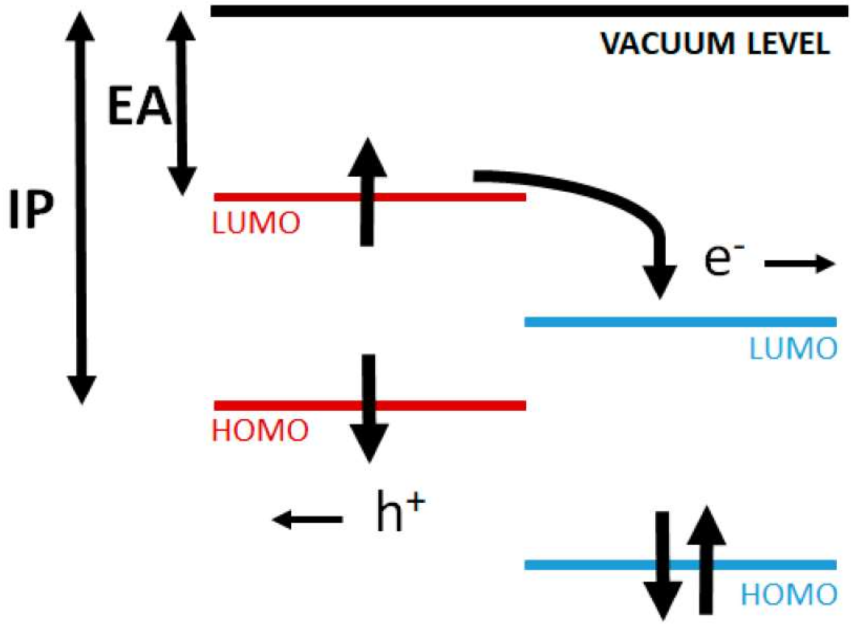

Figure 1.16 Charge seperation mechanism at donor-acceptor interface [21]

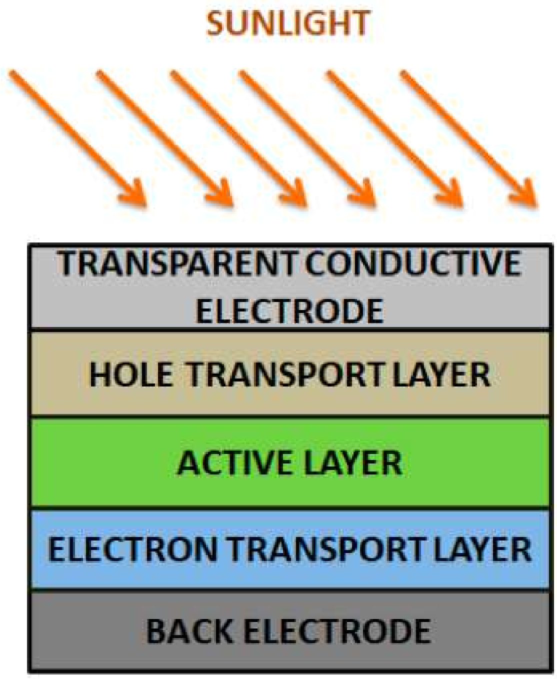

Figure 1.17 Schematic represenation of typical polymer solar cell [30]

4. Perovskite Solar Cells

The first time perovskite material discovered is in 1839 by Gustav Rose in Ural Mountains of Russia. Material is named after Russian mineralogist Lev Perovski. Perovskite is calcium titanium oxide mineral composed of calcium titanate. Perovskite named is applied to the class of compounds whose crystal structure is same as $CaTiO_3$.$^{XII}A^{+2}$ $^{VI}B^{+4}$ $X^{-2}{}_3$ is known as perovskite structure. In perovskite structure, A and B are cations and X is anion. The most studied perovskite absorber is methylammonium lead trihalide, $CH_3NH_3PbX_3$, where X is a halogen ion such as iodide, bromide or chloride. Perovskite materials have many appropriate characteristics to behave as a photoactive material for solar cells. These characteristics are high light absorptivity, great charge-carrier mobility, longer exciton diffusion length and easily tunable bandgap. Perovskite solar cells are favored over conventional silicon solar cells due to simple manufacturing process and low cost. Underlying reason why methylammonium lead iodide extensively studied is that power conversion efficiency of this material is higher than traditional dye-sensitized and organic solar cells. Crystalline structure of Perovskite, unit cubic cell of methylammonium lead iodide and device structure of conventional perovskite solar cell are given below.

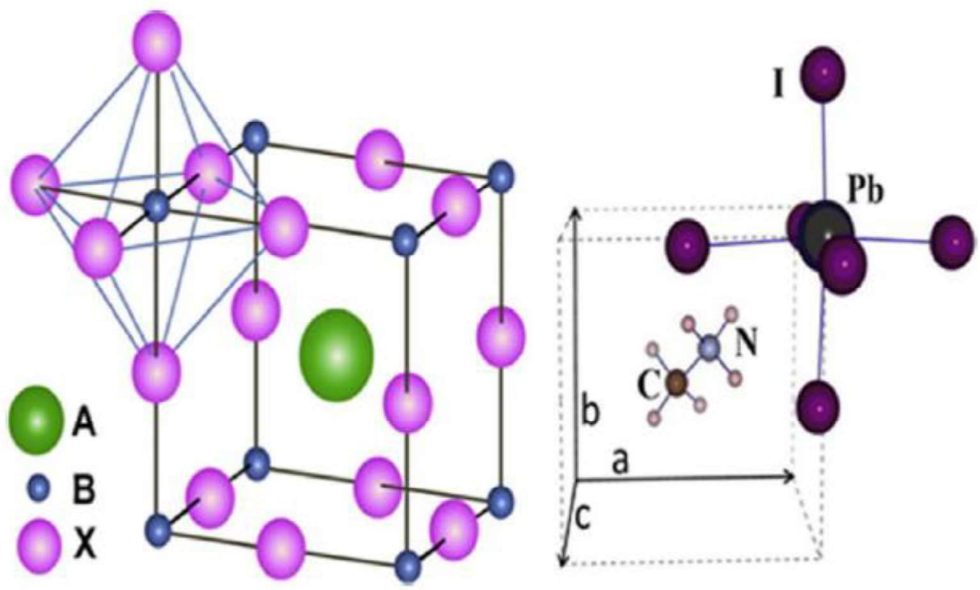

Figure 1.18 Perovskite structure and unit cell of methylammonium lead iodide perovskite [31]

Figure 1.19 Device architecture of conventional perovskite solar cell [32]

5. *Multi-Junction Solar Cell*

Due to SQ-limit, many methods are studied in order to increase efficiency of solar cells. One of the popular method is multi-junction solar cell. Multi-junction solar cell includes multiple pn-junctions made of different semiconductor materials. Each material section is responsible for different portion of sunlight spectrum. Thus, increasing conversion of incident sunlight increases device efficiency. Due to successive structure of the device, multi-junction solar cells are also known as tandem solar cell. Production of multi-junction cell is not an easy job. Therefore, wiring two mechanically seperated thin film solar cells are introduced for tandem solar cell production. To produce tandem solar cells, III-V semiconductors are utilized due to two reasons: they can be grown with excellent quality and they span a wide spectral range.

Theoretical efficiencies of multi-junction solar cells are illustrated as below. Although it seems that as the number of junction increases solar cell efficiency increases too, higher number of junctions make device design difficult. Therefore, it should be optimization among complexity, device efficiency and number of junctions. Also, as it can be seen from the graph below, as the number of junction increases, efficiency jump between number of pn-junctions are decreased, i.e. efficiency saturates after a while. Typical tandem solar cell includes five elements: A transparent electrode covering large band gap cell first to capture the radiation, i.e.

TCO, a recombination layer used as tunnel connection between high-band-gap material and low-band-gap material, higher band gap material, lower band gap material, back contact. Theoretically, multi-junction approach hits the efficiencies from 31% to 86% [33]. On the other hand, technology to reach these efficiencies are higher than conventional silicon solar cells. Therefore, multijunction solar cells are utilized only on space applications.

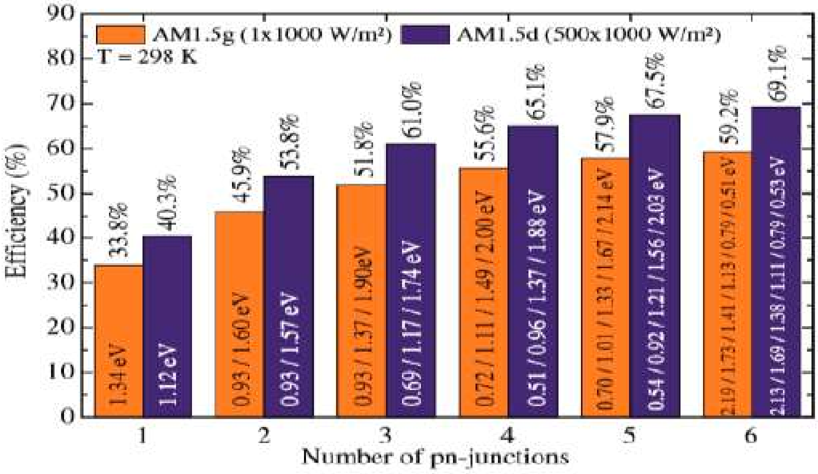

Figure 1.20 Solar cell efficiency as a function of number of junction [34]

Fourth-Generation Photovoltaic Solar Cells

4GEN photovoltaics combines low cost of polymer thin-film materials with good stability of nanomaterials like graphene, carbon nanotube, nanoparticles and its derivatives. These architectures utilize advantage of solution processable devices but incorporate nanomaterials to improve the charge dissociation and charge transport within the cell. Particularly, graphene has highest scientific technological expectations.

1. *Combination of Polymer Thin films with Novel Inorganic Structures*

4GEN photovoltaic solar cells are designed based on the philosophy of low cost and good stability. Inorganic structures are utilized in polymer organic structures to improve stability of the device. One of the most promising inorganic structure is Graphene. Graphene is two dimensional material composed of carbon atoms forming atomically thick layer on the shape of honeycomb. Carbon atoms are linked to each other via Van Der Walls forces. The sp^2 hybridization of carbon atoms determine the fact that free electron of 2px orbital can form π bonds with other atoms. Graphene utilized in electronics industry due to its enormous features by its interesting chemical configuration: Graphene has thermal conductivity of 3000-5000$Wm^{-1}K^{-1}$ [35], 50-300Scm^{-1} electrical conductivity [36], tensile strength of 130GPa and breaking strength of 40N/m [37]. These enormous features make graphene candidate for application in photovoltaics. Although graphene's characteristics are nice for photovoltaic applications, graphene behaves like a transparent material because it absorbs 2.3% of solar radiation [37]. However, thanks to doping, this problem can also be solved. Graphene oxide, shortly GO, is the modified version of Graphene. It includes carboxylic groups at the edges of the sheet, also epoxide and hydroxyl groups within the basal plane [38]. Some characteristic features of GO differ from graphene. GO has lower electron mobility and electrical conductivity, mainly used as insulator, (1012 Ω/squaremeter). Inserting a thin Graphene Oxide (GO) interfacial layer can improve the solar cell efficiency by %100 [39]. Therefore, utilization of Graphene and Graphene Oxide is rather important for solar cells.

1.3 Solar Cell Cooling Methods

Solar cells are best candidate for renewable energy resources nowadays. Although solar light flux increases the electrical power produced, temperature increase due to sunlight radiation reduces the efficiency of the solar panel. Many methods are studied by researchers. Cooling agents for photovoltaic systems are liquid, air and solid. Commonly utilized liquid cooling agent is water. Other special-purpose liquid cooling agents exist. Air is also common in cooling process. Special-purpose solids are utilized by using their phase-change property to reduce operating temperature of the photovoltaic systems. Basically, solar cell cooling methods are divided into two groups: Active Solar cell cooling and Passive Solar cell cooling. If the cooling mechanism consumes power in order to cool down the photovoltaic cell by ventilation or pumping, that mechanism is called as active cooling. On the other hand, if the cooling mechanism does not consume power in order to cool down the photovoltaic cell, e.g. natural ventilation or phase change material, that mechanism is called as passive cooling. Solar cell cooling methods are grouped and depicted as below.

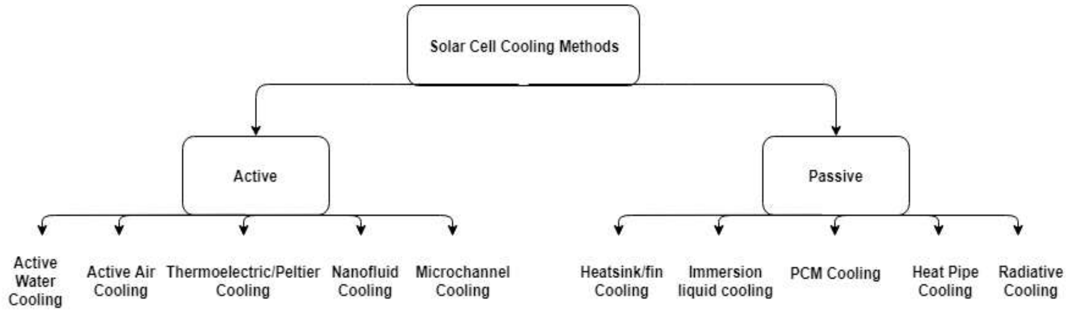

Figure 1.21 Solar cell cooling methods

1.3.1 Active Cooling Methods

Active cooling methods are utilized in photovoltaic power generation systems extensively because the highest efficiency increase by cooling is by active cooling. Consumed power by active cooling like pumping or fan ventilation cultivates efficiency increase from power loss due to temperature rise. There are five active cooling methods: Active Water Cooling, Active Air Cooling, Thermoelectric/Peltier Cooling, Nanofluid Cooling and Microchannel Cooling.

Active Water Cooling

One of the effective way of cooling photovoltaic cell is to reduce operating temperature of its surface. Cooling of solar cell panels is considered the optimum and less expensive technique utilized to improve the performance of photovoltaic cells. Many heat transfer matters are utilized in solar cells. Water is the best and common agent to cool down the surface of the photovoltaic surface. In water cooling systems, there are two ways to cool down the temperature of photovoltaic module: cooling from back of the module and cooling from the surface of the module. In water cooling from back side, water pipe network at the back of photovoltaic modules is utilized. Thanks to this technique, heat is transferred from photovoltaic panel to water and operating temperature of solar cell is lowered. In this technique, operating temperature of solar cell is decreased by 20 K and output power performance is increased by 9% [40]. Other method, aka. cooling from upper side of the photovoltaic panel, increases electrical output power by 10.3% [41]. Although active water cooling increases electrical output of the PV panel, significant amount of pump power is required to circulate the cooling water. In order to obtain net efficiency increase, comprehensive thought is required. However, when spray and jet impingement cooling techniques are considered, it can be seen that decrease in temperature and increase in power output are satisfactory although extra power is utilized for spraying and impinging. Jet-impingement cooling strategy decreases operating temperature of the photovoltaic module by 30 °C and increases output power by 48% [42]. Also, spraying distributes cooling over whole surface and prevents hot spots on cooling surface. All in all, if cooling strategy is utilized effectively, satisfactory results can be obtained though extra power is consumed for cooling, aka. pumping.

Active Air Cooling

One of the easy and effective way to reduce operating temperature of the solar module is via air. Air is the easiest and the most low-cost way to cool down solar modules. As a heat transfer agent, natural air is utilized in active air cooling systems. In active air cooling systems, air is ventilated by using a fan. Moving air over surface of the photovoltaic panel helps to distribute stored heat energy. Excess heat energy is transferred to air moving over the solar cell. Y. M. Irwan et. al compared active air cooling strategy and active water cooling strategy in their studies [43]. They showed that only fan cooling method decreases operating temperature of the photovoltaic module by 6.1 °C and increases output power by 32.23%. On the other hand, Water pump method decreases operating temperature of the photovoltaic module by 6.36 °C and increases output power by 38.98%. These results show that fan cooling method gives weaker performance than water pump method. If ease of installation and uniformity of cooling are considired in fan cooling, it can be said that fan cooling is more preferable although it shows weaker performance.

Thermoelectric/Peltier Cooling

Thermoelectric cooling is another way to cool down the solar module. Underlying idea is based on Peltier effect. Peltier effect is a natural phenomena that when a temperature difference is present between two side, a voltage difference is seen between these two sides, or when a voltage is applied between two sides, heat is transferrred from one side to other. In thermoelectric cooling strategy, a thermoelectric material with heatsink is located at the back side of the photovoltaic module. In study by H. Najafi and K.A. Woodbury [44], they modeled cooling system based on Peltier Effect for photovoltaic cells. They concluded that as temperature increases, required power to cool down the solar module increases, which decreases the net power obtained from PV-TEC module. Also, they investigated that as irradiance increases required power to cool down solar module increases, too. On the other hand, some researchers studied that instead of cooling solar module, electricity generation from excess energy, heat on PV cell. W.G.J.H.M. van Sark studied that PV-TE hybrid structure can generate eletricity from both sunlight and excess heat. Thermoelectric electricity generation can increase annual energy by 14.7- 11.1% [45].

Nanofluid Cooling

Nanofluid cooling is a strong potential candidate to reduce temperature of PV module and to boost the electrical performance of PV module. In this technique, base fluid material is mixed with a proper technique with particles of the order of 10^{-9}m (nanometer size) and new fluid material is named as nanofluid. Resultant fluid has higher heat transfer rate thanks to nanomaterials compared to base material [46]. M. A. Hamdan and K. K. Kardasi conducted a study about performance of nanofluids on PV module cooling. They studied on three PV panel to demonstrate three cases: no-cooling, water-cooling and nanofluid cooling. As nanofluid agent, they studied two nanomaterials Al_2O_3 and CuO. They monitored PV performance for different concentrations of nanofluids and determined the optimum concentration that causes maximum increase in PV performance. They showed that electrical efficiency is increased by 12.57% for nanofluid cooling and 11.39% for water-only cooling. Also, they concluded that temperature of the back-side of the module is decreased by 27°C with nanofluid cooling and by 24°C with water-only cooling. In addition to back-side temperature, output voltage is also affected by cooling method. Under maximum performance giving conditions, open circuit output voltage of PV panel is given as 20.35V for nanofluid cooling, 19.63V for water-only cooling and 17.64V for no-cooling. This temperature drop and high Output voltage is due to the fact that thermal conductivity of nanofluids are higher than water. All in all, although water is a good agent for cooling, nanofluid addition makes base material(water) to better cooling agent.

Microchannel Cooling

Microchannel cooling is another way of cooling to improve the performance of PV module. Microchannels are heat sinks loosely defined by their channel dimensions: typically 10-200 μm but upto 1-3 mm in some cases [47]. There are two types of microchannel cooling: Single-phase and two phase. In single phase method, cooling has single type state of coolant. In two phase method, cooling strategy can involve phase change, such as evaporation or no phase change, bi-phase coolant. As a structural categorisation, there are two ways to place microchannel cooling: single layered and manifold. Basic microchannels consist of series linear channels. The first time such a design proposed in literature is by Tuckerman and Pease. Linear channels have two structural problems: long flow path causing pressure drops and linear flow path causing temperature non-uniformity. Various cross-sectional channel shapes are utilized in microchannels. The most convenient rectangular shape is utilized in designs. However, due to lower performance of square shape, more complex shapes are utilized in designs. Converging channels, channels with stepped increase in pitch are utilized in designs to improve microchannel performance. On the other hand, a new way of microchannel is introduced to solve the problems inhereted by single-layered microchannel. Although many researchers studied microchannel cooling, saying an exact efficiency value is not possible. Water, nanofluid or other cooling agents are circulated through microchannels. Therefore, electrical efficiency also depends on the circulant fluid.

1.3.2 Passive Cooling Methods

Passive cooling methods are used in photovoltaic power generation systems in common because there is no need to utilize external power to drive cooling system. Cooling process is done naturally, e.g. natural ventilation or structurally, e.g. fins. It is possible to increase electrical efficiency when there is a successful design. There are five passive cooling methods: Heatsink/fin Cooling, Immersion Liquid Cooling, PCM Cooling, Heat Pipe Cooling and Radiative Cooling.

Heatsink/fin Cooling

Heatsink. aka fin, cooling method is a passive cooling method to improve PV module performance. In this method, no extra power is utilized to cool down the PV module, which brings that heatsink usage is simple and common in PV module cooling. In heatsink method, fins are utilized to improve cooling performance of the system. In heatsink cooling method, various number, thickness, length of fins are utilized. Also, the material utilized in heatsink changes the cooling performance of system. Generally, aluminium and copper are utilized as heatsink material due to higher thermal conductivity. Z. Arifin et. al. studied effect of heatsink properties on Solar cell cooling systems. They conducted their research on various number fins, two types of heatsink material, various depth of fins. They concluded that as the number of fins increases cooling performance of the system increases. Regarding heatsink material, copper shows best performance in cooling due to higher thermal conductivity. They resulted that temperature decrease of 10.2 and efficiency increase of 2.74% are seen at heatsink cooling [48]. In addition, hybrid cooling systems can be used to improve cooling performance of Heatsink method. E. K. A. Fatoni et al., studied hybrid fan-Heatsink cooling system to obtain best cooling performance. Their results showed that maximum temperature drop is about 20 and maximum efficiency can hit to 28.65% [49]. All in all, adding a heatsink aparatus, simple but robust cooling performance can be obtained.

Immersion Liquid Cooling

Immersion liquid cooling is an attractive cooling method which does not consume power for cooling. There are many types of liquid immersion techniques as the immersion medium varies and immersion liquid varies. PV modules can be immersed into lakes, rivers, seas, pools and oceans. Immersion into natural water resources is a beneficial way of cooling because this way both cools down the operating temperature of photovoltaic panel and avoids excess evaporation of water by covering the water surface. By considering immersion liquid, silicon oil, dielectric water, glycerin, acetone, deionized water can be a candidate for cooling. In immersion liquid selection, refractive index of the liquid is rather important. This value should be optimum to be fitted to concentrate on the module. Immersion liquid cooling technique is studied by many researchers because it is simple but interesting.M. Rosa-Clot and his friends are such researchers. In their study, they analyzed three types of PV modules: panel-1 exposed to air, panel-2 submerged under 4 cm of water, panel-3 submerged under 40 cm of water. They filled pool with water and made a spectral analysis for various depths. Also, they calculated temperature and output power of PV panels at different depths. They concluded that although 40cm depth gives best thermal performance compared to 4cm depth and exposed to air cases, it gives the worst output power due to lowest solar irradiance. The case gives best output power is PV submedged into 4cm depth [50]. On the other hand, Nikhil and Premalatha studied how submerged depth affects the overall efficiency. They studied with only silicon oil. They conducted experiments for different depths and fitted them. They obtained a mathematical expression which says the maximum output power for silicon oil submersion depth [51]. All in all, immersion liquid technique is simple but effective way to boost the performance of solar modules.

PCM Cooling

PCM cooling is another passive way to improve efficiency of photovoltaic modules. All techniques introduced upto now are based only on transfering the excess heat. Excess heat is not stored or re-used somehow. However, PCM cooling method is based on solid-liquid phase transition. Thanks to heat storing ability of PCM materials, excess heat can be used and overall efficiency can be increased. Stored heating can be used for room heating, water heating or even electricity generation [46]. Because of this, phase change materials function like a rechargable thermal battery. PCM materials are categorized under three groups: Organic PCM, Inorganic PCM and Eutectic PCM. Organic PCMs are paraffin and non-paraffin materials. Inorganic PCMs are salt hydrate and metalic materials. Eutectic PCMs are inorganic-inorganic, organic-organic and inorganic-organic. PCM materials can store about 33% more heat compared water-photovoltaic-thermal systems [52]. Theoretically, PCM acts as a heatsink. extraction of excess heat is rather important because for every 1°C rise in cell temperature for crystalline silicon, efficiency of solar cell drops with a value of 0.45% [53]. As an advantage of PCM cooling over water cooling and air cooling, it can be applied to anywhere in world. For example, photovoltaic panels in deserts are over-heated. To cool down the PV modules in desert, water cooling is not good candidate to do this. Water in desert is scarce and there is risk of evaporation. Air cooling is also possible choice to cool down. However, maintainance is a big issue for air cooling systems. On the other hand, PCM materials are good choice to lower operating temperature of PV modules. They are just like install-and-forget systems. The most important point at PCM cooling is melting point. Melting point should be close to ambient temperature. Hot-climate regions require higher melting temperature whereas cold-climate regions require lower melting temperature. Paraffin waxes have tunable melting point due to varying chain lengths of their constituent hydrocarbons [54]. M. J. Huang et al., researched on PCM materials in their studies. They obtained that efficiency of PV/PCM system improved by 7.5% at peak solar hours and temperature difference was 17°C between aluminium flat plate and aluminium box containing PCM [1]. All in all, PCM cooling is a good way due to long-lifespan and cost-effective usage.

Heat Pipe Cooling

Heat Pipe cooling is another passive cooling method to increase solar cell performance. Heat pipe cooling philosophy is based on two principles: Thermal conductivity and phase transition. Heat pipe cooling system includes two major components: Heat pipe and glass evacuated tube. Structurally, heat pipes are made up of envelop material, working fluid and wick material. For -20 to 100, two potential heat pipe wick and wall materials are copper and alumium. A typical heat pipe consists of three main parts: Evaporated section, adiabatic section and condensed section. It these section following operations occur respectively: Evaporation, adiabatic transfer and condensation. Heat firstly passes through evaporated section and provides enough thermal energy for evaporation of working liquid. Next, fluid moves towards adiabatic section where adiabatic transfer happens. After that, fluid arrives to condenser section where vapor turns into liquid by losing its thermal energy. Finally, liquid returns to evaporator section via capillary wick structure and cycle continues. Interestingly, due to the fact that the completely natural movement of working fluid eliminates the necessity of mechanical devices, there is no need to drive a pump to circulate working fluid. In order to increase heat transfer contact area, array of fins are introduced in condenser section of heat pipe. Brahim et al., analzed and investigated the effect of fins on overall efficiency. They resulted that overall efficiency of solar cell increased until number of fins hit to 25. While addition of 5 fins brings 4.73% efficincy improvement, from 10 to 30 brought efficieny is 3.91%. Observations show that usage of lower number of fins is more advantageous [55]. On the other hand, some materials are added to increase thermal performance of working fluid. For example, nanofluids are added to increase thermal conductivity of working fluid. Naphon et al., utilized titanium in their studies and found that heat pipe with 0.10% nanoparticles volume concentration, the thermal efficiency is 10.60% higher than that with the based working fluid [56]. All in all, heat pipe cooling is preferable due to lack of extra power consumption though considerable efficiency increase.

Radiative Cooling

Radiative cooling is another interesting but strong state-of-the-art method to enhance photovoltaic module performance. The underlying phenomena in which radiative cooling based on is the reflection of excess photon energy to atmosphere. Practically, absorbed sunlight is not converted to electricity. Unused part is converted into heat. This heat reduces the efficiency, reliability and lifespan of solar module. This heat is released into space from cooling layer. Cooling layer is chosen so that such a layer does not degrade the optical performance of solar cell. but does generate significant thermal radiation resulting in solar cell cooling by radiatively emitting heat to outer space [57]. There are two types of radiative cooling: below-ambient cooling aims for low steady-state temperatures, ideally to use a cooler with unity emissivity in the transparency window and zero elsewhere. On the other hand, above-ambient cooling aims to absorb no power within the solar spectrum and emit as a blackbody at longer wavelengths [58]. Both types provide emission in atmospheric window, 8-13μm wavelength. Both types absorb solar spectrum, 0-2.5μm wavelength. While above-ambient cooling emits whole spectrum after solar spectrum, under-ambient cooling emits at only atmospheric window. Beacause of this, above-ambient cooling provides maximum cooling power, Many researchers are in rush to design a successful cooling layer. Zhu et al., designed a cooling layer for solar cells. Their cooling layer is nothing but silica pyramid blocks with height of 20μm [57]. They claimed that their simple but robust cooling layer solution reduces the operating temperature by 18.3 °C. Corresponding efficiency increase can be calculated with relation given in [53]. Study of Zhu and his friends are only simulation based work. On the other hand, Wang et al., continued the study of Zhu et al. with fabrication. They built solar cells with pyramid-textured PDMS films [1]. They measured the temperature reduction with PDMS films as 2°C. Alhough it seems low, their study analyzed the model deeply and explained the manufacturing process in detail. All in all, radiative cooling is a strong method including structural modifications on solar cell to enhance the electrical performance, reliability and lifespan of solar cell.

1.4 Building Blocks of Photovoltaic Systems

Photovoltaic systems are designed and installed to power household equipments. Average power consumption of a house reaches the power on the order of kilowatts. Required voltage to power such equipments is 110V/220V. Same thing happens for satellite solar power systems. Satellites are powered only from solar cells installed on it. By considering communication systems, actuators and motors inside the satellite, how much power required for satellite is easy to guess.

Photovoltaic systems are just like complex systems formed of buildings. Each building is formed of flats. Smallest element in the complex system is flat. Just like complex system analogy, Photovoltaic systems are nothing but photovoltaic arrays. Each array is formed of photovoltaic modules. Each module is made up of photovoltaic cells. Underlying idea to combine these building block is to obtain higher power and higher voltage. The relationship between building blocks of photovoltaic elements are illustrated as below.

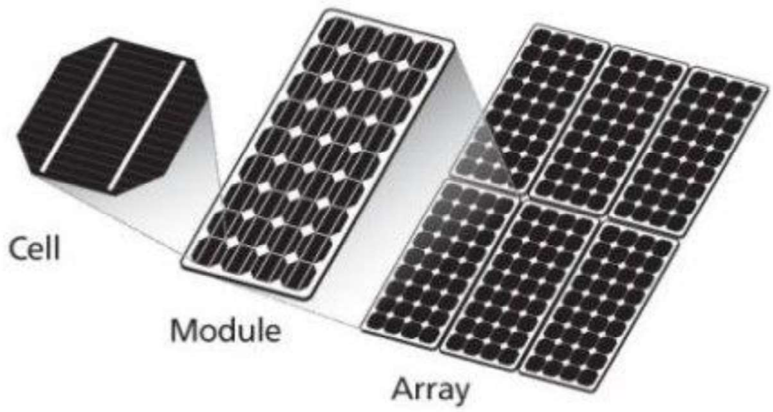

Figure 1.22 Building blocks of photovoltaic systems [59]

PV Cell

The PV cells are the smallest building block of photovoltaic systems. They are specially designed pn junction or Schottky barrier device [60]. Based on the fabrication process, there are two types of PV cells: Monocrystalline PV cell and polycrystalline PV cell. These are illustrated as below.

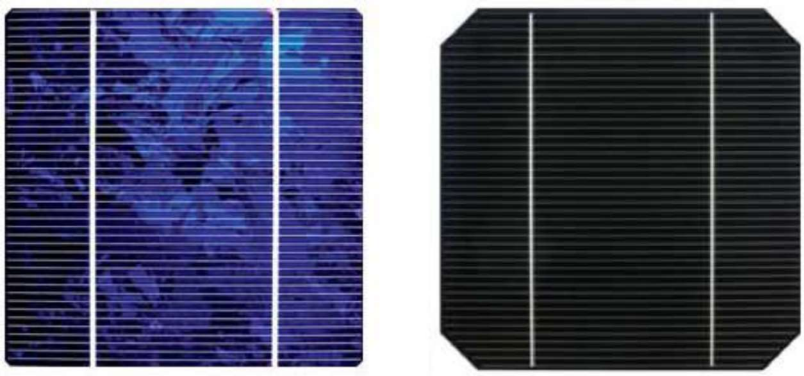

Figure 1.23 polycrystalline PV cell (left) vs. monocrystalline PV cell (Right) [61]

Output voltage of the PV cell is about 0.6-0.8V. It is rather meaningful value by considering a PN-Junction diode. The single solar cell can deliver about 2-3W power. By considering power expectations of a house, there are many solar cells required and to be connected somehow to deliver enough power and voltage.

Current-voltage relationship of a single solar cell can be obtained from simple diode current equation. All characteristics of a photovoltaic system are valid for a PV cell.

PV Module

In order to deliver enough voltage and enough current, PV cells are connected in series and parallel, respectively. Single PV module can deliver 12-18V power. This means, about 30 cell should be connected in series to deliver module voltage. On the order hand, a general photovoltaic module can deliver 100W power, which means more than 30 modules should be connected both in series and paralel to deliver enough voltage and current, respectively. Altough it is stated that general voltage and power ratings for a PV module is 12V and 100W, custom designs can be made and necessary series and parallel combinations are done according to desired module ratings. All characteristics of a photovoltaic system are valid for a PV cell.

PV Array

In order to deliver power more than a module, PV modules are connected somehow. Rooftop photovoltaic systems and solar fields are good examples for PV arrays. There are other methods to increase delivered power for PV arrays. Solar concentration and solar cell cooling methods are one of these. If high current is desired to drive a load, e.g. to drive a loaded-motor, PV modules are connected in parallel. If high voltage is desired to drive a load, e.g. to power residential area, PV modules are connected in series. Generally, PV arrays are connected to grid and utilized to supply enough power to grid. Although PV arrays deliver DC-Voltage, utility grids are based on AC-Voltage. Therefore, some sophisticated DC-to-AC converters are utilized to connect PV Arrays to utility grids.

1.5 Figure of Merits for Photovoltaics

Photovoltaics are semiconductor devices to convert optical energy to electrical energy. There are many main parameters to define this conversion performance. Photovoltaic cell efficiency, open circuit voltage, short circuit current, fill factor and MPPT are those parameters.

Photovoltaic Cell Efficiency

Efficiency is the parameter to show how good the conversion process is. Efficiency of a photovoltaic cell is defined as the ratio of incoming incident light power to converted electricity power. Many researchers, scientists and engineers are in rush to obtain as high efficiency as possible. According to Shockley-Queisser limit, maximum solar conversion efficiency is around 33.7% for a single pn-junction photovoltaic cell. This limit comes from sunlight spectrum and energy band gap of silicon. In literature, there are ways to push this limit: multi-junction structure and solar concentration are the ways to break this limit. Upper limit for multi-junction cell with infinite number of layer is 68.7% [62] and upper limit for concentrated multi-junction cell is 86.8% [63]. There are two authorities in world to measure efficiency of solar cells and give a golden standard to efficiency measurement: NREL and Fraunhofer Institute. Annually, NREL and Fraunhofer Institute scientists announce the maximum efficiency for solar cells [64]. Efficiency is rather important performance parameter for investors to obtain higher power from photovoltaics. The most important limiting factor for photovoltaics is module temperature. Module temperature degrades performance of photovoltaics severely. Efficiency is one of the merits showing performance of photovoltaics. There are many expressions showing temperature effect on efficiency in literature [53]. The most well known and used expression for temperature vs efficiency relation is Evan's Formula and it is given below [65].

$$\eta_c = \eta_{Tref} \left[1 - \beta_{ref}(T_c - T_{ref})\right]$$

In this expression, η_{Tref} and β_{ref} are given by manufacturer of photovoltaic module. If it is not stated in datasheet of the module, it can be obtained from flash tests at two temperatures [53]. Temperature coefficient, β_{ref}, is defined as below. In the expression below, T_{ref} is reference temperature and T_0 is the high temperature at which efficiency of photovoltaic drops to zero. For crystalline photovoltaics, this temperature is 270 °C [66].

$$\beta_{ref} = \frac{1}{T_{ref} - T_0}$$

Open Circuit Voltage (V_{oc})

Open Circuit Voltage is a main parameter determining electrical performance of photovoltaics. The maximum terminal voltage can be obtained when there is no load and zero current case. Open circuit voltage is based on light-generated current due to forward bias. Open circuit voltage varies with irradiance and temperature. As irradiance increases open circuit voltage increases. On the other hand, if temperature increases open circuit voltage decreases. Open circuit voltage can be increased by connecting solar cells in series. Graphically, determination of open circuit voltage is given below. Formula for open circuit voltage and temperature dependence of open circuit voltage are given below.

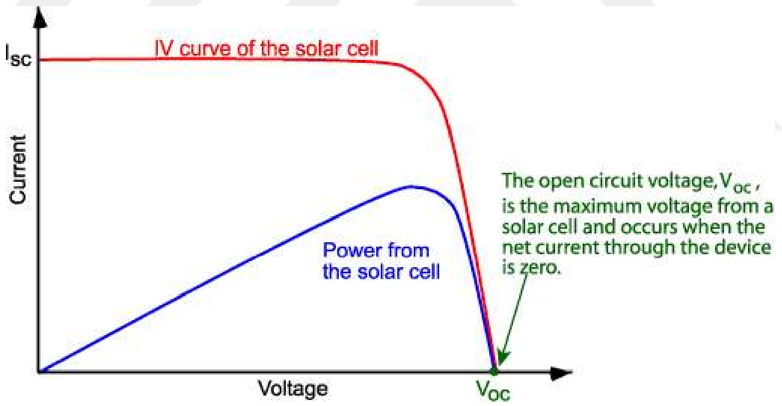

Figure 1.24 Determination of open circuit voltage from I-V and power curve [67]

$$V_{oc} = \frac{kT}{q} \ln\left(\frac{I_{sc}}{I_o} + 1\right)$$

$$\frac{dV_{oc}}{dT} = \frac{V_{oc}}{T} + V_{th}\left(\frac{1}{I_{sc}}\frac{dI_{sc}}{dT} - \frac{1}{I_o}\frac{dI_o}{dT}\right) \; where \; V_{th} = \frac{kT}{q}$$

Short Circuit Current (I_{sc})

Short Circuit current is another main parameter to evaluate photovoltaics electrically. Short circuit current depends on incident photon fluxes which depends on solar spectrum. It is limited by reflection losses, ohmic losses, shadowing losses and recombination losses. On the other hand, photovoltaic cell area determines short circuit current. The wider solar cell area, the more current. Short circuit current varies with irradiance. As irradiance is increased, short circuit current is increased, too. On the other hand, there is not that much increase of it for increased temperature. If temperature is increased, short circuit current is slightly increased. Experimental studies validate this fact. However, some researchers assume that temperature does not affect short circuit current. Short circuit current can be increased by connecting solar cells in parallel. Graphically, determination of short circuit voltage is given below.

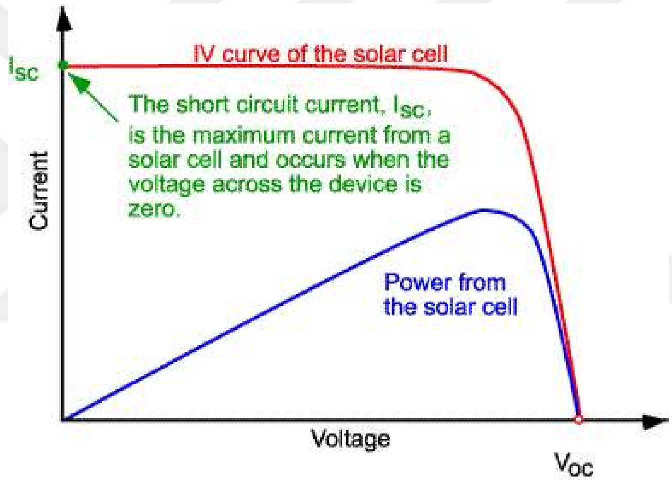

Figure 1.25 Determination of Short Circuit Current from I-V and Power Curve [68]

Fill Factor (FF)

Fill factor is another parameter which gives the photovoltaic performance. It expresses output efficiency of the system. Fill factor is defined as the ratio of multiplication of maximum power point voltage and maximum power point current to multiplication of open circuit voltage and short circuit current. In general, rule of thumb for fill factor is assumed to be over 60% for acceptable photovoltaic system. Fill factor below 60% are considered to be insufficient [69]. Although fill factor(FF) is known as a performance parameter, there are other factors affecting FF: series resistance of solar cell, parallel and shunt resistance of solar cell, recombination current in the space charge region and reverse saturation current [70]. The higher FF, the better performance. If FF is low, then affecting factors are visited to improve FF. To determine FF visiually, FF is depicted as below. FF is the ratio of A over B. An expression having excellent accuracy is proposed by Green [71] and it is given below.

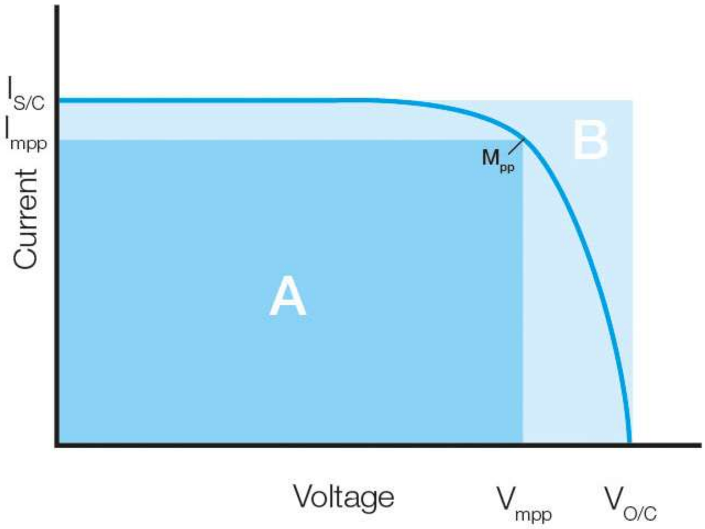

Figure 1.26 Depiction of Fill Factor

$$FF = \frac{v_{oc} - \ln(v_{oc} + 0.72)}{v_{oc} + 1} \quad where\ v_{oc} = V_{oc}/V_t$$

Maximum Power Point Tracking

Photovoltaic systems are installed to power loads. However, when power curve of photovoltaics are considered, it is seen that it is not possible to obtain same amount of power for every current and voltage. The voltage and current where the maximum amount of power obtained is named as maximum power point. Due to nonlinear behaviour of photovoltaic devices, MPPT is one of the hot research topic nowadays. From 2000, there is a increase in the number of articles about MPPT algorithms [72]. MPPs for different irradiance levels are depicted as below. It can be seen below that as irradiance increases, power obtained increases. As a result of this, maximum power point increases, too.

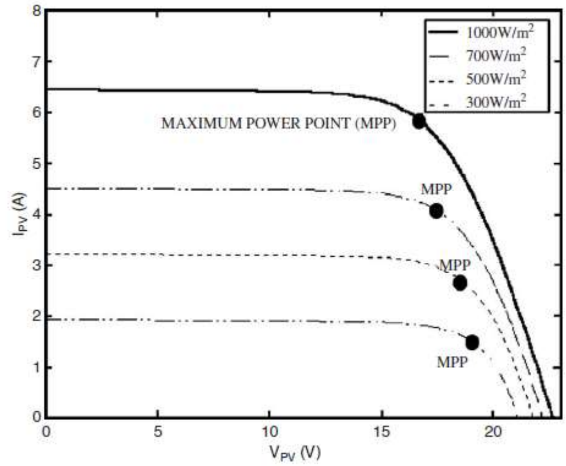

Figure 1.27 Maximum Power Points for Different Irradiance Levels [73]

It can be seen below that when solar cell is illuminated it provides power, 1st quadrant. When it is not illuminated, dark case scenario, diode behaves like a diode. Behaviour of curvature and breakdown voltages are similiar to diode characteristics.

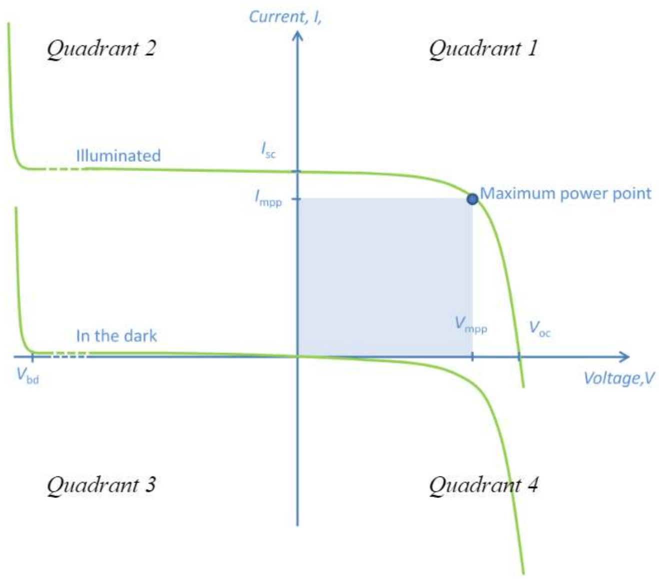

Figure 1.28 Current-Voltage Characteristics of Solar cell in different Illumination Scenarios [74]

1.6 Modelling of Photovoltaics

1.6.1 Equivalent Circuit Models

Photovoltaics are semiconductor devices which provides electrical power to load. Modelling is essential to analyze the produced electrical output. Photovoltaic modeling provides the analyze the characteristics of photovoltaics. Modelling is essential for power system applications and maximum power tracking applications [75].

Photovoltaic modelling is essential to analyze performance of photovoltaics. It provides analysis of characteristics of solar cells. Equivalent circuit modelling is a way to model photovoltaics electrically. Equivalent circuit models can predict voltage and current output for photovoltaics. It is used for circuit simulators, MPPT applications, power system applications and solar cell analysis. Representation is done by utiling lumped circuit elements, those are current source, diode and resistor. Environment-dependent characteristics of photovoltaics are modelled by utilizing temperature and irradiance dependent circuit components. Equivalent circuit models are able to predict the electrical output at all points along the I-V curve and the P-V curve. Modelling allows to perform joint simulation of solar devices with power electronics by creating interfaces. In literature, there are many equivalent circuit models to represent photovoltaics ranging from the simplest one to the most complex one. While the simplest model is composed of a current source and a temperature-dependent diode, the most complex one is formed of multiple diodes as well as series and shunt resistors. The simplest model is ideal equivalent circuit model**.** It is depicted as below. Current source represents photo-generated current, diode represents thermal losses. As temperature increases, some part of the generated current passes through the temperature-dependent diode which reduces output power. Although it work very well with ideal photovoltaics, it fails to represent realistic photovoltaics. In practice, a shunt resistor is used to represent current leakage due to nonlinearity of the semiconductor. On the other hand, metalic connections and resistance of the semiconductor material are represented by a series resistance. To advance the realistic representation model of the equivalent circuit, other methods are proposed. Four-parameter model is one of them. Although it is originated from single diode model, it includes a series resistance. Series resistance is added to the model in order to represent the contact losses between semiconductor and metals, semiconductor material losses, metalic losses, cell and busbar losses. Increase in series resistance decreases the output voltage. Four parameter model is named as simplified single diode model (SSDM) and depicted as below. In SSDM model, there are four unknown parameters to be solved: Photogenerated current (I_{ph}), diode saturation current (I_o), diode ideality factor (A) and series resistance (R_s). To solve these unknown parameters, four independent equations are required. Generally, the derivative of power with respect to voltage, temperature coefficient and voltage coefficient are used as the fourth equation. Four parameter model gives a reasonably good accuracy whose accuracy is similiar to two diode model but still it is inadequate to fit experimental I-V curve [76]. Also, performance of 4-parameter model is not good for temperature variations at high temperatures. To improve the performance of SSDM, shunt resistance is added to the model to represent manufacturing defects**.** When this resistance is added, representation performance of the model is improved especially at lower sunlight intensities. Decrease in shunt resistance leads to drop in output current. The effect of shunt resistance is seen in case of low light levels because less photo-generated currents are produced at low sunlight intensities. Resultant shunt resistor-added model is named as 5-parameter model. This model is named as Single Diode Model (SDM). Circuitry of SDM is given as below. There are five unknown parameters to be solved: Photogenerated current (I_{ph}), diode saturation current (I_o), diode ideality factor (A), series resistance (R_s) and shunt resistance (R_{shunt}). There should be five independent equations. Five parameter model works well under low temperature fluctuating conditions but it does not perform well for amorphous and thin-film technologies as well as medium and high temperature variations. The standard five-parameter model is capable to predict performance of monocrystalline and polycrystalline modules within %6 [77]. To improve the performance of 5-parameter model further, an extra diode is added to the model to represent recombination losses. Resultant model is named as double diode model (DDM). DDM model is depicted as below. There are seven unknown parameters to be solved: Photogenerated current (I_{ph}), first diode saturation current ($I_{o,1}$), first diode ideality factor (A_1), second diode saturation current ($I_{o,2}$), second diode ideality factor (A_2), series resistance (R_s) and shunt resistance (R_{shunt}). There should be seven independent equations. This model is proposed by Ishaque et al. [78]. DDM model performs well for medium and high temperature variations. Additional dependence intrduced by seven-parameter model has less than a %1 RMS error to represent performance of power predictions for amorphous technology [77].

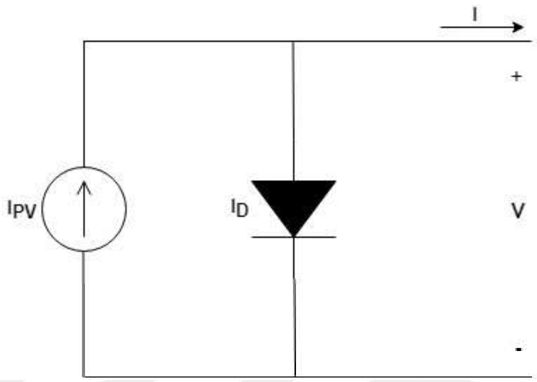

Figure 1.29 Ideal model of photovoltaics

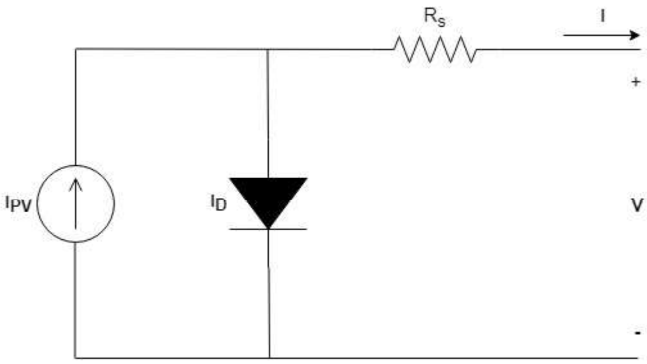

Figure 1.30 Simplified single diode model

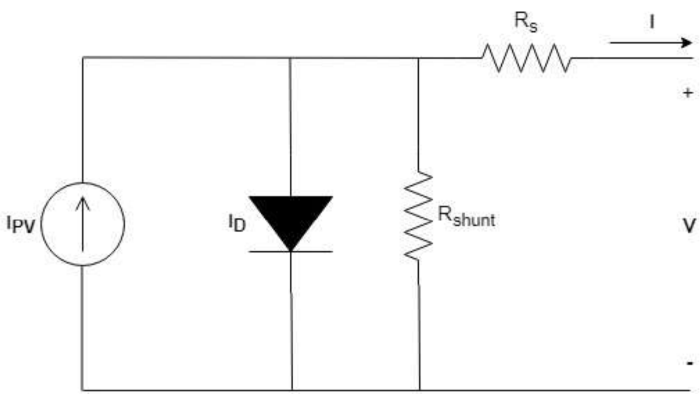

Figure 1.31 Five-parameter model

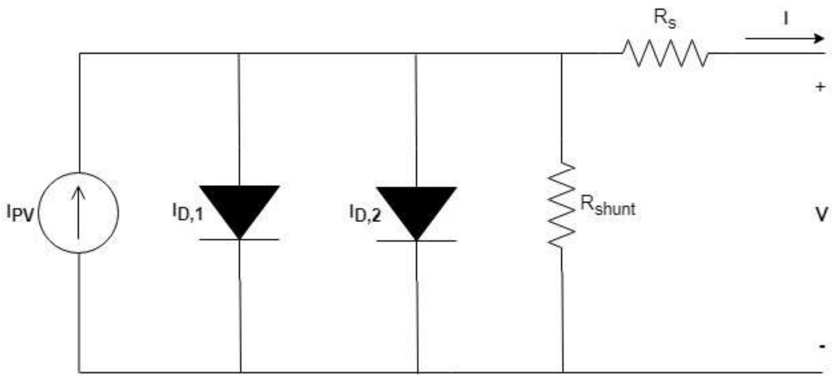

Figure 1.32 Seven-parameter model

Although there are many models proposed to represent the electrical performance of photovoltaics, the most used and well known model is 5-parameter model, SDM model. It is preferred because of efficiency and simplicity. Current-voltage equation for SDM model is given as below.

$$I = I_{pv} - I_s\left(\exp\left(\frac{q(V+IR_s)}{A.K.T}\right) - 1\right) - \left(\frac{V+IR_s}{R_{shunt}}\right)$$

Photogenerated current is given as follows:

$$I_{pv} = \left(\frac{G}{G_{STC}}\right)[I_{pv\ at\ STC} + K_i(T - T_{STC})]$$

Diode saturation current is given as follows:

$$I_o = I_{o\ at\ STC}\left(\frac{T}{T_{STC}}\right)^3 \exp\left[\left(\frac{q \cdot E_g}{A \cdot K}\right)\left(\frac{1}{T_{STC}} - \frac{1}{T}\right)\right]$$

By considering Energy Band gap, Varshni equation gives the exact definition for energy band gap. $E_g(t)$ energy band gap depending on temperature is given as follows:

$$E_g(t) = E_g(0) - \frac{\alpha T^2}{\beta + T}$$

For α and β coefficients, in case of crystalline silicon, $E_g(0)$ = 1.1557 eV, $\alpha = 7.021 \cdot 10^{-4}\ evK^{-1}$ and $\beta = 1108K$ [79].

Output current vs output voltage relation is depicted as below. I-V characteristic of photovoltaic is superposition of current source and diode characteristics. By considering ideal model of photovoltaics, resultant characteristic is based on this model. Additional components modifies shape of I-V characteristic but fundamental characteristic is based on ideal model of photovoltaics.

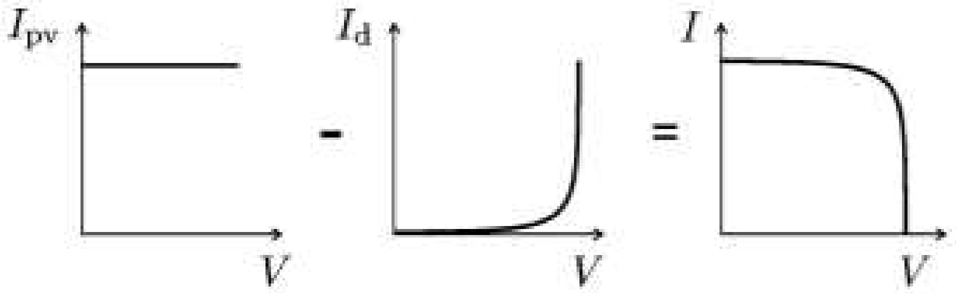

Figure 1.33 Superposition of current source and diode characteristics [80]

To obtain five unknown independent parameters, $\mathbf{I_{ph}}$,I_o, A, R_s and R_{shunt}, there should be five independent equations to be solved. Three of five equations depend on short-circuit, open-circuit and maximum power cases for KVL equations around output of photovoltaics. Five independent equations giving five independent parameters are given as below [81].

The first equation comes from short-circuit case (I =I_{sc} and V=0):

$$I_{sc} = I_{pv} - I_s\left(\exp\left(\frac{q(I_{sc}R_s)}{A.k.T}\right) - 1\right) - \left(\frac{I_{sc}R_s}{R_{shunt}}\right)$$

The second equation comes from open-circuit case (V =V_{oc} and I=0):

$$0 = I_{pv} - \ I_s \left(\exp\left(\frac{q(V_{oc})}{A.k.T}\right) - 1\right) - \left(\frac{V_{oc}}{R_{shunt}}\right)$$

The third equation comes from maximum power case (I =I_{mp} and V =V_{mp}):

$$I_{mp} = I_{pv} - \ I_s \left(\exp\left(\frac{q\left(V_{mp} + I_{mp}R_s\right)}{A.k.T}\right) - 1\right) - \left(\frac{V_{mp} + I_{mp}R_s}{R_{shunt}}\right)$$

The fourth equation comes from the assumption that derivative of power versus voltage at the MPP is null:

$$I_{mp} - \ I_s \left(\exp\left(\frac{q\left(V_{mp} + I_{mp}R_s\right)}{A.k.T}\right)\left(\frac{q\left(V_{mp} - I_{mp}R_s\right)}{A \cdot k \cdot T}\right)\right) - \left(\frac{V_{mp} - I_{mp}R_s}{R_{shunt}}\right) = 0$$

The fifth equation comes by eliminating shunt resistance, reformulating four independent equations and using the approximation $I_{pv} \gg I_s \left(\exp\left(\frac{q(I_{sc}R_s)}{A.k.T}\right)\right)$ [82] :

$$\frac{AkT}{q}\left(\frac{I_{sc}}{I_{sc} - I_{mp}} + \ln\left(\frac{I_{sc} - I_{mp}}{I_{sc}}\right)\right) - 2V_{mp} + \ V_{oc} = 0$$

By using independent equations, exact expressions of five parameters are given as below [83]:

$$I_s \ = \frac{I_{ph} - \left(\frac{V_{oc}}{R_{sh}}\right)}{e^{\frac{V_{oc}}{A}} - 1}$$

$$A = \ \delta V_{oc}$$

$$R_{sh} = \frac{V_{mp} + \ I_{mp}R_s - A}{I_{ph} + \ I_s - I_{mp} - \frac{A}{\frac{V_{mp}}{I_{mp}} - R_s}}$$

$$R_s = \frac{A\ln\left(\frac{I_{sc} + I_s - \frac{V_{mp}}{R_{sh}} - I_{mp}}{I_s}\right) - V_{mp}}{I_{mp}}$$

$$I_{ph} = I_{sc} + I_s\left(e^{\frac{I_{sc}R_s}{A}} - 1\right) + \frac{I_{sc}R_s}{R_{sh}}$$

Effect of photogenerated current, series resistance and parallel resistance on current-voltage characteristic of photovoltaics is given below.

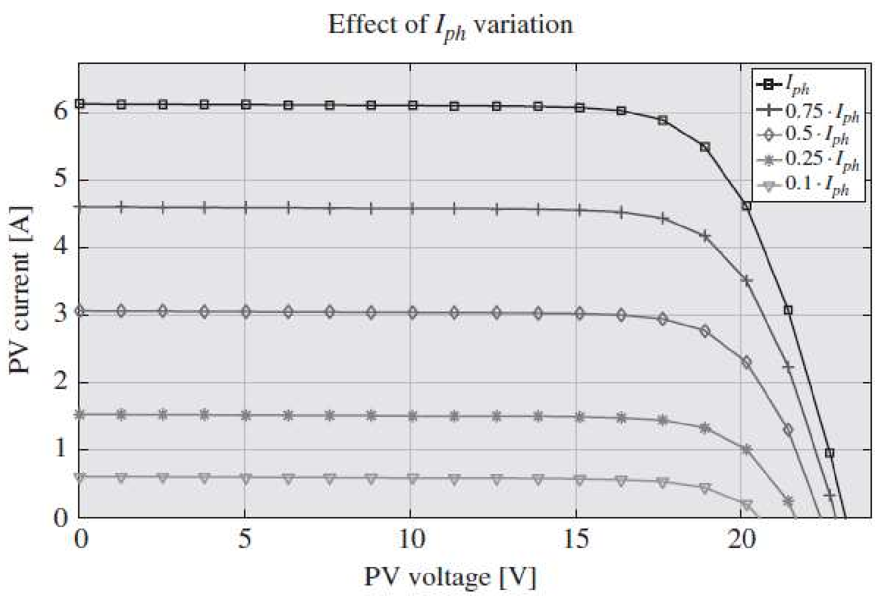

Figure 1.34 Effect of photogenerated current on I-V characteristic of photovoltaics [84]

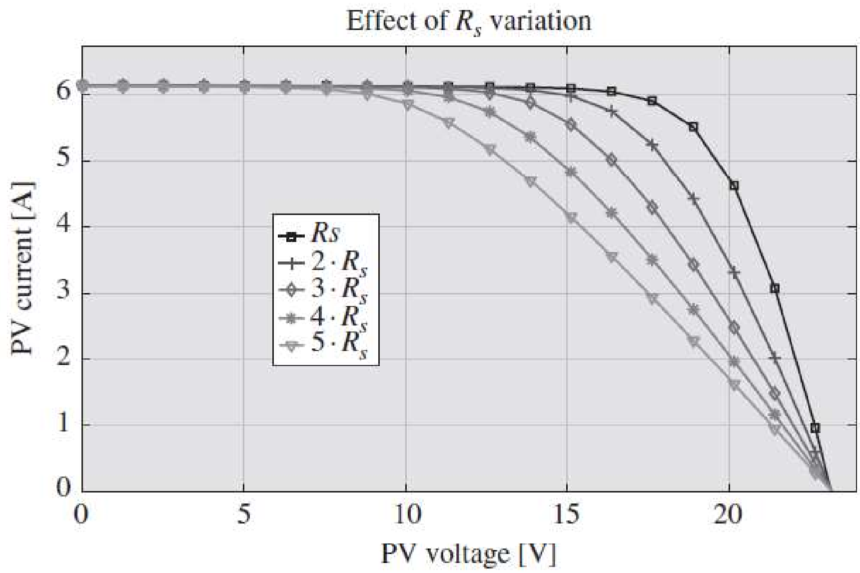

Figure 1.35 Series resistance effect on I-V characteristic of photovoltaics [84]

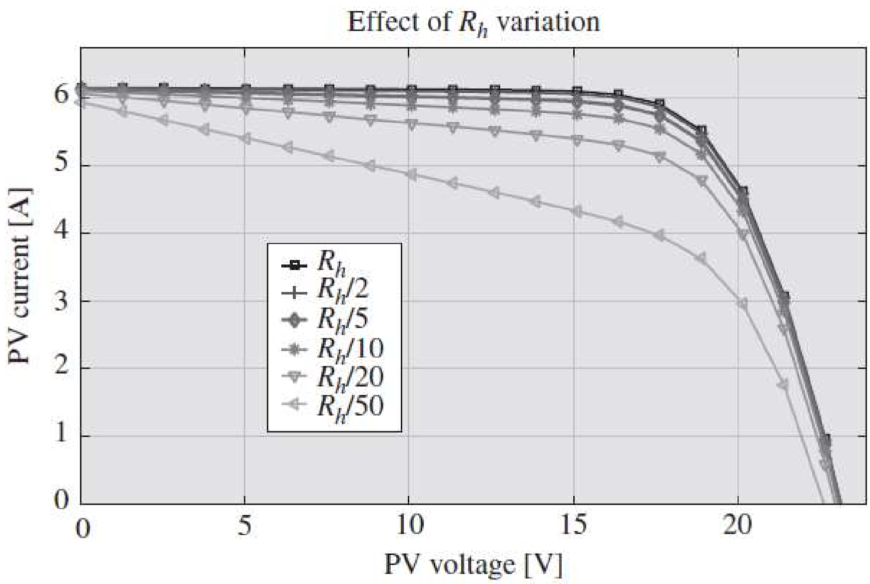

Figure 1.36 Parallel resistance on I-V characteristic of photovoltaics [84]

As it can be seen from above figures, photogenerated current increases electrical performance of photovoltaics. Generated power in photovoltaics are directly related to photogenerated currents. For series and parallel resistances, they degrade electrical performance of photovoltaics. Series resistance decreases maximum power, which also decreases fill factor. Effect of series resistance can be seen with intuition. Series resistance behaves as extra load resulting power reduction. Just like series resistance, parallel resistance also degrades the electrical performance of photovoltaics. It decrases output current resulting to decrease in maximum power, which also reduces the fill factor. Effect of parallel resistance can be seen by intuition that considerable amount of parallel resistance results to loss of output current.

1.6.2 Temperature Effect on Photovoltaic Parameters

There are two basic environmental factors affecting photovoltaics: Irradiance and temperature. In this work, basically temperature effect on photovoltaics are studied. Temperature severely affects the performance of photovoltaics because most of the physical mechanism involved in the photovoltaic conversion process is temperature dependent. In this topic, temperature effect on photovoltaics parameters are studied.

Temperature Effect on Efficiency

Efficiency is an important term showing harvest performance of photovoltaic power generation. Due to semiconductive structure of photovoltaic devices, temperature is an important environmental factor affecting photovoltaic performance. Many researchers observed that efficiency of photovoltaics degrades inevitably. Perraki and Kounavis observed temperature effect on three types of solar cells, mono crystalline silicon, polycrystalline silicon and CIS photovoltaic samples. In their study, they observed that as temperature increases efficiency decreases linearly [85]. Similiar observartions are done by Achouby et al. They observed the performance of a polycrystalline module for many irradiance levels for a certain temperature range. In their study, they observed that efficiency decreases for each irradiance level as temperature increases [86]. To enhance efficiency of photovoltaics at high ambient temperatures, active and passive cooling methods are introduced to compansate losses due to module temperature rise.

Temperature Effect on Open Circuit Voltage

Thermal sensivity of photovoltaics are rather important concept because 80-90% of temperature coefficient is due to open-circuit voltage deviation. Maximum thermal influence is seen cell temperature. Based on EN60904-5 universal photovoltaic standard, if thermal effect of photvoltaics are desired to observe, variation of output voltage should be measured. Open circuit case is the fact that total rate of photogeneration equals to recombination so that no current circulates the system.

Many studies are conducted to show the effect of temperature on output voltage of photovoltaics and they concluded that temperature rise degrades the open circuit voltage performance. Singh and Ravindra observed the thermal effect on many kind of solar cells and their observations is that open circuit voltage of the tested photovoltaics decreases as temperature increases. Their observations are valid for a long thermal interval [87]. Similiar observations are done by Chander et al. They measured the I-V characteristic of monocrystalline silicon module and they observed that I-V characteristic curve of the photovoltaic shifts towards left, which means reducing the open circuit voltage. In addition, they measured thermal sensitivity of open circuit voltage and it is given below [88]. Also, expression of open circuit voltage deviation for temperature change is given below [87].

$$\frac{1}{V_{oc}}\frac{dV_{oc}}{dT} \approx -(0.0022\ to\ 0.0025)\ per\ {}^{\circ}C$$

$$\frac{dV_{oc}}{dT} = \frac{V_{oc}}{T} + V_{th}\left(\frac{1}{I_{sc}}\frac{dI_{sc}}{dT} - \frac{1}{I_o}\frac{dI_o}{dT}\right)$$

Temperature Effect on Short Circuit Current

Contrary to other figure of merits, temperature rise behaves on short circuit current as additive. Generally, short circuit current increases as temperature increases. This interesting effect is mainly due to the fact that most semiconductor bandgaps decrease with temperature. Short circuit current depends on the number of photons those are capable to create electron-hole pair. Lowering the energy band gap increases the number of photons those are capable to create electron-hole pair resulting increase in short circuit current. However, temperature-energy band gap relation is valid for perovskite semiconductors. In pervoskites, bandgap increases as temperature increases. Many studies are conducted by scientists. In the work performed by Perraki and their friends, they observed that short circuit current characteristics of Mono-C silicon, Poly-C silicon and CIS solar cells for changing temperateraturе. They observed in all solar cells that short circuit current slightly increases as temperature increases [89]. Similiar observations are performed by Chander et al. In their study, it is observed that current-voltage characteristic of a

Mono-C Silicon module and they observed that I-V characteristic of the photovoltaic shifts upward, which means increasing the short-circuit current. In addition, they measured thermal sensivity of short-circuit current and it is given as below [88].

$$\frac{1}{I_{sc}}\frac{dI_{sc}}{dT} \approx 0.002\, per\ ^{\circ}C$$

Temperature Effect on Fill Factor

Fill Factor is related to extractable maximum power from a cell to the product of open-circuit voltage and short-circuit current. It indicates the minimum effort of extracting the photogenerated charges from cell into the load and it corresponds to optimal current/voltage trade-off. This optimum depends on photogeneration-recombination balance but also relates to transport losses at maximum power point. Fill factor is one of the most difficult parameter to measure. Many studies are conducted to show the thermal effect on fill factor. In the study Singh and Ravindra, many types of solar cells are tested for a longe range of temperature. They observed that in all kind of photovoltaics fill factor vanishes as temperature increases. Interestingly, the most dramatic increase in fill factor is seen in Germanium photovoltaics [87]. Similiar observations are done by Chander et al. They have seen that fill factor is reduced as temperature is increased. Also, they measured thermal sensitivity of fill factor and it is given as below [88]. Also, expression of fill factor deviation for temperature variation is given below [87].

$$\frac{1}{FF}\frac{dFF}{dT} \approx -0.0013\, per\ ^{\circ}C$$

$$\frac{dFF}{dT} = \frac{\frac{dV_{oc}}{dT} - \frac{V_{oc}}{T}}{V_{oc} + V_{th}}\{\frac{\frac{V_{oc}}{V_{th}} - 0.28}{\frac{V_{oc}}{V_{th}} + 0.72} - FF\}$$

CHAPTER 2

EXPERIMENTAL PROCEDURE

In the experimental process, a prototype of double-faced photovoltaic system, solar simulator system and dynamic cooling control system are established. The objective of the experiments are to analyze thermal and cooling effects on double-faced photovoltaic system performance, thermal response of dynamic control system and realistic sunlight performance of double-faced photovoltaic system.

In double-faced photovoltaics system, both PV modules are mounted together to be used with any platform. It can be utilized with solar simulator system and solar-tracking system. Both solar cells are identical. It is rather easy to conduct experiments and obtain meaningful experimental data due to symmetrical structure of the PV system. In solar simulator system, double-faced PV system is illuminated with two identical sunlight-like light sources. Heating effect is mimiced by using air blower with heating property. Fan-cooling is performed by utilizing air blower which is identical to heater. Thanks to portable and isolated properties of the solar simulator system, it is possible to conduct PV experiments in any season and at any time of the day. For dynamic control system, there are two temperature sensors giving ambient and solar simulator temperature information. By comparing these two temperature informations, it triggers to cooling mechanism.

In this chapter, firstly equipments used in the experimental procedure are given. Secondly, working principles of experimental systems are given. Later, experimental information about measurement of the systems is given.

2.1 Experimental Materials

In the experiment to observe thermal and cooling effect on double faced photovoltaic system performance, two air blowers, two identical photovoltaic modules, two sunlight-like light sources, digital thermometer, digital multimeter are utilized.

Figure 2.1 Overall solar simulator system

Figure 2.2 Inside view of solar simulator system

Overall and inside views of solar simulator systems are given above. Centered identical light sources illuminate double-faced photovoltaic system as it can be seen in inside view of solar simulator system. Heating effect of sunlight is given via heater at the bottom. Fan cooling effect is given via cooler at the top. Temperature of solar simulator is measured via digital thermometer. Thanks to heater and light sources, thermal and optical effects on photovoltaics are observed independently. To understand the details of the experimental systems, components of the systems are explained in details.

2.1.1 Light Source

As a light source, two identical LED light sources are utilized. They are selected as high-power and easily-replacable light sources. They can be replaced with the one in local store. Size of light source is 95mm x 45mm x 40 mm. By concerning light color, cool daylight color is chosen for light source because it must simulate the spectral properties of sunlight. Cool daylight is the best candidate to simulate sunlight spectrum. Optical properties of the light source are given in the table below. To maximize the incident flux obtained by solar cell, light sources are located as horizontally being parallel with solar cells. Each light source is located at big walls of the solar simulator, those are face to face. By using lid at the top of the solar simulator, it is ensured that inside of solar simulator is illuminated only via light sources. Light sources are good enough to measure performance of photovoltaics. However, they are not powerful like sunlight. They only triggers to flow rather low current, on the order of leakage current but they can generate a potential difference on the photovoltaic. Therefore, it must be considered that by using only light source, it is not possible to obtain reasonable amount of current from photovoltaics but it is possible to obtain satisfactory voltage values. Just by obtaining only voltage value is enough to measure temperature effect on photovoltaic performance. Figure below is for light source.

Table 2.1 Optical characteristic of light source

Illuminance Strength of The Light Source	Power of Light Source
5700lux	$20W/m^2$

Figure 2.3 Identical light sources

2.1.2 Solar Cells

In the solar simulator setup, two identical polycrystalline solar cells are utilized. Double-faced photovoltaic modules are located between two identical light sources. They are so located that they are illuminated equally via each identical light sources. Being a prototype, solar cells are selected as small and compact. The selected photovoltaics ease the usage of double faced photovoltaic modules. Return time of double-faced system are reasonable time.

Efficiency of polycrystalline solar cell is the smallest one among solar cell types. Experimental procedures of the thesis are not an efficiency challenge. Therefore, it is required to prefer low-cost and small modules in order to demonstrate making more profit with double-faced photovoltaics systems.

Figure below demonstrates the two identical solar modules. Each module has 12 lines and 4 columns of solar cells resulting to 48 solar cells. Each cell has 9 fingers.

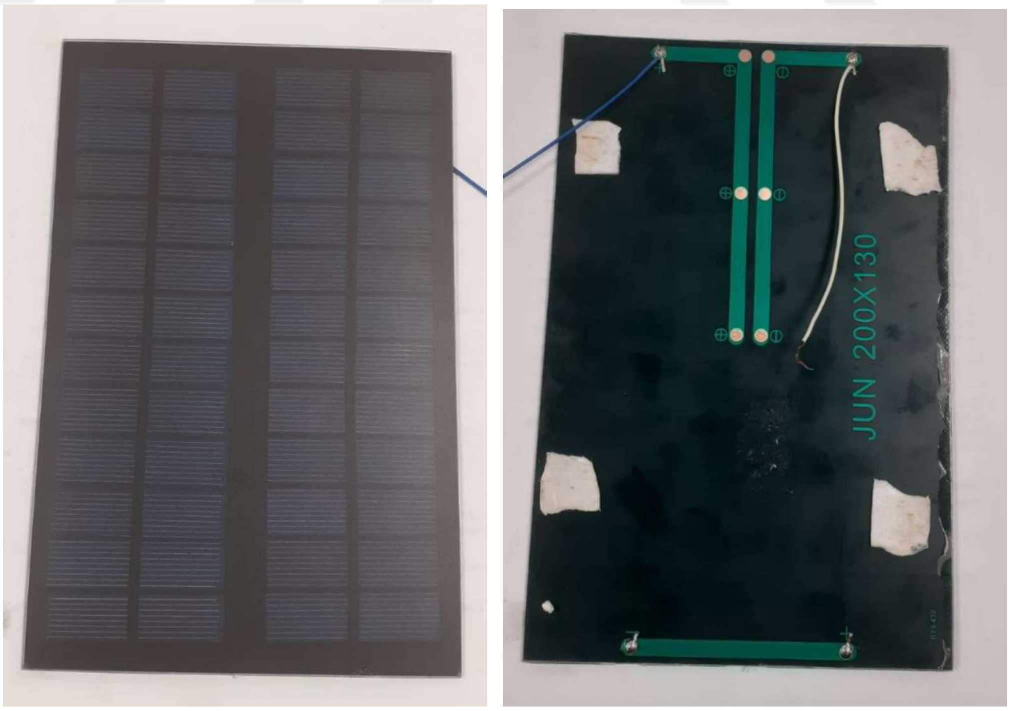

Figure 2.4 Back and front sides of the solar cell

Properties of solar cells are given as [90]:

Manufacturer: JUN

Maximum Power: 6W

Output Voltage: 12V

Maximum Supply Current: 0.5A

Dimensions: 20cm x 13cm

Weight: 73gr

2.1.3 Digital Thermometer

In the solar simulator system, K-type thermo couple digital thermometer is utilized. K-type thermocouple is a formation of Chromel (90% nickel and 10%chromium) and Alumel (95% nickel, 2% manganese, 2% aluminium and 1% silicon) wires and it has a range of -270°C - 1260°C and it has approximate sensitivity of 41 µV/°C. It has output voltage value ranging of -6.4mV to 54.9mV. This long range is one of the advantages over other temperature transducers like thermistors, NTCs or resistance temperature detectors. Thermocouples are electrical devices formed of two dissimiliar electrical conductors creating an electrical junction. At this electrical junction, an electrical voltage is generated thanks to Seebeck Effect. Thermocouple output voltage vs temperature and table of characteristic thermocouples are given below. Also, equivalent circuit of thermocouple is given as below.

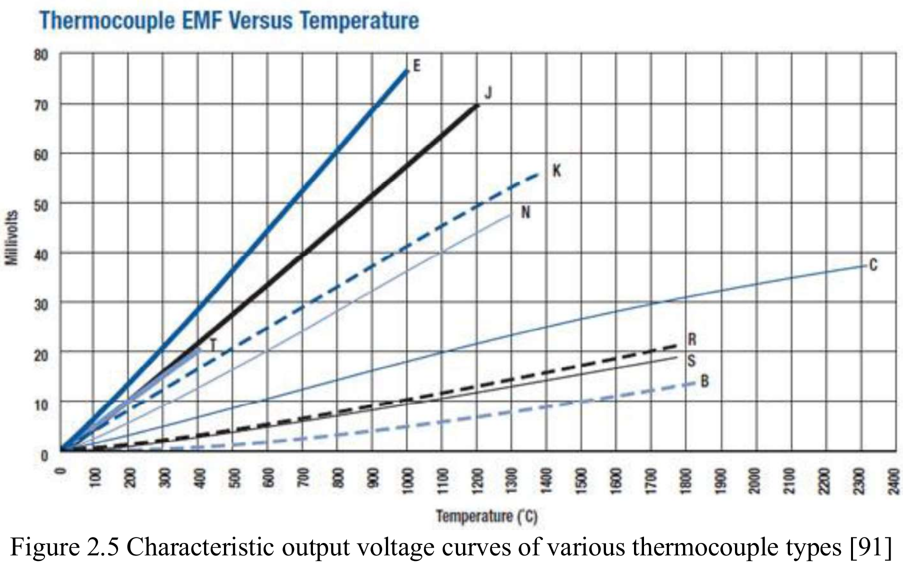

Figure 2.5 Characteristic output voltage curves of various thermocouple types [91]

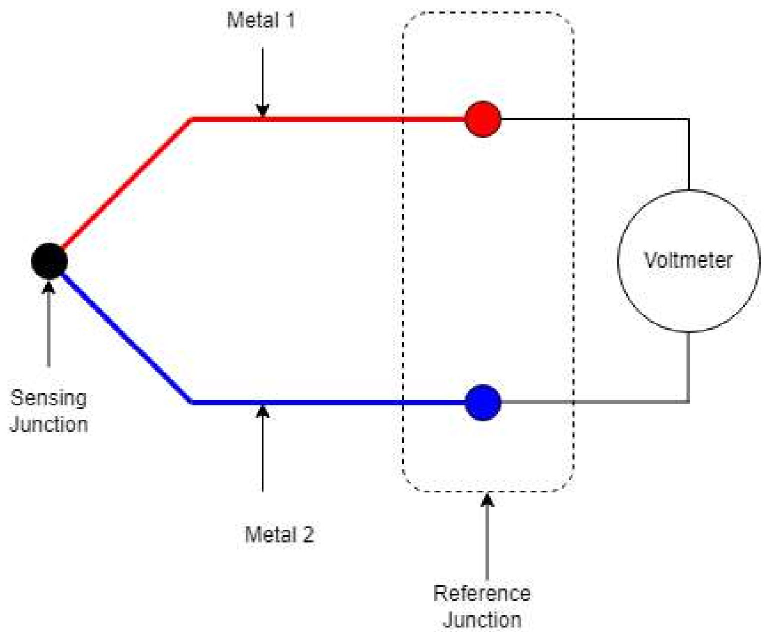

Figure 2.6 Thermocouple equivalent circuit

Table 2.2 Characteristics of various thermocouples

Thermocouple Type	**Formation**	**Temperature Range**	**Temperature Sensitivity**
E	Chromel – constantan	-270°C – 740°C	68 µV/°C
J	Iron – Constantan	-40 °C – 750°C	50 µV/°C
K	Chromel – Alumel	-200°C – 1350°C	41 µV/°C
N	Nicrosil – Nisil	-270°C – 1300°C	39 µV/°C
T	Copper – Constantan	-200°C – 350°C	43 µV/°C

Digital thermometer in solar simulator system is utilized to monitor solar simulator ambient temperature. It is selected as low-cost, high accuracy, digital thermometer. It can be replacable with one from local store. For further phases of this study, it is possible to use a precise semiconductor thermometer, NTC or thermistor. Temperature data can be transferred to computer environment like Matlab and processed there. By measuring delta temperature between solar simulator ambient and ambient temperature outside the solar simulator, it is possible to design advanced dynamic control systems. At this phase, only photovoltaic performance in terms of output voltage variation over temperature change can be monitored by using this digital thermometer. Picture of digital temperature is given as below.

Figure 2.7 Digital thermometer

Characteristics of the digital thermometer is given as below [92]:

Manufacturer: TT Technic

Temperature Range: -50 - 400°C

Resolution: 1°C

Accuracy: ±(1%+4)°C

Number of Channel: 1

Probe Type: K

Battery: 9V

Dimensions: 24 x 72 x 108mm

2.1.4 Digital Multimeter

To observe output voltage of the photovoltaic as a performance metric for changing solar simulator system temperature inside, digital multimeter is utilized. It is selected as digital, high sampling rate and also general purpose. It can be replacable with one from local store. For further phases of the study, this output voltage data can be received by arduino system and transferred to computer environment like Matlab. By collecting previous voltage data and comparing it with temperature data, it is possible to create output voltage vs. temperature relationship. Thanks to this simple but robust system, it is possible to create advanced output voltage monitoring system, data acquisition system. Digital multimeter is utilized only for output voltage monitoring because illumination power inside the solar simulator system is not enough to create photogeneration current. Therefore, it is not risky to damage multimeter while measuring current, i.e. there is no need to measure current of photovoltaics. It is enough to monitor only one of the identical photovoltaics in the solar simulator system to observe thermal performance of double-faced photovoltaics. If it is required to measure output voltages of identical photovoltaics, another general-purpose multimeter can be utilized. Further development of data acquisition system enables to observe multiple output voltages simultaneously. Picture of the multimeter is given as below. Although it is not stated in datasheet, sampling rate of newer version of the same digital multimeter is 4 times/second [93].

Figure 2.8 Depiction of digital multimeter

Properties of the digital multimeter is given as below [93]:

Manufacturer: Uni-Trend
Model: UT136B
DC Voltage Range: 400mV/4V/40V/400V/500V (Auto Range)
DC Voltage Measurement Accuracy: ±(0.8%+1)
Input Impedance: 10MΩ
Power: 9V Battery
Dimension: 72mm x 137mm x 35mm
Weight: 200g

To measure optical characteristics of light sources, special-purpose lux meter and power meter is utilized.

2.1.5 Lux Meter

To observe the amount of lux density of identical light sources, special-purpose lux meter is utilized. Lux meter is utilized to measure illuminance of a light source. Illuminance is a consept that measures how much luminous flux is spread over a certain area. Analogiously, luminous flux is a measure of total amount of visible light present, and illuminance is the intensity of illumination over a certain area. Illuminance is inversely proportional with the surface area while keeping illuminous flux constant. Unit of illuminance is “lux”. Conversion relation between related SI units are given below. Another common non-SI unit for illuminance is foot candles(FC). Conversion relation between lux and FC is given below. Lux is utilized in photometric measurements.

$$1\ lx = \frac{1\ lm}{m^2} = 1\ cd \cdot \frac{sr}{m^2}$$

$$10.752\ \cdot FC = 1\ lx$$

Illumination values of some daytime conditions are given in the table below.

Table 2.3. Illumination values for various daytime conditions [94]

Condition	Illumination (Lux)
Sunlight	107,527
Full Daylight	10,752.7
Overcast Day	1,075.3
Very Dark Day	107.53
Twilight	10.75
Deep Twilight	1.08
Full Moon	0.108
Quarter Moon	0.0108
Starlight	0.0011
Overcast Night	0.0001

For photometric measurements, spectrum of the measured light ray is rather important. To characterize a certain light ray, it is required to match spectrum of light ray and spectrum of the measurement instrument. Color of the light sources is cool daylight. Therefore, spectrum of the light sources should be rather close to visible portion of the sunlight. Spectrum of the visible light and spectrum response of measurement device is given below. It can seen how better to match measurement device spectrum with the spectrum of light source.

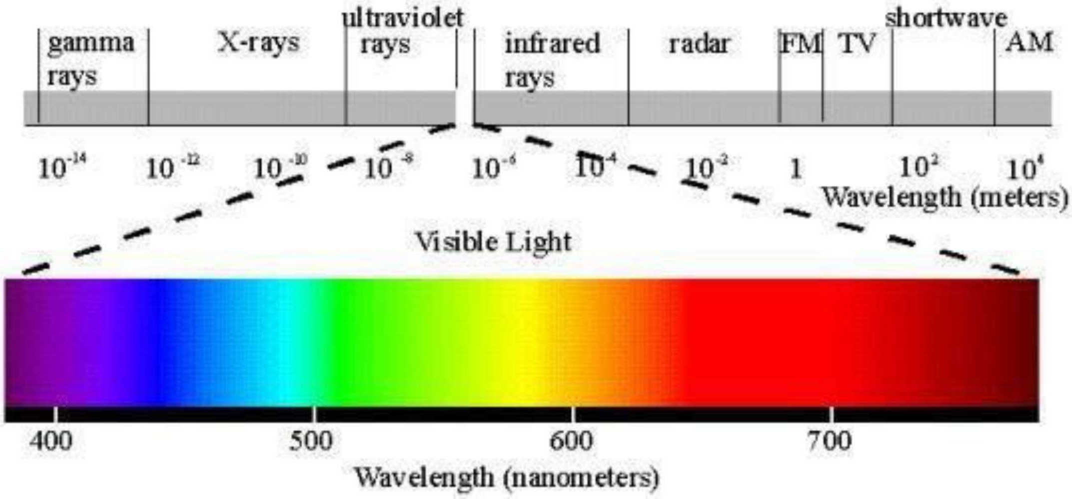

Figure 2.9 Visible light spectrum in the radio frequency spectrum [95]

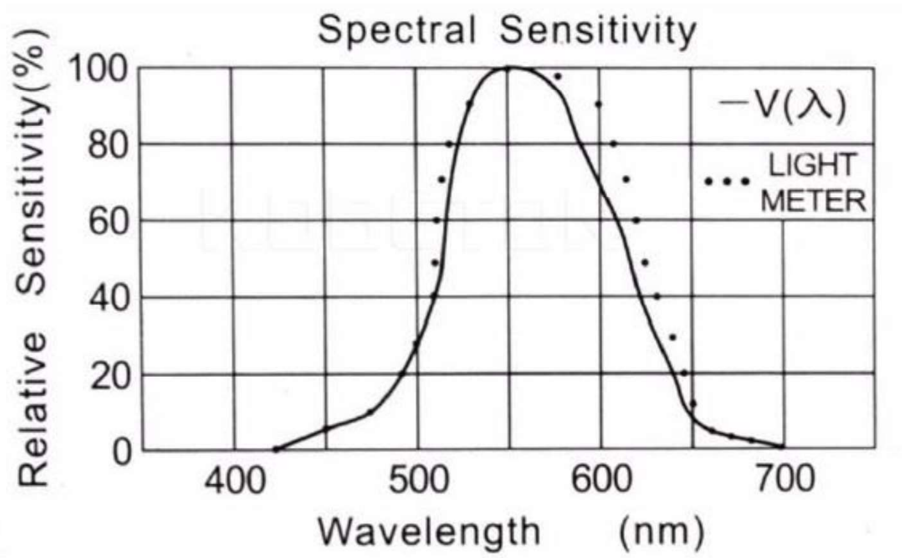

Figure 2.10 Spectral response of luxmeter [96]

Picture of the instrument utilized to characterize light sources is given as below.

Figure 2.11 Special-purpose lux meter to characterize light sources

Technical specifications of the luxmeter is given as below [97]:

Manufacturer: Alion

Model: Lx1010B

Lux Range: 1-50,000 lx

Resolution: 1 lx

Accuracy: <10,000 lx: ±4%

>10,000 lx: ±5%

Repetability: ±2%

Temperature Characteristic: ±0.1%/°C

Test Rate: 0.4sec.

Operation Temperature: -10°C to 40°C

Power: 9V battery, average current consumption 2mA

Dimensions: 230x72x30 mm (meter body)

106x57x26mm (photo detector)

Weight:190g

2.1.6 Solar Power Level Meter

To characterize the identical light sources, solar power level meter is utilized in addition to lux meter. Lux meter is used to measure luminous flux. On the other hand, solar power level meter is utilized to measure illuminance power of the identical light sources. In photometric measurements, lux meter is utilized. Photometry is measurement of visible light. In radiometric measurements, power level meter is utilized to measure spectrum power level of optical radiation covering electromagnetic spectrum from 300GHz to 30000 THz.

Sunlight comes from sun to World by passing through atmosphere. This journey results to well-known two solar spectrum types to explain sunlight spectra. These spectrums are defined by American Society for Testing and Materials. One of the spectra is named as AM1.5 spectra. Standard code for this spectrum is ASTMG173. Prefix AM is named as “air mass” and is defined below.

$$AM = \frac{1}{\cos(\theta)} \; with\ the\ zenith\ angle\ \theta.$$

Atmospheric conditions for AM1.5 are given below [98]:

a. The 1976 U.S. Standard Atmosphere with temperature, pressure, air density etc. Specified in 33 layers.
b. An absolute air mass of 1.5 (solar zenith angle 48.19)
c. Angstrom turbidityat 500nm of 0.084c
d. Total coloumn water vapor equivalent of 1.42cm
e. Total coloumn ozone equivalent of 0.34cm
f. Cell is tilted by 37° from the horizon
g. Cell has no optical concentration
h. As CO_2 level is rising, a higher CO_2 level is taken (370ppm)
i. Haziness is fine-tuned (to a turbidity value of 0.084 at 500nm)
j. Total Irradiance is 1000W/m^2

There are two types of AM1.5 spectrum types. AM1.5 Global spectrum is designed for flate plate modules, especially for photovoltaics, whereas AM1.5 Direct spectrum is designed for solar concentrator Works. While AM1.5G spectrum assumes 1000W/m^2 total irradiance, AM1.5 Direct spectrum assumes 900W/m^2 power density.

In addition to AM1.5 spectra, there is also AM0 spectra. Calculation of AM1.5 spectra is originated from AM0 spectra. While there is non-zero zenith angle in AM1.5 spectra calculation, there is zero zenith angle in AM0 spectra. Modified calculations are added onto AM0 spectra. Derivative of other spectrums can be obtained by manipulating the AM0 spectra data on NREL website [99].

Like AM1.5 spectra, AM0 spectra has also characteristic code for itself. Air mass zero reference spectrum, aka. AM0 spectra, is code by ASTM as ASTM E-490. Total irradiance strength of AM0 spectra is 1366.1 W/m^2. Other alternative units for AM0 total irradiance is given below [99].

$$
\begin{aligned}
Solar\ Constant &= 1366.1\frac{W}{m^2}\,[SI\ unit] \\
&= \frac{0.13661W}{cm^2} \\
&= 1.3661\ \cdot\ 106erg \cdot cm^{-2} \cdot s^{-1} \\
&= 126.9\ W \cdot ft^{-2} \\
&= 1.959cal \cdot cm^{-2} \cdot min^{-1} \\
&= 0.0326cal \cdot cm^{-2} \cdot s^{-1} \\
&= 433.4\ Btu \cdot ft^{-2} \cdot h^{-1} \\
&= 0.1202\ Btu \cdot ft^{-2} \cdot s^{-1} \\
&= 1.956\ Langleys \cdot min^{-1}
\end{aligned}
$$

Designed spectrums and their related zenith angles are depicted in the figure below.

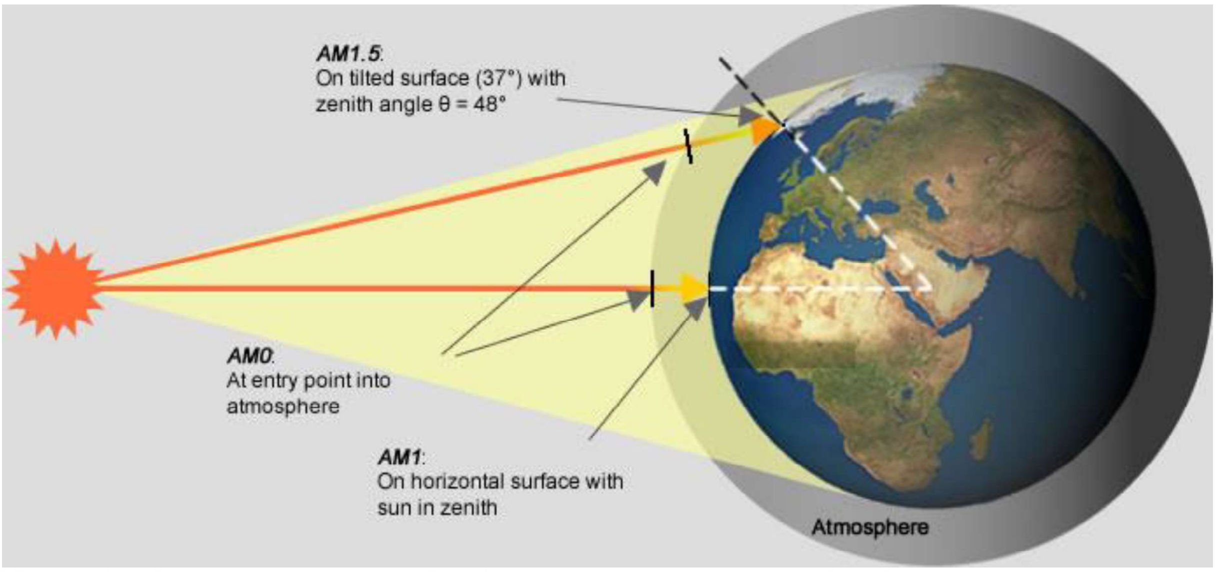

Figure 2.12 Designed sunlight spectrums and their related zenith angles [100]

Spectrum components and their corresponding spectral irradiance strengths are given in the figure below.

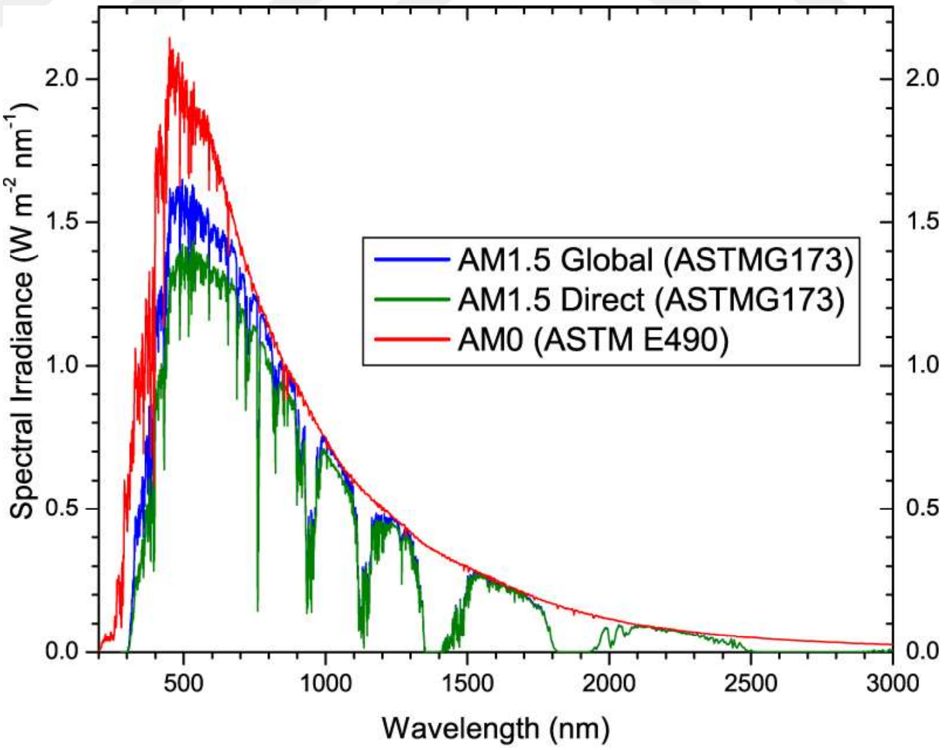

Figure 2.13 Spectrum components vs. spectral irradiance strength characteristic [101]

The most utilized solar radiation model in commercial terrrestial PV applications is AM1.5G solar spectrum model [102]. Therefore, solar power meters are adjusted to AM1.5G spectra. Lux density and illumimance strength are two orthogonal measurement methods. While illuminance strength measurements are done by more expensive instruments, lux density measurements are performed by using low-cost instruments. In addition, solar power level meters are not reliably at low irradiance levels. In literature, although there is not a rule of thumb to convert lux density to power density, it is stated that for 1 sun power density, 1000W/m^2, lux density varies between 21,000lx to 688,449lx. Peter Michael analysed whole solar data and considered measurement uncertainities, equipment calibration and standards, concluded that solar irradiance of 1 sun (1,000W/m^2) equals approximately to 120,000lux, i.e. 120lux per 1W/m^2 [103]. If optical characteristics of identical light sources are analyzed it is seen that lux density per unit power is equal to 285lux/W/m^2. This value is consistent with the solar value in literature. In other worlds, our identical light sources can replace with sun. On the other hand, proposal by Peter Michael shows that our identical light sources are more powerful than sun power.

Instrument utilized to characterize identical light sources are given as below.

Figure 2.14 Solar power level meter to characterize identical light sources

Technical specifications of solar power level meter is given as below [104]:

Manufacturer: Extech Instruments

Model: SP505

Measurement Range: 0-3999 W/m^2

Resolution: 0.1 W/m^2

Accuracy: ±10 W/m2

Sampling Rate: 0.25 sec

Operating Temperature: 5 to 40°C

Operating Altitude: 2000 meters

Power: 2 x 1.5V AAA battery

Dimensions: 108 x 48 x 23mm

Weight: 80gr

In the experiment to observe thermal response of dynamic control system, electronic components, OPAMP, NTC thermistors, NPN transistors, PNP transistors, 1N4001 power diodes, plenty of resistors, DC motor and DC power supply are utilized.

2.1.7 DC Power Supply

In dynamic control system, to energize and test the designed system, tabletop DC Power Supply is utilized. It is selected as low-cost, reliable, stable, variable, powerful. It can be replacable with one from local store. If designed system is examined, it can be seen that there are two different voltage sources required. The tabletop DC power supply can give output from two channels simultaneously. From variable voltage power output channel, dynamic control system is energized. From fixed 5V-2A power channel test motor is energized. Experimental DC source is given in the figures below. To use both power channels simultaneously in the circuit, negative polarities of each channel are in common.

Figure 2.15 DC power supply front and auxiliary views

Technical specifications of the DC power supply is given below [105]:

Manufacturer: Mervesan

Model: MS-305B

Number of Channels: 2 Channels (1 Variable Voltage + 1 Fixed Voltage)

Power Supply Voltage: 220V/110V ±10% 50Hz/60Hz

Operating Range: 0-30V/0-5A

Power Stability: <0.01%+3mV

Load Stability: <0.01%+5mV

Recovery Time: 100µS

Ripple Noise: <0.5mV

Temperature Coefficient: <300PPM/°C

Operating Temperature:0-40°C

Dimensions: 285x128x145mm

2.1.8 Electronic Components

Dynamic control system is established in a prototype manner. This study is open to revisions and modifications, it is established on a breadboard prototyping board. Discrete components are utilized in order to easily pick or place. Electronics components are selected as reliable, stable, general-purpose, open to customization and replacable. Any of the component can be replacabled with one from local electronics store or online electronics store. Design of the dynamic control system is based on analog electronics. This philosophy is selected because analog systems are low-cost, more reliable, fundamental. Although design of digital system-on-chip solutions are more flexible than analog system, they are not open to customization due to compactness. In discrete analog systems, every components can be modified, changed or upgraded.

Prototype view of dynamic control system on breadboard is given as below.

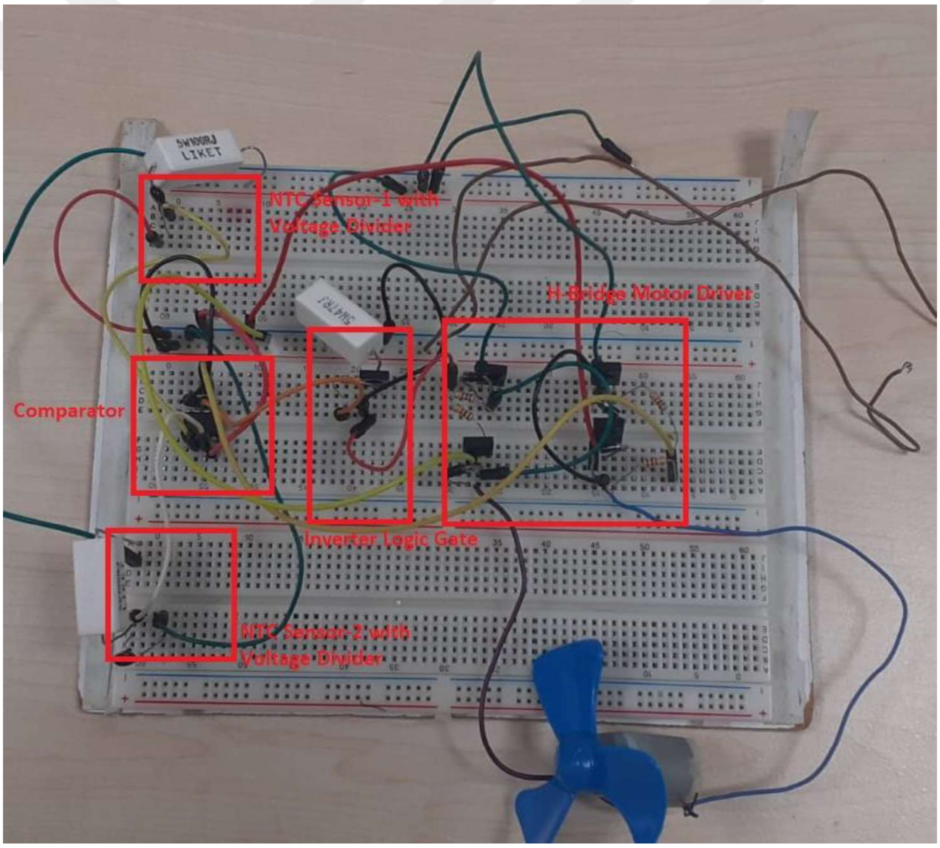

Figure 2.16 Dynamic control system prototype on breadboard and system blocks

Dynamic control system is simple circuit consisting of 2 NTC sensors, 2 voltage divider circuits, comparator circuit, logic inverter circuit and H-bridge motor driver circuit. All components are energized by DC power supply. Technically, electronic components in the system are listed as below:

NTC (Negative Temperature Coefficient) Sensor: NTC sensors are one type of thermistor device. Such sensors are categorized under thermistor group. Thermistor is a type of resistor whose resistance is more strictly dependent to temperature than conventional resistors. Name “thermistor” is combintion of “thermal” and “resistor”. In history, the first time NTC was invented by Michael Faraday in 1833 on his work related to semiconductive behaviour of silver sulfide. He noticed that resistance of silver sulfide decreases dramatically as temperature increases [106]. Later on, many studies are conducted but any product cannot be produced until 1930s. In 1930, the first commercially viable thermistor is invented by Samuel Ruben [107]. NTC sensors are utilized as current limiters, temperature sensors or over-current self-resetting systems. Operating temperature range of thermistors are typically between -100°C to 300°C. In Negative temperature coefficient sensors, resistance decreases as temperature increases. Physics behind this phenomena is that thermal agitation from valence band bumps up conduction electrons. Increase in conduction electrons increases conduction. Therefore, conduction is eased, resistance is decreased. The things in PTC is reverse of NTC. As temperature increases, resistance decreases. Although NTC thermistors are known as thermally sensitive resistors, in reality they are semiconductor devices. Though exact mixture of NTC sensors are proprietary secret of each manufacturer, they are actually formed of powdered metal oxides, those are chromium, manganese, cobalt, iron and nickel [108][109][110].

Nowadays, they can reach up to ±0.1°C temperature accuracy within 0°C to 70°C, which temperature range is more than enough for many product operating in room temperatures. Circuit symbols for NTC sensors are given in the figure below. Symbols in the first row are used in U.S. convention, those in the second row are utilized in European convention. NTC thermistors utilized in the study can be given in the figure below.

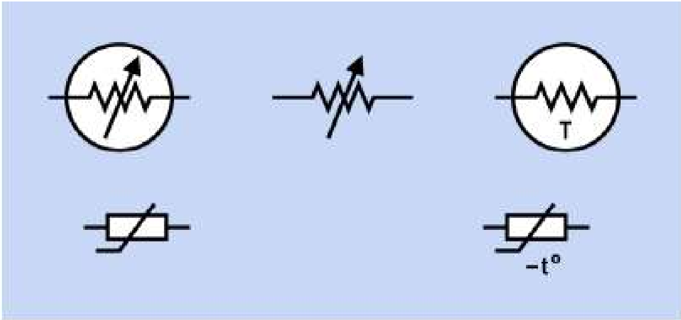

Figure 2.17 Circuit symbols of NTC thermistors [110]

Figure 2.18 NTC sensors in the study

Basically, for a certain range of temperature, mathematical relation between temperature and resistance of thermistor is linear and it is given as below.

$$\Delta R = k \cdot \Delta T$$

Where ΔR is change in resistance, Δt change in temperature and k is temperature coefficient. If k value is positive, then the type of thermistor is PTC. If k value is negative, then the type of thermistor is NTC. This method is assumption of first order approximation. Although it is valid for certain temperature range, it is invalid for wider temperature range. For wider temperature ranges, to obtain more precise values, more complex resistance-temperature transfer functions are utilized. One of the high performance transfer function is Steinhart-Hart equation. It is a widely used third order approximation and given as below.

$$\frac{1}{T} = a + b \cdot lnR + c(lnR)^3$$

Where, a, b and c are called as Steinhart-Hart parameters and they are device-specific parameters. T is temperature and R is resistance. If the equation above is solved for lnR, it is found as below.

$$lnR = \frac{b}{3c \cdot x^{\frac{1}{3}}} - y^{\frac{1}{3}}$$

Where

$$y = \frac{1}{2c} \cdot \left(a - \frac{1}{T}\right)$$

$$x = y + \sqrt{\left(\frac{b}{3c}\right)^3 + y^2}$$

Another way to solve Steinhart-Hart equation for only R value is given below.

$$R = \exp\,[\left(\beta - \frac{\alpha}{2}\right)^{\frac{1}{3}} - \left(\beta + \frac{\alpha}{2}\right)^{\frac{1}{3}}]$$

Where

$$\alpha = \frac{A - \left(\frac{1}{T}\right)}{C}$$

$$\beta = \sqrt{\left(\frac{B}{3C}\right)^3 + \frac{\alpha^2}{4}}$$

Error in Steinhart-Hart equation is less than 0.02°C, which is strongly accurate than linear approximation.

Steinhart-Hart equation can be written in the form of B-parameter equation, which is given as below.

$$\frac{1}{T} = \frac{1}{T_0} + \frac{1}{B} \ln\left(\frac{R}{R_0}\right)$$

Equation above is nothing but normal Steinhart-Hart equation with $a = \frac{1}{T_0} - \left(\frac{1}{B}\right) lnR_0$, $b = \frac{1}{B}$ and $c = 0$ Steinhart-Hart parameters.

If the B-parameter equation is solved for R, it is found as below.

$$R = R_0 e^{B(\frac{1}{T} - \frac{1}{T_0})}$$

Where R_0 is the resistance at the certain temperature T_0. Apart from temperature, there are other performance metrics of thermistors in datasheet, those are given as below.

Thermistor Value: When reviewing a datasheet, first thing to look is thermistor value. Thermistor value is strictly dependent to application. If the application is for temperature measurement, higher value is selected, which is not suitable for inrush current limiting applications. On the other hand, if the application is for inrush current limiting application, lower value is selected, which is not suitable for temperature measurement.

Reference Temperature: Reference temperature is the temperature at which many figure of merits of thermistor, temperature coefficient, resistance etc., are measured. Although reference temperature is 25°C for many thermistor applications, in some cases, this value is selected as 0°C. Reference temperature is abbreviated as T_{REF}.

Reference Resistance: Reference resistance, as it can be guessed, is the resistance at the reference temperature. In datasheet of thermistors, it is shown as "R25" or "R_{25}", which is the temperature at 25°C.

Temperature Coefficient: Temperature coefficient is shown as TC, which is sensitivity of the thermistor. Value is percentage change in resistance for each change in temperature of 1°C. For example, if resistance value is decreased from 100ohm to 95 ohm for temperature change from 28°C to 29°C, TC=-5%. Sometimes, this value is expressed in parts per million(ppm) instead of percentage. To convert ppm values to percentage value, ppm value is divided by 10000.

Applications for NTC thermistors are inrush current limiter, wheatstone bridge circuit, temperature measurement in devices like 3D printers, dishwashers, toasters, laser printers, modern automobiles and medical equipments. In this study, two NTC sensor are utilized to sense solar simulator system temperature inside and ambient temperature outside. Because they are easy to find in local stores, 100Ω NTC sensors are utilized.

OPAMP: OPAMPs are abbreviation of operational amplifiers. They are coming from birth of computers. The first computers were analog computers. Such devices were utilizing pre-programmed equations and input data to execute operations. Programming of computers were a big business at that time. It was based on hard-wired operations and an operator was required to plug-unplug hard wires with a series of circuits. Counterpart of today's computer's brain was operational amplifiers for analog computers. They can be configured to perform many mathematical operations like multiplication, addition, subtraction, division, integration an differentiation for input signals. Analog computers are replaced with digital computers. However, popularity of OPAMPs are increased year by year. This device accepts differential inputs and generally gives single-ended outputs. Popularity of the device comes from its versatility. If negative feedback is used in OPAMPs, circuit's overall gain and response is determined by feedback network rather than open-loop gain. Ideal OPAMP has some characteristics, given as below:

a. Infinite open-loop gain, $V_{out}/V_{in} \approx \infty$
b. Inifinite input impedance, $R_{in} \approx \infty$
c. Zero output impedance, $R_{out} = 0$

These characteristics result some circuit design rules:

1. In closed-loop circuit, output is taken a value that voltage difference between input ports are zero.
2. Input ports do not draw current.

Many operations can be performed by configuring negative feedback circuit, like summation, multiplication, division. If any circuit is not constructed as negative feedback circuit around OPAMP, then OPAMP behaves as a comparator. In this study, two voltages coming from NTC sensors, are compared and single-ended output is fed into inverse logic and H-Bridge motor driver circuit. As an OPAMP IC, UA741 is chosen for OPAMP comparator. UA741 comes after UA709. UA709 is invented by Robert J. Widler from Fairchild Semiconductor.It has some problems regarding design but many engineers prefered it in their design. After UA709, UA741 is invented by Dave Fullagar. Fame of UA741 is much more positive than UA709. Due to It's wider power supply requirements, it is preferred a lot [111]. There are some performance parameters in datasheet of OPAMPs, those are also considered in the study, and they are given as below.

Supply Voltage: Supply voltage is required voltage to drive OPAMP. It is given by power supply. It is sometimes referred as bias voltage. It is shown as V_{CC} or V_{DD}. In addition to power required for operation, supply voltage is critical for output signal saturation voltage levels. There are two way to power-up OPAMPs: Single-supply design or dual-supply design. In single supply design, positive polarity is connected to "V^{+}" pin of OPAMP whereas negative polarity, aka. ground, is connected to "V^{-}" pin of OPAMP. In dual supply design, there are two voltage levels: one of them is positive voltage level, other one is negative voltage level. In dual supply designs, ground is not connected to supply pins of OPAMP. Instead, a virtual ground is somehow created in the circuit. In dual supply design, if magnitude of voltage levels are same, then design is named as split-supply design. Generally, split-supply power supplies are used to enhance input voltage range of OPAMPs. However, magnitudes of supply voltages may not be same. This fact is directly dependent to design demands. In any case, it is suggested to create a virtual ground for the circuit. All in all, in both cases, maxima and minima of output voltage levels, aka. saturation voltage levels, are determined by supply voltage levels, aka. positive and negative rail voltages.

Input Resistance: In ideal OPAMP circuit, input resistance of OPAMP is assumed to infinite, ideal OPAMP circuit is given as below. Because of this, input current drawn by OPAMP is assumed to be zero. However, this is not the case. Input resistance of OPAMPs are higher but finite. In this study, input resistance of UA741 is stated as 2MΩ. Generally, for negative feedback circuitry, resistances on the order of kiloohm is prefered. Therefore, it does not affect the input signal of OPAMPs. Major advantage of higher input resistance is by keeping input current on the order of leakage current, it is satisfied that devices satisfying input signal are protected, they are not loaded. In this study, in input stage of OPAMP, resistances on the order of ohm is prefered.

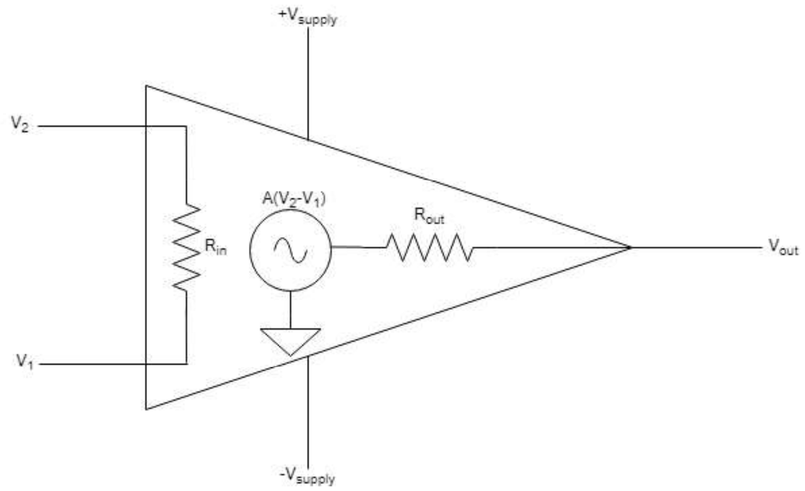

Figure 2.19 Ideal OPAMP circuit

Input Voltage Range: Input voltage range is another figure of merit for operational amplifiers. Input voltage can be two cases: Common-mode input voltage and differential-mode input voltage. In datasheet of OPAMPs, generally total input voltage range is given. Although it is stated in datasheets on OPAMPs that voltage range is a certain value, it should be prefered that input voltage is not selected higher than supply voltage. In better analog design, input signal should be selected lower than supply voltage, i.e. there should be tolerance margin. In this study, input signals have both common-mode and differential mode input. By using voltage division circuits, a common-mode input voltage is fed into each differential input pins. By utilizing temperature variations between NTC sensors, differential-mode input voltage is introduced. In this study, input voltage levels are selected much more lower than supply voltage range of OPAMP in order to operate properly.

Output Voltage Swing: Output voltage swing is another less-known but critical figure of merit. Output voltage swing is output voltage range that OPAMP can provide. It is strictly dependent to supply voltages. General-purpose, most-known OPAMPs can provide voltage swing less than supply voltage range. However, this may result to trouble while designing a single-supply circuit design. If a transistor is biased with supply voltage of OPAMP and it is used as a switch, it is not possible to switched via output signal of OPAMP due to difference between output voltage maxima and supply voltage. This difference will forward bias the transistor always. In order to solve this problem, rail-to-rail OPAMPs are designed and released into market. Such powerful devices force the limit of saturation voltages, sticking to supply voltages. Thanks to such devices, it is possible to design single-supply switch-mode analog designs. Therefore, this figure of merit is a challenge for today's analog designers. LMV321, LMV358, LMV324, OPA342, OPA2342, OPA4342 are example for low-cost rail-to-rail output OPAMPs. Although they are stated as low-cost, still they are much more expensive than general-purpose, most-known OPAMPs like UA358,UA741. Although, UA741 is not a rail-to-rail output OPAMP, dual power supplies are utilized in analog circuit design. Lower voltage is selected to bias PNP-type transistors. Although, output of OPAMP is not rail-to-rail, output voltage loss does not affect the switching of transistors. It is ensured that transistor is off when output of OPAMP is high.

Transistor: Transistor is a semiconductor device which amplifies signal or control the conduction of electrical current. Transistors are fundamental electronic device in today's modern electronics. Transistors have at least three terminal for electrical connection. A small electrical current is applied between two terminals of the device and current through other terminals are controlled. This mechanism provides the amplification of signal. The first time transistors are designed and invented by John

Bardeen and Walter Brattain while they were working at Bells Labs. Their invention brought 1956 Nobel Prize in Physics to them. There are many types of transistors: Bipolar Junction Transistor (BJT), Field Effect Transistor (FET), Metal Oxide semiconductor field effect transistor (MOSFET). Today, the most preferred transistor type is MOSFET due its high performance. Transistors are mostly produced from silicon materials. The reasons are that silicon is abundant in earth crust and performance of silicon is rather appropriate for transistor devices. Other materials are also preferred to produce such devices, e.g. Germanium, carbon, Gallium etc. By considering transistor physics, in bipolar junction transistors, there are two kind of charge carriers, whereas in field effect transistors, there is only one kind of charge carrier. Former version transistors, vacuum tube devices, were able to work at higher frequencies and higher power ratings compared to transistor counterpart but they were bigger in size and consuming more power compared transistors. Also, fabrication of vacuum tube devices were more difficult compared to transistors. Fame of transistors were spread and vacuum tube devices are replaced with transistors. They broke fresh ground in analog electronics and opened the door of digital electronics. Today, although MOSFETs are preferred more than BJTs due to higher performance and more advanced technology, BJTs are also still in use due to the fact that they are budget-friendly, simple to use solutions for electronics designs. There are two type of BJT transistors: NPN type and PNP type. In NPN type, charge carriers are electrons, whereas in PNP types, charge carriers are holes. BJTs can be used as two purposes: Signal amplification in analog electronics and switching electrical current in digital electronics. In switching operation, transistor is used as a switch, as it can be inferred by name. Transistor can be either in an “ON” or “OFF” state based on biasing of transistor. Such operation is used in SMPS and logic Gates. When the voltage at Base, one of the pins of BJT, is increased, resistance between collector and emitter, other two pins of transistor, is decreased. Therefore, current can easily pass through collector to emitter. Such mode of operation is named as Saturation mode. In saturation mode, when gate pin is biased, then transistor is named as “ON”. The only thing required to make BJT in saturation mode is that considerable amount of current should be drawn by transistor from it’s base terminal. If BJT is intended to operate as Switch mode, it is required to choose a proper base resistor value so that considerable amount of current is drawn by base of the transistor and it is ensured that BJT is in saturation mode of operation. In switching-mode, rather higher currents are utilized to switch the transistor. On the other hand, in signal amplification, small input signal in base is amplified in BJT. Small input signal variations results to larger signal changes in output voltage. As in negative feedback circuitry around OPAMP, various circuit topologies can be constructed around terminals of transistor and it can be obtained many kind of possibilities: voltage gain, current gain, trans-resistance or both of them. Signal amplification can be used in everywhere signals exist: from televisions to radios, radars to mobile phones. They are used for sound reproduction, radio transmission and signal processing. Although initial transistors are on the order of mW, today transistors on the order of hundreds of watts are released to market. To sum up, switch-mode operation is utilized in DC-mode operation, whereas signal amplification is utilized in AC-mode operation. In this study, transistors are utilized in DC mode operation. Power requirement of this study is from hundreds of miliampers to currents on the order of amper. Best candidate for this study is to use power transistors. They can handle currents on the order of ampers compared to currents of on the order of hundreds of miliampers by general-purpose transistors. Best candidate for such requirement is “BD” transistor family. Best match products of this family are “BD139” and “BD140”. BD139 is NPN type transistor, BD140 is PNP type transistor. They have same electrical charactertic but only difference is that they are complementary of each other. Replacements of these devices are “BD135” and “BD136” pairs. BD135-136 pair has better small signal amplification performance. Other electrical characteristics of these are exactly same with BD139-BD140. In this study, only DC-Switch mode operations are utilized. Therefore, it is not a problem to replace BD135-BD136 with BD139-BD140, respectively. Transistors utilized in the study is given as below.

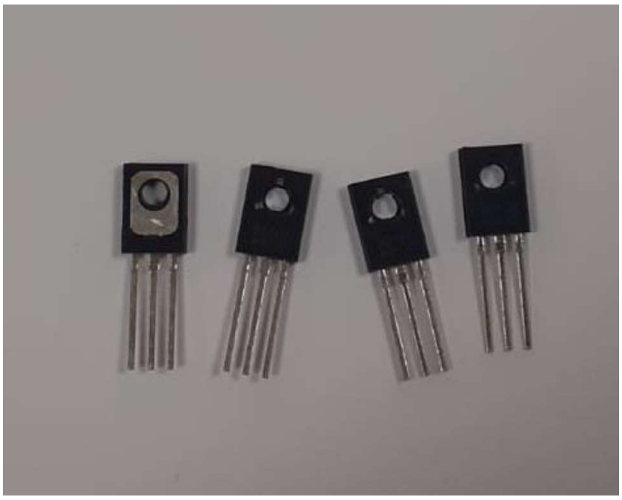

Figure 2.20 BJT transistors in the study

There are some figure of merits of BJT transistors to be used in circuit design. In this study, such performance metrics are also considered.

Collector-Emitter Voltage: Collector-Emitter Voltage is stated in datasheet of transistor that maximum voltage that can be applied between collector and emitter terminals. This voltage is also the voltage that transistor can handle when it is OFF. Beyond that value, breakdown occurs and transistor is burnt. This voltage value is considered while designing the circuit. Supply voltage and collector resistors are determined based on this value. In this study, supply voltages are much more lower than the maximum collector-emitter voltage stated in datasheet of the transistor. In the design, maximum collector-emitter voltage is stated as 80V for BD139-BD140.

Emitter-Base Voltage: This value is considered when base-emitter junction is reversed biased, i.e. not-conducting. This value stated in datasheets is the maximum voltage that base-emtter junction is reversed biased. This concept should not be confused with Base-Emitter voltage. Base-Emitter voltage is the voltage between base and emitter terminals when this junction is forward-biased and this value is about 0.7V silicon devices. BJT transistors have lower emitter-base voltages compared to MOSFET that have Source-Gate Voltage. While emitter-base voltage value is about 5V for BJTs, Source-Gate voltage of MOSFET can reach up 20V. This figure of merits make MOSFET more preferable. In circuit design of the study, there are two voltage supply levels are utilized. While one of them is 5V, other one is 9V. H-Bridge circuit is powered with 5V while OPAMP is powered via 9V power supply. There is a trade-off in the design that supply voltage of OPAMP should be increased for better performance but emitter-base voltages of transistors in H-bridge should not be exceeded. Voltage difference between positive saturation output voltage level of OPAMP and H-bridge motor driver circuit supply voltage is kept 4V by ensuring that BJTs in H-Bridge driver circuit are in safe.

Collector Current: Collector current is another performance characteristic of transistors. It is stated in datasheet of transistors that collector current is the maximum current that transistor can handle. There are two types of collector currents: continuous collector current and peak collector current. Continuous current is the current that transistor can handle continuously. Peak collector current is the current that transistor can handle momentarily. Although there is not a time duration is specified what continuous is or what peak is, by "rule of thumb" peak collector current is assumed to be two times of maximum collector current. In circuit design, current values beyond maximum continuous collector current should be exceeded because it may result to permanent damage to device. Collector current does directly depend on transistor family and transistor packages. Power transistors are considered to convey more current than other conventional transistors. TO-220, TO-39, TO-247 packages can handle more current than other packages like TO-92. Also, such packages permit to use heatsink in order to push the power ratings of transistors. In this study, designed circuit is simulated with circuit simulator programs and it is observed that current passing through transistors is on the order of hundred miliamps and it is not required to use heatsink with it.

Base Current: This concept is another figure of merit that transistor can handle. Base current is the maximum current which can be applied to base terminal of transistor. Although it is not a concern in amplification of small signal, base current is important for switch mode transistor operations. In small signal amplification, small input signal variations are required at the base terminal of transistor which ensures that transistor works in linear-mode of operation which leads to small base current. However, in switch-mode of operation for transistors, BJTs should be work in saturation mode of operation and current in saturation mode is greatly higher than current in linear mode. This figure of merit is a concept related to device design like collector current. Wider terminal surface leads to higher current. Base resistance should be adjusted so that base current does not exceed maximum rated current. In circuit design, there is a trade-off for base terminal resistance. If transistor is intended to operate as a switch mode, then base current should be increased, i.e. base resistance is decreased, to operation in saturation mode of operation. However, there is a limit for maximum base current rating. Base resistance should not be lowered to exceed maximum base current. In this study this trade-off is considered and base resistances are adjusted based on this philosophy. Transistors used in this study has base current value of "0.5A" which is rather higher than operating point of transistors.

Collector-Emitter Saturation Voltage: This performance parameter is another critical concept used in circuit design. Collector-Emitter saturation voltage is the maximum voltage drop can be seen between collector and emitter terminals of the transistor. This voltage is the minimum voltage that collector current remains essentially constant as base current or base emitter voltage is increased. This voltage is a limit for transistors to operation in linear mode of operation. This voltage limit is critical especially for logic Gates in digital electronics. If emitter grounded switch exists in design, as in the study, when input signal is "HIGH", inverter logic should give "LOW" output voltage. This output voltage corresponds to Collector-Emitter voltage. Because transistors are in saturation mode of operation in switch mode operation, Collector-Emitter Saturation Voltage is seen as output in the inverter gate. This value should in the pre-defined so-called "LOW" voltage because it might feed another BJT, as in this study. In this study, inverter logic transistor is connected to transistors in H-Bridge motor driver. Based on "HIGH" or "LOW" value of input/output, BJTs in H-Bridge are turned as "ON" or "OFF". Alhough, it is assumed to 0.2V for Collector-Emitter Saturation Voltage for BJTs as a convetion, transistors used in this study has $V_{CE,SAT}$ as 0.5V, stated in the datasheet. Still this value, as in "LOW" state, is not enough turn base-emitter junction, whose voltage is 0.7V.

Diode: Diode is a two-terminal semiconductor device which conducts electricity in one direction. While it has lower resistance in one direction, it has higher resistance in other direction. Ancestor of diodes is vacuum tube diode or thermionic diode which has two electrodes. Electron travels from heated cathode to plate. On the other hand, diodes are semiconductor materials having two types of materials. One side is named as P-type material in which there are holes more than electrons, other side is named as N-type material in which there are electrons more than holes. Diodes are building blocks of other semiconductor materials, basically bipolar junction transistors. The first time asymmetrical electrical conduction across the contact between a crystal and a metal is done by Ferdinand Braun in 1874. Most diodes nowadays are made up on silicon. However, other types of materials are also used, like Gallium and Germanium. When diode is in conduction, it is called as forward-biased. P-type region is biased with more voltage than N-type region. However, there is voltage barrier called as threshold voltage. Threshold voltage is created across depletion region. This value is material-dependent. When threshold voltage is exceeded, electrical conduction occurs. This specific threshold voltage can be utilized as reference voltage. Therefore, diodes are used as voltage reference in circuit design. Current-voltage characteristic of the diode is nonlinear. It depends on temperature. Because of this, diode can be used as a temperature sensor. If voltage is applied in reverse direction in that of forward-bias, conduction stops. However, this can be observed up to a certain voltage level. This level is named as avalanche breakdown voltage. Beyond that voltage, diode starts to conduct electricity in reverse direction. Structurally, there are two types of diodes, PN-junction diodes and Schottky diode. While two types of semiconductor materials are utilized in PN-junction, metal-semiconductor junction is used in Schottky diodes in order to reduce junction capacitance and increase switching speed. Functionally, there are many types of diodes: Light emitting diodes, aka. LEDS, Laser diodes, photodiodes, PIN diodes, varicap and zener diodes. IN JEDEC standardization, diodes have prefix as 1N, due to two terminal devices. Diodes are used as many purposes: rectification, current steering, temperature measurement, over current protection, device protection. In this study, transistors in H-Bridge motor driver provides current to DC motor. As switcing changes, other transistor pair starts to conduct. However, due to inductive structure of DC-motor, current is keen on to conduct. However, proper transistors are OFF and it is not allowed to pass. Due to current-voltage characteristic of inductor, momentary changes of current creates extreme level voltage spikes.

Collector emitter voltage of transistor is limited with a certain value and it cannot handle this voltage spike. As a result of this, transistor experiences break-down. In order to eliminate this problem, protection diodes are placed across transistor terminals. Power MOSFETs have such diodes internally. In this study, general-purpose power diodes are used. The most well-known family is 1N400x. In the design, 1N4001 is used. It is selected because it is low-cost, high power and easy-replace from local store. Because ordinary conduction ability is used, all members of 1N400x family, 1N4002, 1N4003, 1N4004, 1N4005, 1N4006, 1N4007 can be replaced with 1N4001 diode. There are some figure of merits regarding the current conduction control semiconductor device, diode and they are given as below.

Average Forward Rectified Current: This value is maximum allowable current that diode can handle. This current basically related to thermal capability of device. This parameter is directly related to structural design of the device. Terminal width is adjusted so that certain amount of current can pass through without any problem. Also, packaging type directly affects the amount of forward current. While packaging type DO-41 can handle lower values, packaging type TO-220 and TO-247 can handle higher amount of current. Also, high current capable packages make heatsink usage possible. Momentary or surge currents are tens of times of continuous currents. In this study, diodes are used as protection devices. Current values of DC-motor is on the order of hundred miliamps. Therefore, momentarily, surge current on the order of tens miliamps can be handled by the selected diode.

Maximum Instantaneous Forward Voltage: This voltage comes from depletion region. This voltage level is also named as built-in voltage. Built-in voltage is a material-specific value. Silicon diodes have 0.7V forward voltage drop, germanium devices have 0.3V built-in voltage. In this study, diodes are used to protect transistors against high voltage spikes. High voltage spikes can easily handle the threshold voltage. It is not a business to open protection diodes for high voltage spikes. Diodes used in the study has threshold voltage value of 1.1V.

Maximum Repetitive Peak Reverse Voltage: This voltage is another figure of merit for diodes. This voltage is the maximum reverse-biased voltage that diode can protect to reverse conduction. This voltage is also named as DC blocking voltage.

Although, in repetitive mode, this value is on the order of 50A or hundreds amps, momentarily, diode can handle more reverse voltage values. In this study, DC-motor is powered up via 5V power supply. It is expected for DC-motor not to create higher reverse voltage across diodes to damage the semiconductor device.

Resistor: Unlike OPAMP, BJT, resistors are passive two-terminal electrial component like NTC or diode. It implements electrical resistance across it as a circuit element. In electronic circuits, they are used to reduce current flow. They are utilized for adjusting signal levels, voltage division, bias active devices. There are two types of resistors: low power resistors and high power resistors. While low power resistors are formed of carbon material, high power resistors are made upon ceramic material. High power resistors are also called as wire-wound resistor. In this study, both low power and high power resistors are utilized. Low power resistors are used to bias transistor, whereas high power resistor is used for voltage division for NTC sensors.

2.2 Working Principles of Study Subsystems

This study comprises of three subsystems: Solar simulator system, dynamic control system and double-faced photovoltaic system. Although all study subsystems are designed to operate together, each of the study subsystem can operate stand-alone. In this topic, stand-alone operation of each study subsystem is explained.

2.2.1 Solar Simulator System

Solar simulator system is designed to observe electrical performance of double faced photovoltaic system. Electrical performance depends on both structural and environmental parameters. Modifying structural parameter is not an easy job. Therefore, environmental parameters are the only ones to modify. Changing irradiance is possible excluding concentration. Temperature is the only environmental parameter to change. Although many studies are conducted in literature to show cooling effect on photovoltaic performance, In this study fan cooling is chosen to improve electrical performance of photovoltaics because it is easy to install, not required to maintain, budget-friendly and easy to observe its effects on performance improve. Not only fan is installed for cooling effect but also a heater is installed to observe thermal effect on electrical performance of photovoltaics. Theoretical model of proposed cooling system is given as below:

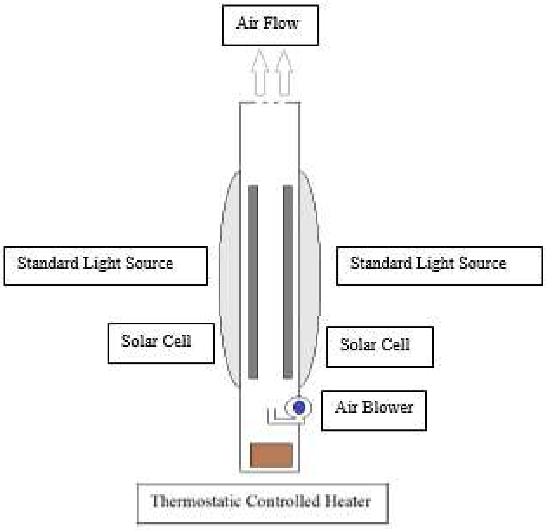

Figure 2.21 Proposed solar simulator system model

In this model, there is a thermostatic controlled heater at the bottom. By choosing a desired fan speed and radiator temperature from dual-modes, temperature of solar simulator reaches to desired temperature. This process can be monitored in a real-time manner via digital thermometer whose probe installed inside. Simultaneously, output voltage as an electrical performance can be monitored via digital multimeter. Identical photovoltaics inside the solar simulator are illuminated via identical light sources with single mode. Therefore, it is not possible to change illumination intensity of light sources.

Working procedure of solar simulator is given as below. First, lid of the solar simulator is opened and identical light sources are powered-up, multimeter probes are connected to output of double-faced photovoltaics and lid of solar simulator is closed. It is chosen that whether it will be heated or cooled. If heated, fan speed and resistance temperature are set. in case of thermostat, desired system temperature is set. If it does not exist, by manually penetrating or pulling, i.e. by manual thermostatic control effect, it is observed that solar simulator system ambient temperature reaches to set temperature. Meanwhile, system ambient temperature is measured via digital thermometer. If cooled, fan speed is set and it is activated. By monitoring ambient temperature, process is controlled. Same manual thermostatic control effect can be applied to fan cooling process, i.e. by manually penetrating or pulling the fan cooler. Throughout these procedures, output voltages of double-faced photovoltaic systems are measured. Output voltage as an electrical performance versus temperature as an environmental factor can be extracted.

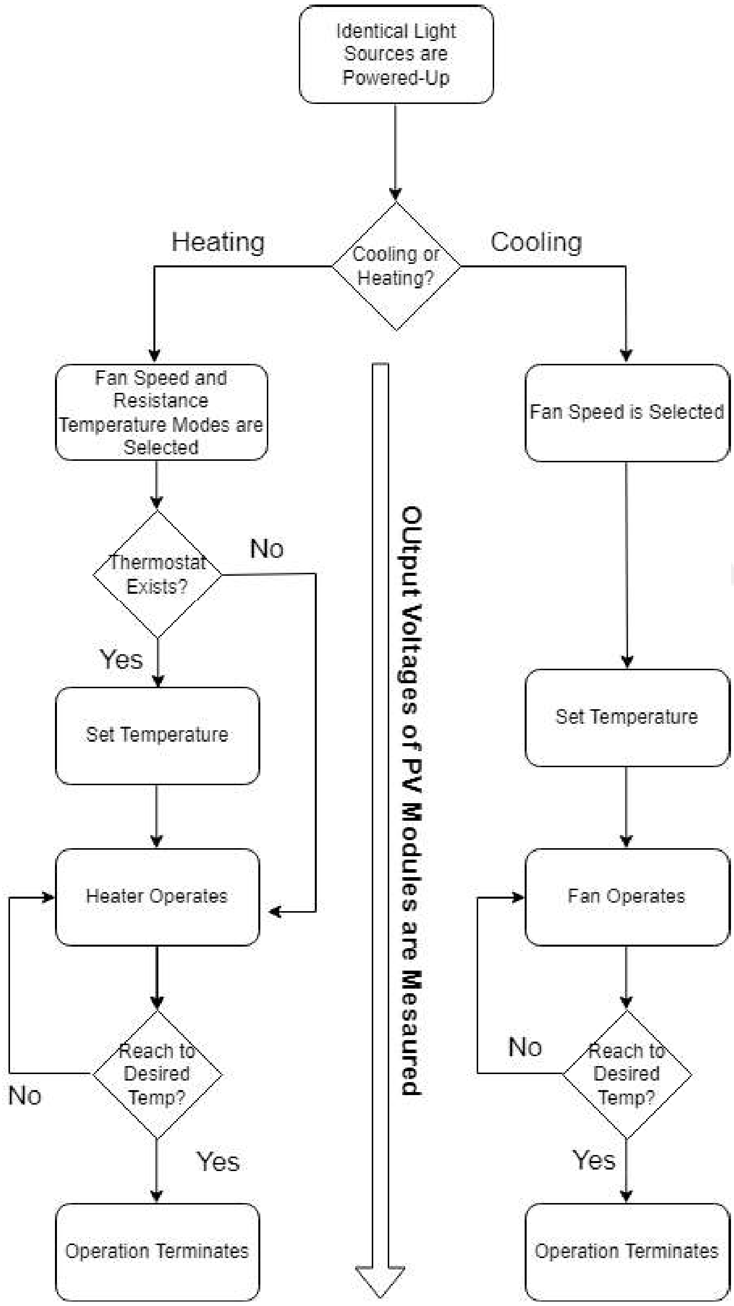

Figure 2.22 Flowchart of heating and cooling processes

Bill of materials for solar simulator is given as below.

Table 2.4. Bill of materials (BOM) of solar simulator system

Component	**Quantity**
Air Blower	2
Light Source	2
Digital Thermometer	1
Digital Multimeter	1

2.2.2 Dynamic Control System

Dynamic cooling system is designed to operate with solar simulator system. It is tested stand-alone in prototyping phase. Basically, it consists of four building blocks for this subsystem: Sensor circuitry, comparator circuitry, logic NOT circuitry and H-Bridge motor driver circuitry.

System representation of dynamic control system is given as below. In sensor circuitries, 5V supply voltage is biased through a high power resistor and a NTC sensor. As temperature changes, resistance of NTC changes, too. This results to voltage variation. Voltage variations between sensor circuitries are compared at compactor circuitry. If inside ambient temperature of solar simulator system is higher than outside ambient temperature of solar simulator system, comparator gives HIGH signal. If not comparator circuit gives LOW signal. To operate H-Bridge motor driver circuit, it is required another signal which is complement of original control signal. To do that, logic NOT circuitry is established.

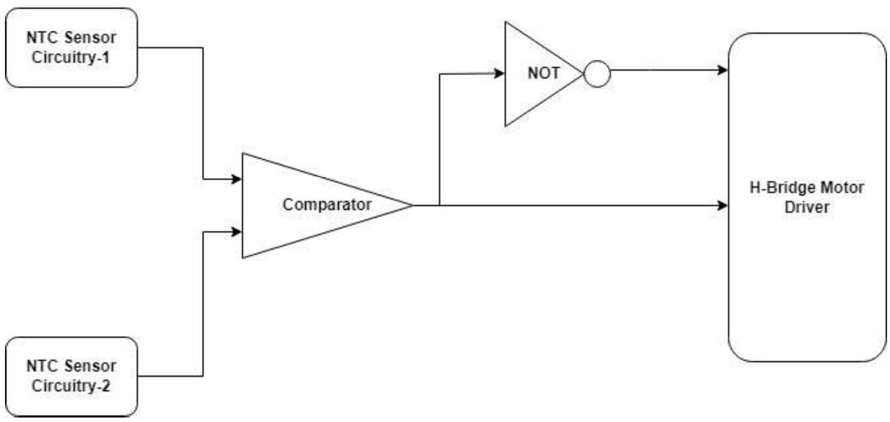

Figure 2.23 System representation of dynamic control system

H-Bridge Motor Driver circuit consists of two PNP BJT, two NPN BJT for switching and four diodes for reverse current protection. Switch-1 and Switch-4 are controlled via signals coming from comparator output. Switch-2 and Switch-3 are controlled via signals coming from logic NOT circuit. Two signals are complement of each other. Therefore, it is not possible to switch-ON for all four switches. While one pair is ON, motor rotation is clockwise (CW), other pair is ON, motor rotation is counter-clockwise(CCW). This is due to the effect of current on rotation direction. Truth table for each case of the sensors are given below.

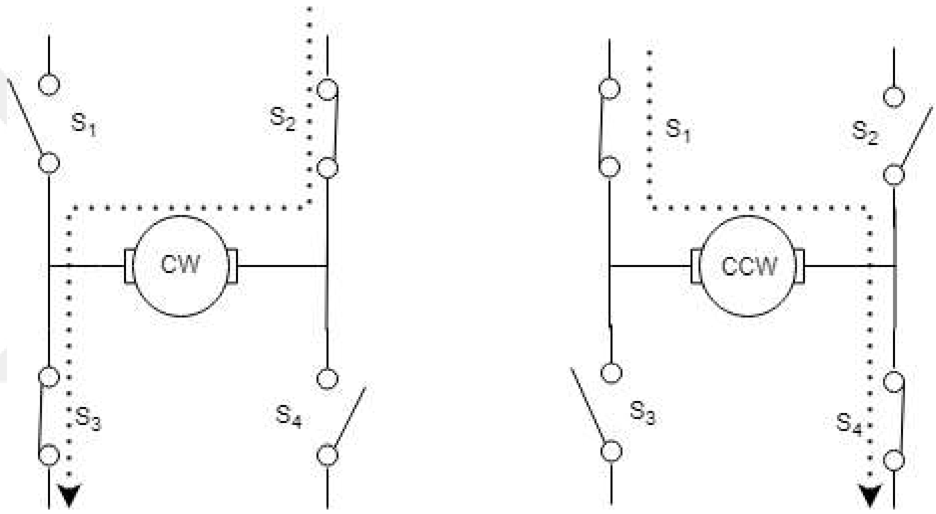

Figure 2.24 H-Bridge motor controller working mechanism

Table 2.5 Truth table for dynamic control system

	$\text{Comp}_{\text{output}}$	**$\text{NOT}_{\text{output}}$**	**S_1**	**S_2**	**S_3**	**S_4**	**$\text{Motor}_{\text{direction}}$**
$T_{inside} > T_{outside}$	HIGH	LOW	LOW	HIGH	HIGH	LOW	CW
$T_{inside} < T_{outside}$	LOW	HIGH	HIGH	LOW	LOW	HIGH	CCW

Bill of material for dynamic control system is given below.

Table 2.6. Bill of material(BOM) for dynamic control system

Component	Quantity
LM741 OPAMP	1
100Ω NTC Sensor	2
¼ W Resistor	6
5W Resistor	2
BD139 NPN Transistor	3
BD140 PNP Transistor	2
1N4001 Power Diode	4

2.2.3 Double-faced Photovoltaic System

Double-faced photovoltaic system is designed to operate together with solar simulator system. By activating identical light sources, electrical performance of double-faced photovoltaic system is observed. Though joint-operation purpose, it can be operated stand alone. However, for stand-alone operation, well-oriented mirror pair is required to illuminate other face of the system. Prototype demonstration of double-faced photovoltaic system operation under sunlight is given as below. It is important to use well-adjusted mirror pair to use with double-faced photovoltaic system under sunlight. Bill of material (BOM) list for this subsystem includes only two identical photovoltaic system.

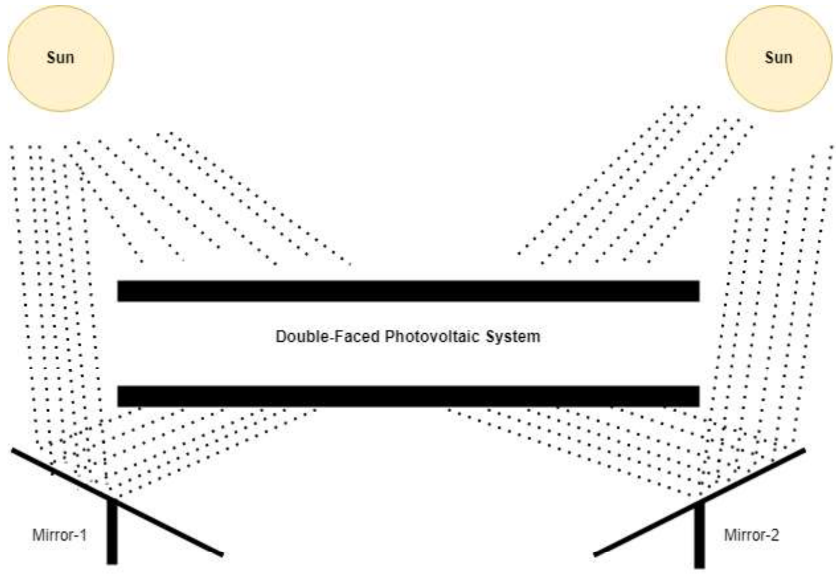

Figure 2.25. Operation of double-faced photovoltaic system under sunlight

CHAPTER 3

EXPERIMENTAL RESULTS

In experimental phase, study subsystems are designed to operate stand alone. Study subsystems are tested under different conditions and in different environments. They are tested in different environments and under different conditions. Mesaurement are taken in computer environment, under laboratory conditions and real-time real-conditions. Solar simulator system is tested under laboratory conditions, dynamic control system is tested in computer environment and double faced photovoltaic system is tested under real-time and real-conditions. In this topic, test measurements of study subsystems in different environments and under different conditions are given.

3.1 Measurements Taken in Computer Environment

Thanks to digitalization, physical experiments can be conducted in computer environment. In physical experiments, it is required to use experimental materials each time to conduct experiment. Also, it may not be posssible to control experimental procedure. Obtaining multiple results and conducting multiple analysis may not be possible in physical experiments. However, in computer simulation environments, physical experimental environment is created in simulation environment. Physical parameters on experimental enviroment is transferred to digital environment. By stating experimental parameters, they are observed in computer simulation environment.

Almost every engineering study utilizes computer-aided technologies to conduct analysis. Today, almost any physical experiment can be simulated in computer environment. Analysis of Computational Fluid Dynamics, finite element methods, Monte Carlo methods, electromagnetic analysis are one of these. Every company utilizes to simulate their studies in computer environments. This capability makes them to repeat their study many times without paying for experimental materials. Also, it is possible to conduct analysis in detail.

In this study, analog circuit of dynamic control system is designed. It has NTC sensors in the input stage, H-Bridge motor driver at the output stage. Thermal signal is given as input signal to the system, electrical current is taken as output signal from the system. To observe eletrical characteristic of each subcomponent of the system, there are instruments required to monitor electrical components. It is not a cost-effective way to conduct experiments physically for electronic circuits. Therefore, computer-aided simulation environments are good alternative to analyze electrical characteristics of the circuit. In this study, NI Multisim 14.2 is used as simulation environment. Dynamic control system is analyzed in a electrical manner using NI Multisim 14.2.

3.1.1 Dynamic Control System

There are four components of dynamic control system: NTC sensor circuitry, comparator circuit, inverting NOT logic circuit and H-Bridge motor driver circuit. In this topic, comparison performance of comparator circuit, inverting performance of NOT logic circuit and driving performance of H-Bridge motor driver circuitry is analyzed.

Although all components of the circuitry is complete analog components, behaviour of whole circuitry is binary. When one of the NTC sensor gives higher voltage than other, H-Bridge motor driver drives the dc motor in a certain way, vice versa. Fort the cases in which voltage of NTC sensor in the solar simulator is higher than voltage of NTC sensor outside the solar simulator and vice versa are given below.

$\underline{T_{solar\ simulator} > T_{ambient}}$:

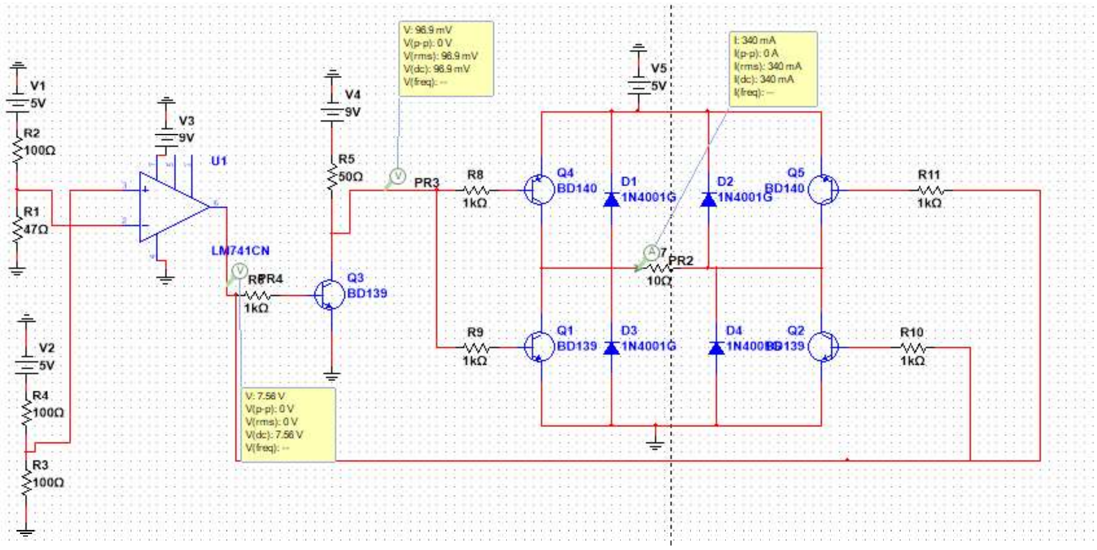

Figure 3.1 The case in which solar simulator system temperature higher than ambient temperature

$T_{solar\ simulator} > T_{ambient}$:

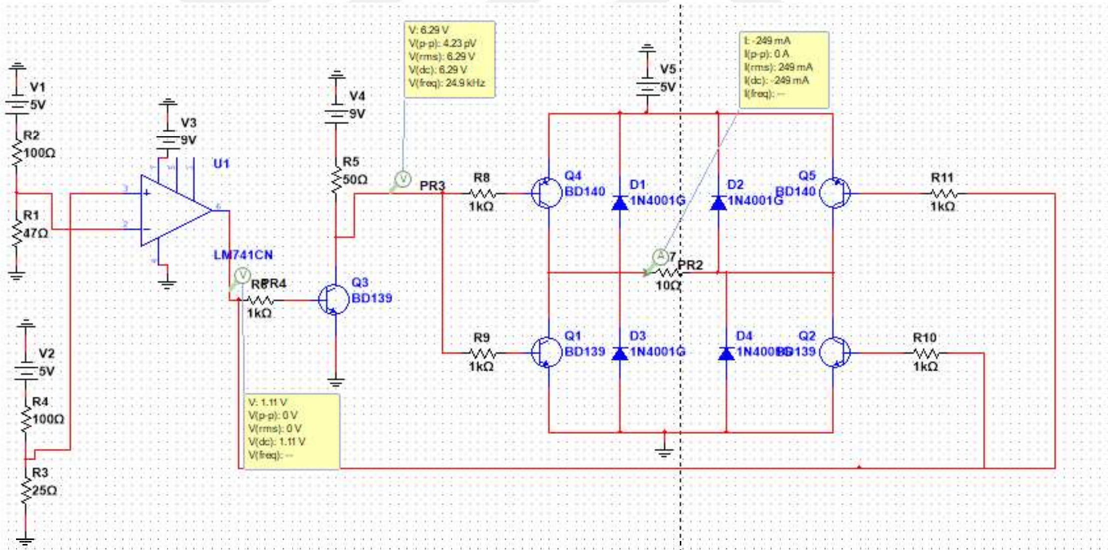

Figure 3.2 The case in which ambient temperature higher than solar simulator system temperature

Comparator: Analog system have better sensitivity compared digital. In this study, analog compator circuit, LM741 is selected. The most crucial parameter for this subsystem is comparison sensitivity of comparator. Although it is not stated in datasheet of LM741, it has 1mV differential input sensitivity. Transfer characteristic of LM741 as a comparison performance is given below. 20mV input signal range is enough to characterize the comparator. Analysis below shows that selected comparator has a rather better comparison performance for a narrow input range. Its characteristic is almost step-wise at 0mV.

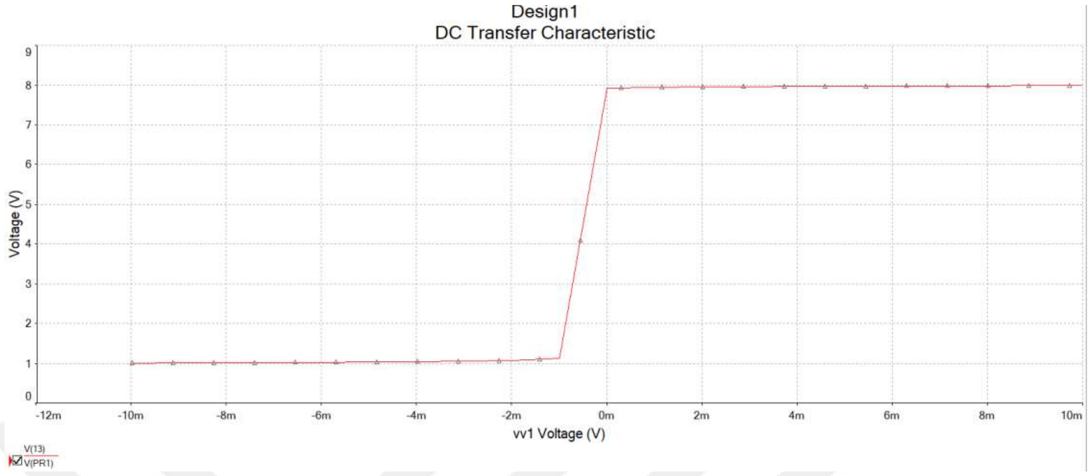

Figure 3.3 Comparator DC transfer characteristic.

Inverter: In this design, inverter topology is constructed by using discrete transistors. Avantage of it is easy to construct. Disadvantage of it, it is not as sharp as digital, special purpose logic inverters. In this topology, BJT transistor is used as a switch. The underlying philosophy behind this is not to loss collector-emitter voltage in Switch-ON case, in which transistor brings ground voltage when switch is on. To control the BJT whether it is operating in active region or saturation region, $\beta_{forced}<\beta$. To ensure it is in saturation mode, base current is increased. In this design, BJT is driven via 9mA maximum. Maximum beta value is given as 250 in datasheet of transistor. It is assumed 100 for simplicity. Puting 50 ohm resistor in collector of BJT, it gives forced beta value as 2. It is completely ensured that it is in deep saturation. How quiescent point is far away from edge of saturation, it gives less collector emitter voltage. This state is named as deep saturation. However, upper limit for collector voltage is input resistance of next stage. In next stage, base resistance of 1k ohm is connected. Voltage division is occured in case of transistor is OFF. To obtain a safe voltage division, 1/10 of resistance on lower side is chosen to dominate whole voltage. For 1k ohm base resistance, 100 ohm is upper limit for collector resistance. As a result of this design considerations, a successful logic inverter is designed. DC transfer characteristic of the designed logic inverter circuit is given as below. The designed inverter has output HIGH input range of 0-600mV. It has 0.6-2.4V transition input range, which stands for 1.8V. This transition range should be avoided in order to ensure logic inverter gives exact output HIGH or output LOW. Logic inverter has 2.4-9V input range for LOW output signal. Therefore, for a input range of 0-9.0V, persentage of input signal range which stands for meaningful output voltage is %80.

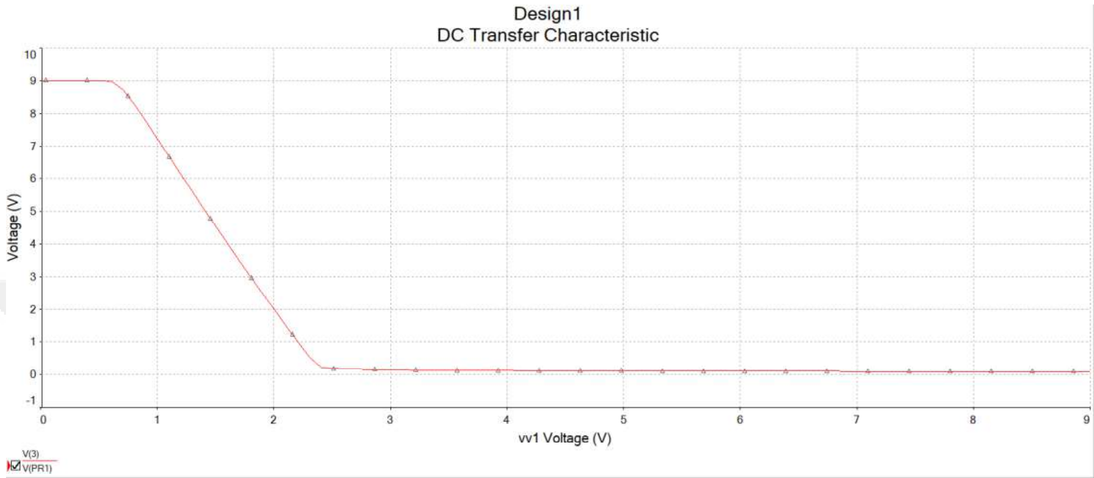

Figure 3.4 DC transfer characteristic of logic inverter circuit

H-Bridge Motor Driver: In this design, switch-mode h-bridge motor driver circuit is constructed by using discrete components. It is constructed by using discrete components to show operation principles and to customize design of the circuit. Just like logic inverter circuitry, transistors in h-bridge motor driver are operating in saturation region. The underlying reason behind this is that transistors are only to guide current, i.e. current steering. Therefore, voltage loss due to collector emitter voltage drop is not desired. Advantages of discrete design are easy to customize, easy to replace, easy to observe operation. Disadvantage of it is that working performance is not as sharp as other packaged solutions, e.g. L298. To operate transistors in saturation mode of operation, higher current is applied to the bases of transistors. As a design parameter, base resistors of transistors are selected as 1k ohm. Lower limit for base resistor is the collector resistor in previous stage. In case of voltage division, at least 10 times higher resistance should be selected to dominate whole voltage. Therefore, there is a design trade-off between lower resistance to sature transistors in h-bridge and higher resistance to dominate voltage division. Switching performance of h-bridge motor driver circuit is given as below. In h-bridge motor driver topology, there are two controlling input to driver transistors in h-bridge. By using common parameter, parameter sweep is performed in the analysis below. In the analysis, higher operating performance is obtained for 0-0.6V and 8.4-9.0V input ranges. In this input ranges, performance of h-bridge motor driver is almost stable and at maximum. For 0.6-2.6V and 6.4-8.4V input ranges, driven motor rotates in a certain direction. For input range of 2.6-6.4V, h-bridge motor driver is at full conduction. This is a pathological case. All transistors are ON and no current passes through motor. Also, power supply is in case of short circuit because two successive transistor switches are ON. This case is a design consideration for switch-mode designs. Even control signal is reversed, HIGH to LOW or vice versa, there is a possibility that transistor switch is already ON. Forcing other transistor switch to ON short circuits the power supply. In order to avoid such a catastrophic case, "dead time" is introduced into controlling signal to ensure transistor switch which was already ON is OFF. In the designed h-bridge motor driver, control signals must be exactly LOW or HIGH. For input ranges of 2.6-6.4V, the circuit damages power supply.

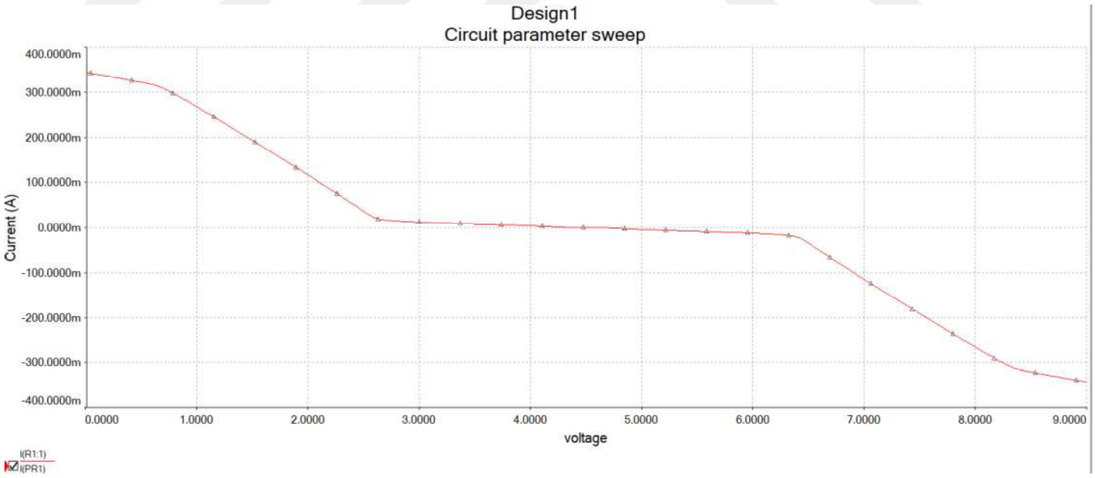

Figure 3.5 Switching characteristic of h-bridge motor driver

3.2 Measurements Taken in Laboratory Environment

Thanks to flexible operating property of designed solar simulator system, electrical performance of double-faced photovoltaic system can be observed in every time of day, every month of year, every season of year. Electrical performance measurements of double-faced photovoltaic system is performed in Yıldırım Beyazıt

University 15 Temmuz Şehitleri Campus laboratories. Also, temperature resistance characteristic of NTC sensors are rather crucial for dynamic control system. For further phases of this system, it is expected to introduce adaptive off-set temperature for ambient and solar system NTC sensors. In this topic, studies conducted in laboratory environment those show thermal effect on electrical performance of double faced photovoltaic system and temperature-resistance relation of 100Ω NTC sensor.

3.2.1 Solar Simulator System

Electrical performance is rather important for solar cells. They are used as power generators. Anything increasing electrical performance of solar cells are welcome for investors and researchers. Electrical performance is open to be affected by environmental factors. There are two major environmental factors affecting performance of solar cells: irradiance and temperature. Irradiance is not easy to change but concentrated solar cells are studied by researchers to increase irradiance of solar cells from one sun to hundreds of suns. However, even concentration introduces temperature rise in solar cells. Therefore, temperature is fundamental problem to be solved. Temperature rise affects electrical performance of solar cell in a destructive manner. It decreases fill factor, open circuit voltage but slightly increases short circuit current. Open circuit voltage is the most temperature dependent parameter among electrical performance parameters. If parameter variation per temperature rise is analyzed it is concluded that temperature affects open circuit voltage at most [88]. International Electrotechnical Comission, as a authority, releases a standard, IEC 60904-5, regarding panel temperature and open circuit voltage. In the standard, it is said that temperature measurement of solar cell does not give exact values by using distributed sensors. To give an average single value, equivalent cell temperature (ECT) of photovoltaic devices are introduced in the standard. Open circuit voltage can give equivalent cell temperature of photovoltaic devices. In this laboratory measurement, temperature vs. open circuit voltage relation is observed.

By using solar simulator system and activating heater, effect of temperature on open circuit voltage is seen. Temperature of the system is measured by using digital thermometer inside the solar system. Temperature is increased from 28°C to 50°C with steps of 2°C. Going beyond 50°C may result to permanent damage on solar cell. Then, it is safe not to go beyond it. During measurement process, it was only possible to record only one single photovoltaic device data. However, it can deduced from solar simulator system design, data of other photovoltaic panel would be rather close to recorded data. Measured data and light source parameters are tabulated as below.

Table 3.1. Solar simulator open circuit voltage measurements

Light Source Measurements:3860 lux, 50W/m^2	
$T_{solar\ simulator}$(°C)	**V_{oc}(V)**
28	7.22
30	7.20
32	7.19
34	7.15
36	7.11
38	7.09
40	6.88
42	6.84
44	6.80
46	6.75
48	6.68
50	6.60

To see visually trend of this measurement, these twelve data points are drawn as a graph in Excel. Also, in the same environment, linear regression analysis is performed and a linear behaviour is obtained effect of temperature on open circuit voltage. R-squared value is calculated in Matlab. In physical science, linear regression with R-squared having a value greater than 0.9 is known as strong relation. In this analysis, R-squared value of the linear regression is 0.9749. This values could be more higher because solar simulator system designed is rather difficult to control. During mesurement, heater is manually pulled or penetrated by observing system temperature. In future versions of this system, it is possible to set a system temperature and observe more stable and more reliable open circuit voltage values thanks to advanced thermostatic control. Line fit for the collected dataset in Excel, resultant linear relation between temperature and open circuit voltage and R-squared value are given as below.

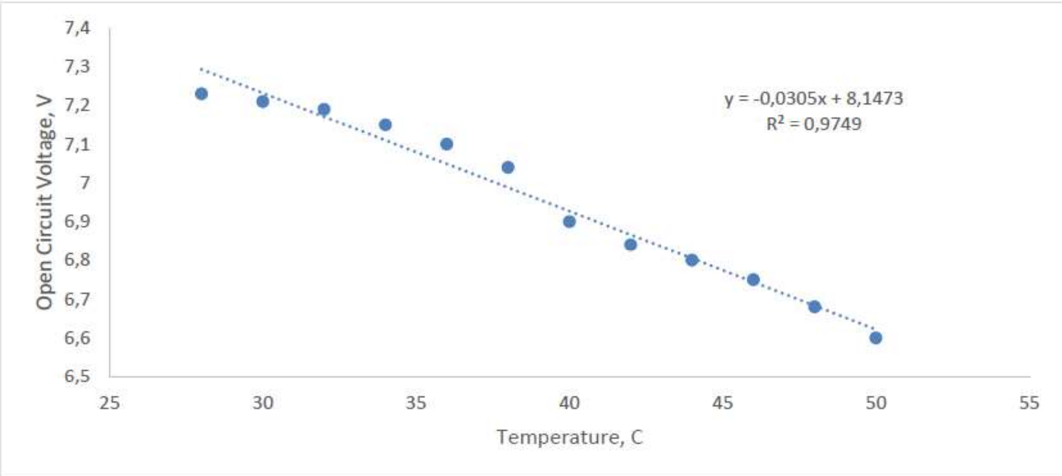

Figure 3.6 Line fit for experimental dataset

3.2.2 100Ω NTC Sensor

NTC sensor is utilized to convert temperature input to voltage output. It sits at the input stage of the dynamic control system. In dynamic control system, two NTC sensors are compared in a binary manner. Exact resistance or temperature is not needed to be known. However, in future phases of the system, a dynamic offset temperature is considered to be introduced. Although temperature vs resistance characteristic of NTC sensors are not necessary, it is required for next versions of the system. Research on this device will be a fundamental for future studies. NTC has a identical temperature vs resistance characteristic. Temperature vs. resistance curve depends on a β parameter which is between 3000-5000 for 25°C and 100°C given in datasheets of thermistors. In this study, β value for concern temperature range 25-50°C is found and characteristic curve is extracted. Collected dataset is compared with Steinhart-Hart equation.

Tap water is filled into the mug. NTC sensor is immersed into tap water in mug for equal temperature. Starting temperature of tap water is 22.7°C. Just after fill-empty process, temperature of tap water is gradually increased. The time to heat from 22.7°C to 92°C lasts 30 minutes including measuring the temperature of the tap water and resistance of NTC sensor.

Collected data to characterize NTC sensor is tabulated as below.

Table 3.2. NTC sensor characterization dataset

Temperature(°C)	**Resistance(Ω)**
22.7	136
26.1	117.6
29.6	108.3
34.8	92.6
36.5	87.4
38.3	83.1
40.7	76.0
44.2	68.9
49.4	60.0
52.2	55.2
57.5	48.8
62.4	42.4
68.4	36.4
73.1	32.7
75.3	30.8
80.3	27.7
83.5	25.8
87.0	23.7
88.0	23.1
88.6	22.9
89.8	22.2
91.5	21.2
92.0	21.0

Collected data is forced to fit in the resistance equation given below.

$$R = R_0 e^{\beta\left(\frac{1}{T}-\frac{1}{T_0}\right)}$$

Here, reference values are used as rated values. In NTC sensors, rated resistance is for room temperature (25°C). In Matlab's Curve Fitting Toolbox, collected dataset is forced to fit into the expression given above. Fitted line and collected dataset is graphed as below

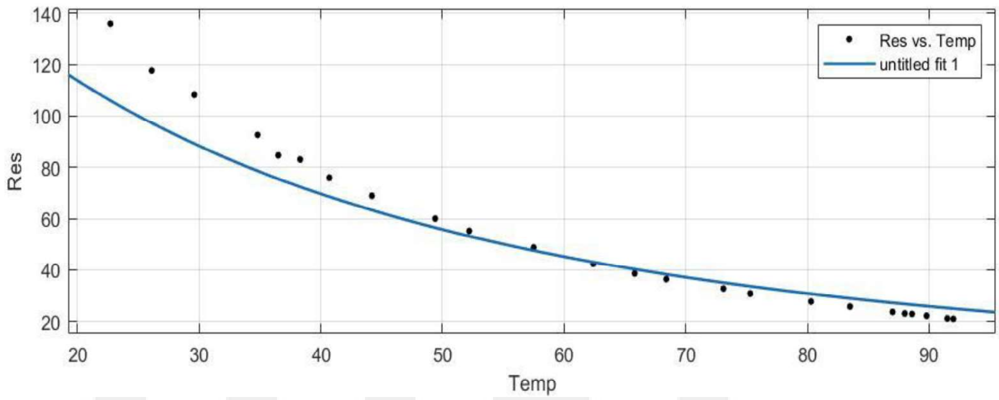

Figure 3.7 NTC characterization fitting process

Fitting performance details:

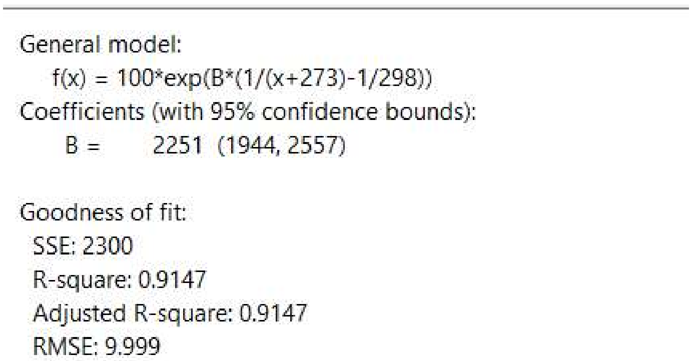
General model:
f(x) = 100*exp(B*(1/(x+273)-1/298))
Coefficients (with 95% confidence bounds):
B = 2251 (1944, 2557)

Goodness of fit:
SSE: 2300
R-square: 0.9147
Adjusted R-square: 0.9147
RMSE: 9.999

Figure 3.8. NTC characterization fitting performance details

CHAPTER 4

DISCUSSION AND CONCLUSION

Energy is the most important building block of human life. Reproduction, movement, growth all of the functional abilities directly depend on energy. As civilization progresses, global energy demand increases, too. Transportation, communication, computation all technologies require high amount of energy. Today's energy production comes from fossil-based fuels. Such fuels result to environmental issues. Global warming, climate changes are ones of them. Researchers study to find more environment-friendly fuels. Renewable energy sources are best candidate to satisfy higher energy demand and protect environment.

There are many renewable energy sources in nature. Alternative energy sources are another saying for it. Solar, wind, tidal, hydropower, biomass are one of these sources. The most available and highest efficiency energy resource is solar energy resources. Every country can reach solar energy regardless of it's geography. Also, the highest power can be obtained by solar energy resources. They can utilized for both water heating and electricity generation. With the invention of photovoltaic power modules, popularity of solar electricity generation increases year by year. Thanks to its portable and easy to install properties, attention on photovoltaics increases year by year.

Researchers and investors search for methods to increase electrical performance of photovoltaics. Thanks to double-faced photovoltaic systems, energy output from the system is doubled. On the other hand, environmental factors decrease electrical performance of solar modules. Temperature is the most fundamental factor affecting electrical performance of photovoltaics. Due to semiconductive structure of photovoltaics, performance parameters of photovoltaics are affected in a bad way. Solar cooling methods are proposed by researchers to enhance electrical performance of photovoltaics. Although there are many active and passive methods to cool down photovoltaic panel operating temperature, fan cooling is best candidate method to improve performance of solar modules due to it's easy to establish, easy to maintain and low-cost establishment properties. In this thesis, effect of temperature rise on electrical performance of double faced solar power modules are observed. As a solution, electrodynamic fan cooling system is proposed. It’s prototype model is designed and established.

In the first part of the thesis, introductory informations and comprehensive literature search are given. Definition of photovoltaics, timeline of photovoltaic developments, working principle of solar modules, structural definitions of solar modules, types of photovoltaics, alternative solar cell cooling methods, figure of merits of photovoltaics, equivalent circuit models for photovoltaics and temperature effect on photovoltaic performance are given.
In the second part of the thesis, experimental procedure is given. Basically, detail information about experiments are given in this part. In experimental procedure part, study subsystems, solar simulator system, electrodynamic control system and double faced photovoltaic system are introduced. Experimental materials used in these study subsystems are introduced and background information regarding working principles of subsystem materials are given. Intsruments to characterize these subsystems and obtain experimental measurements form these subsystems are introduced. Working principle of study subsystems are explained in this part of the thesis.

In the third part of the thesis, experimental results are given. In this part, experimental results regarding electrodynamic control system, solar simulator system and double faced photovoltaic system are given. Design considerations and simulation results of electrodynamic control system is given. Performance analysis results of building blocks of electrodynamic control system is given. Laboratory measurements of solar simulator system is given. Temperature effect on electrical performance of photovoltaic is given. In addition to solar simulator system, NTC sensor is also experimented in this part. Characterization of NTC sensor is performed and results are given in this part.

In the fourth part, conclusive informations and dissussions on experimental results are given. Summary of whole thesis is given.

When simulation results of dynamic control system are examined, it can be said that although some building blocks of the system show considerably higher performance, some other blocks show moderate performance. Overall performance of system directly depends on the block having lower performance. However, comparator circuit gives rather high performance output signal, lower performance is not a concern for this design. In future versions of this system, higher performance components can be replaced with ones in the design. For solar simulator experimental results, it can be seen that temperature rise directly affects electrical performance of photovoltaic system. As an electrical performance, only output voltage is selected to monitor. It is rather correct selection because IEC 60904-5 standard says best way to monitor temperature effect is to observe open circuit voltage. Also, temperature vs open circuit voltage characteristic is as expected from literature. Rate of change of output voltage per temperature rise is rather close to values in literature. Performance degradation due to temperature rise makes necessary that some external output stage circuit is required to stabilize output voltage. If this photovoltaic drives a load or if it is connected to utility, it may lead to dangerous results. To prevent such problems, voltage stabilizer systems can be connected to prevent output voltage fluctuations due to temperature rise. NTC sensor characterization is important for future phases of the study. Although, in this thesis, temperature control is performed in a binary manner, in next versions of the study, it is expected to introduce adaptive offset temperature in dynamic control system. Thanks to this property, there will be some tolerance temperature in order to save energy. However, on higher temperature those are risky to panel, tolerance will be skept and system will operate if system temperature is higher. Collected dataset to characterize NTC sensors are as expected. Resistance of the sensor reduces exponentially as temperature increases. Also, based on reference values, dataset is forced to fit thermistor resistance expression and rather successful fitting process is performed on Matlab enviroment. In curve fitting process, room temperature values are used as reference values. Difference between room temperature datasheet value and experimental measurement value reduces performance of curve fitting. However, R-square value of 0.9147 is rather powerful correlation. Beta value of 2251 is close to theoretical value of beta.

To sum up, designed double faced photovoltaic system with electrodynamic cooling system works properly. It can be used to observe temperature effect on electrical performance of photovoltaic system. Also, it can be used to observe effect of fan cooling on electrical performance of photovoltaic system. Although this system is designed for prototype model, vast advantage of this system can be seen on big solar farms. This study can be beneficial for researchers and investors.

REFERENCES

[1] The Editors of Encyclopaedia Britannica, Photovoltaic effect. Retrieved March 17, 2021, from https://www.britannica.com/science/photovoltaic-effect. 2008.

[2] Davidson, M. W. Pioneers in Optics: Alexandre Edmond Becquerel and William Henry Bragg. Microscopy Today, 19, 20, 42-44. 2011

[3] Xu, J., Zhang, J., Kuang, K. Manufacturing Solar Cells: Assembly and Packaging. Conveyor Belt Furnace Thermal Processing. (1st Edition) pp. (35-41). Springer International Publishing. 2017

[4] Xu, J., Zhang, J., Kuang, K. Manufacturing Solar Cells: Assembly and Packaging. Conveyor Belt Furnace Thermal Processing. (1st Edition) pp. (35-41). Springer International Publishing. 2017

[5] Baker, L. A new age of energy dawns at ASU. Retrieved March 18, 2021, from https://news.asu.edu/20200917-arizona-impact-new-age-energy-dawns-asu. 2020

[6] Wolfe, P. R. What is Photovoltaics?. The Solar Generation: Childhood and Adolescence of Terrestrial Photovoltaics. (1st Edition) pp. (9-24). IEEE. 2018

[7] Ali Md. F., Hossain Md. F. Influence of Front and Back Contacts on Photovoltaic Performances of p-n Homojunction Si Solar Cell: Considering an Electron-Blocking Layer. International Journal of Photoenergy, 2017, pp. 1-6, 2017

[8] Periodic Trends – Metals, Semiconductors and Insulators. Retrieved August 28, 2021, from https://chem.libretexts.org/@go/page/183355. 2021

[9] Light- Absorption, Reflection and Transmission, Retrieved March 30, 2021, from https://www.physicsclassroom.com/class/light/Lesson-2/Light-Absorption,-Reflection,-and-Transmission. n. d.

[10] Riordan M., Hoddeson L. The origins of pn junction. IEEE Spectrum, (34), 6, 46-51, 1997

[11] Belyakov, N. Solar Energy Sustainable power generation: Current status, future challenges, and perspectives. (1st Edition) pp.(417-437). Academic Press. 2019

[12] Green, M. A., Hishikawa, Y., Dunlop, E. D., Levi, D. H., Hohl-Ebinger, J., and A. W. Y., & Ho-Baillie, A. W. Y. Solar cell efficiency tables (version 51). Progress in Photovoltaics: Research and Applications, (26) 1, 3-12.2017

[13] Panasonic HIT® Solar Cell Achieves World's Highest Energy Conversion Efficiency of 25.6% at Research Level. Retrieved June 17, 2021, from

https://news.panasonic.com/global/press/data/2014/04/en140410-4/en140410-4.html. 2014

[14] Parida, B., Iniyan, S., & Goic R. A review of solar photovoltaic technologies. Renewable and Sustainable Energy Reviews, (18), 3, 1625-1636. 2011

[15] Torres-Martínez, L. M.,Kharissova, O. V., Kharisov, B. I., (Ed.). Handbook of Ecomaterials (1st Edition), (1034-1050), Springer. 2019

[16] Repins et al., 19·9%-efficient ZnO/CdS/CuInGaSe2 solar cell with 81·2% fill factor. Progress in Photovoltaics: Research and Applications, (16), 3, 235-239. 2008

[17] O-Regan, B., & Gratzel, M. A low-cost, high-efficiency solar cell based on dye-sensitized colloidal TiO2 films. Nature, (353), 6346, 737-740. 1991

[18] Tang, C. W. Two-layer organic photovoltaic cell. Applied Physics Letters, (48), 2, 183-185. 1986

[19] Gong, J., Sumathy, K., Qiao, Q., & Zhou, Z. Review on dye-sensitized solar cells (DSSCs): Advanced techniques and research trends. Renewable and Sustainable Energy Reviews, (68), 234-246, 2017

[20] Conibeer, G. Third-generation photovoltaics. Materials Today, (10), 11, 42-50. 2007

[21] Luceño-Sánchez, J., Díez-Pascual, A., & Peña Capilla, R. Materials for Photovoltaics: State of Art and Recent Developments. International Journal of Molecular Sciences, (20), 4, 976. 2019

[22] Kivambe, M., Aissa, B., & Tabet, N. Emerging Technologies in Crystal Growth of Photovoltaic Silicon: Progress and Challenges. Energy Procedia. (130), 7-13. 2017

[23] Green, M. A., et al. Solar cell efficiency tables (version 50). Progress in Photovoltaics: Research and Applications, (25), 7, 668-676. 2017.

[24] Mark Osborne, Stion claims CIGS cell conversion ef?ciency of 23.2%. Retrieved June 21, 2021, from https://www.pv-tech.org/stion_claims_prototype_cigs_mini_module_conversion_efficiency_of_23-2/. 2014

[25] Lorelle Mansfield, Copper Indium Gallium Diselenide Solar Cells. Retrieved June 21, 2021, from https://www.nrel.gov/pv/copper-indium-gallium-diselenide-solar-cells.html. n. d.

[26] PROFESSOR GRÄTZEL WINS THE 2010 MILLENNIUM TECHNOLOGY GRAND PRIZE FOR DYE-SENSITIZED SOLAR CELLS. Retrieved June 23,

2021,fromhttp://web.archive.org/web/20100613065310/http://www.millennium mprize.fi/news/165/111/PROFESSOR-GRaeTZEL-WINS-THE-2010-MILLENNIUM-TECHNOLOGY-GRAND-PRIZE-FOR-DYE-SENSITIZED-SOLAR-CELLS/d,news_en/. n. d.

[27] Calogero, G., et al. Efficient Dye-Sensitized Solar Cells Using Red Turnip and Purple Wild Sicilian Prickly Pear Fruits. International Journal of Molecular Sciences, (11), 1, 254-267. 2010

[28] Snaith, H. J. Estimating the Maximum Attainable Efficiency in Dye-Sensitized Solar Cells. Advanced Functional Materials, (20), 1, 13-19. 2010

[29] Tvrdy, K., & Kamat, P. V. Quantum Dot Solar Cells. Comprehensive Nanoscience and Technology, 257-275. 2011

[30] Díez-Pascual, A., Luceño Sánchez, J., Peña Capilla, R., & García Díaz, P. Recent Developments in Graphene/Polymer Nanocomposites for Application in Polymer Solar Cells. Polymers, (10), 2, 217. 2018

[31] Giorgi, G., Fujisawa J. I., Segawa, H., & Yamashita, K. Small Photocarrier Effective Masses Featuring Ambipolar Transport in Methylammonium Lead Iodide Perovskite: A Density Functional Analysis. The Journal of Physical Chemistry Letters. (4), 24, 4213-4216. 2013

[32] Ansari, M. I. H., Qurashi, A., & Nazeeruddin, M. K. Frontiers, opportunities, and challenges in perovskite solar cells: A critical review. Journal of Photochemistry and Photobiology C: Photochemistry Reviews, (35), 1-24. 2018

[33] Dimroth, F., & Kurtz, S. High-Efficiency Multijunction Solar Cells. MRS Bulletin. (32), 3, 230-235. 2007

[34] Philipps S. P., & Bett, A. W. III-V Multi-junction solar cells and concentrating photovoltaic (CPV) systems. Advanced Optical Technologies, (3), 5-6, 469-478. 2014.

[35] Balandin, A. A., et al. Superior Thermal Conductivity of Single-Layer Graphene. Nano Letters, (8), 3, 902-907. 2008

[36] Chen H., Müller, M. B., Gilmore, K. J., Wallace G. G., & Li, D. Mechanically Strong, Electrically Conductive, and Biocompatible Graphene Paper. Advanced Materials, (20), 18, 3557-3561. 2008

[37] Weiss, N. O., et al. Graphene: An Emerging Electronic Material. Advanced Materials. (24), 43, 5782-5825. 2012

[38] Liu, S., et al. Antibacterial Activity of Graphite, Graphite Oxide, Graphene Oxide, and Reduced Graphene Oxide: Membrane and Oxidative Stress. ACS Nano, (5), 9, 6971-6980. 2011

[39] Jiao, K., Wang, X., Wang, Y., & Chen, Y. Graphene oxide as an effective interfacial layer for enhanced graphene/silicon solar cell performance. J. Mater. Chem. C, (2), 37, 7715-7721. 2014

[40] Krauter, S., et al. Combined photovoltaic and solar thermal systems for facade integration and building insulation. Solar Energy, (67), 4-6, 239-248. 1999

[41] Krauter, S. Increased electrical yield via water flow over the front of photovoltaic panels. Solar Energy Materials and Solar Cells. (82), 1-2, 131-137. 2004

[42] Javidan, M., & Moghadam, A. J. Experimental investigation on thermal management of a photovoltaic module using water-jet impingement cooling. Energy Conversion and Management, (228), 113686. 2021

[43] Irwan, Y. M., et al. Comparison of solar panel cooling system by using dc brushless fan and dc water. Journal of Physics: Conference Series, (622), 012001. 2015

[44] Najafi, H., & Woodbury, K. A. Optimization of a cooling system based on Peltier effect for photovoltaic cells. Solar Energy, (91), 152-160. 2013

[45] Van Sark, W. G. J. H. M. Feasibility of photovoltaic – Thermoelectric hybrid modules. Applied Energy, (88), 8, 2785-2790. 2011

[46] Kumar, R., Deshmukh, V., & Bharj, R. S. Performance enhancement of photovoltaic modules by nanofluid cooling: A comprehensive review. International Journal of Energy Research. (44), 8, 6149-6169. 2020

[47] Gilmore, N., Timchenko, V., & Menictas, C. Microchannel cooling of concentrator photovoltaics: A review. Renewable and Sustainable Energy Reviews, (90), 1041-1059. 2018

[48] Arifin, Z., Suyitno, S., Tjahjana, D. D. D. P., Juwana, W. E., Putra, M. R. A., & Prabowo, A. R. The Effect of Heat Sink Properties on Solar Cell Cooling Systems. Applied Sciences, (10), 21, 7919. 2020

[49] Fatoni, E. K. A., Taqwa, A. & Kusumanto, R. Solar Panel Performance Improvement using Heatsink Fan as the Cooling Effect. Journal of Physics: Conference Series. (1167), 012031. 2019

[50] Rosa-Clot, M., Rosa-Clot, P., Tina, G. M., & P. F. Scandura. Submerged photovoltaic solar panel: SP2. Renewable Energy, (35), 8, 1862-1865. 2010

[51] Nikhil, P. G., & Premalatha M. Performance enhancement of solar module by cooling: An experimental investigation. International Journal of Energy and Environment, (3), 1, 73-82. 2012

[52] Islam, M. M., Pandey, A. K., Hasanuzzaman, M., & Rahim, N. A. Recent progresses and achievements in photovoltaic-phase change material technology: A review with special treatment on photovoltaic thermal-phase change material systems. Energy Conversion and Management, (126), 177-204. 2016

[53] Skoplaki, E., & Palyvos, J. A. On the temperature dependence of photovoltaic module electrical performance: A review of efficiency/power correlations. Solar Energy, (83), 5, 614-624. 2009

[54] Heinz, A., & Streicher, W. Application of phase change materials and PCM slurries for thermal energ storage. Proceedings of the Ecostock 2006, 2006

[55] Shafieian, A., Khiadani, M., & Nosrati, A. A review of latest developments, progress, and applications of heat pipe solar collectors. Renewable and Sustainable Energy Reviews. (95). 273-304. 2018

[56] Naphon, P., Assadamongkol, P., & Borirak, T. Experimental investigation of titanium nanofluids on the heat pipe thermal efficiency. International Communications in Heat and Mass Transfer. (35), 10, 1316-1319. 2008

[57] Zhu, L., Raman, A., Wang, K. X., Anoma, M. A., & Fan, S. Radiative cooling of solar cells. Optica, (1), 1, 32. 2014

[58] Wang Z. et al. Lightweight, Passive Radiative Cooling to Enhance Concentrating Photovoltaics. Joule, (4), 12, 2702-2717. 2020

[59] Afrouzi, H. N., Mashak, S. V., Abdul-Malek, Z., Mehranzamir, K., & Salimi, B. Solar Array and Battery Sizing for a Photovoltaic Building in Malaysia. Jurnal Teknologi, (64), 4. 2013

[60] Messenger, R. A., & Abtahi, A. Photovoltaic Systems Engineering, (2nd Edition), CRC Press.2003

[61] POLYCRYSTALLINE VS MONOCRYSTALLINE SOLAR PANELS, Retrieved 7 September, 2021, from http://www.solarquotes.com.au/panels/photovoltaic/monocrystalline-vs-polycrystalline/, n. d

[62] De Vos, A., & Pauwels, H. On the Thermodynamic Limit of Photovoltaic Energy Conversion. Applied Physics, (25), 2, 119-125. 1981

[63] Vos, A. D. Detailed balance limit of the efficiency of tandem solar cells. Journal of Physics D: Applied Physics, (13), 5. 839-846.1980

[64] Green, M., Dunlop, E., Hohl-Ebinger, J., Yoshita, M., Kopidakis, N., & Hao, X. Solar cell efficiency tables (version 57). Progress in Photovoltaics: Research and Applications, (29), 1, 3-15. 2020

[65] Evans, D. L. Simplified method for predicting photovoltaic array output. Solar Energy, (27), 6, 555-560. 1981

[66] Evans, D. L., & Florschuetz, L. W. Terrestrial concentrating photovoltaic power system studies. Solar Energy, (20), 1, 37-43. 1978

[67] Open-Circuit Voltage, Retrieved September 7, 2021, from https://www.pveducation.org/pvcdrom/solar-cell-operation/open-circuit-voltage. n. d.

[68] Short-Circuit Current, Retrieved September 7, 2021, from https://www.pveducation.org/pvcdrom/solar-cell-operation/short-circuit-current. n. d.

[69] Çobankaya, Mustafa Latif. Design and Development of a Novel Photovoltaic System with Reflectors and a Sun Tracker. Unpublished Masters dissertation, Ankara Yıldırım Beyazı University, 2017.

[70] Saha, U. What factors in solar cell can affect the fill factor? Retrieved September 8, 2021, from https://www.researchgate.net/post/What_factors_in_solar_cell_can_affect_the_fill_factor. 2018

[71] Green, M. A. Accuracy of analytical expressions for solar cell fill factors. Solar Cells, (7), 3, 337-340. 1982

[72] Sechilariu, M., Locment, F. Urban DC Microgrid: Intelligent Control and Power Flow Optimization, (1st Edition), Butterworth-Heinemann. 2016

[73] Salas, V., Olias, E., Barrado, A., & Lazaro, A. Review of the maximum power point tracking algorithms for stand-alone photovoltaic systems. Solar Energy Materials and Solar Cells, (90), 11, 1555-1578. 2006

[74] Skaaland, A., Ricke, M., Wallevik, K., Strandberg, R., & Imenes, A. G. Potential and Challenges for Building Integrated Photovoltaics in the Agder Region. Agderforskning Technical Report. 1-120. 2011

[75] Elbaset, A. A., Ali, H., & Abd-El Sattar, M. Novel seven-parameter model for photovoltaic modules. Solar Energy Materials and Solar Cells. (130), 442-455. 2014

[76] Khezzar, R., Zereg, M., & Khezzar, A. Modeling improvement of the four parameter model for photovoltaic modules. Solar Energy, (110), 452-462.2014

[77] Boyd, M. T., Klein, S. A., Reindl, D. T., & Dougherty B. P. Evaluation and Validation of Equivalent Circuit Photovoltaic Solar Cell Performance Models. Journal of Solar Energy Engineering, (133), 2. 2011

[78] Ishaque, K., Salam, Z., & H. Taheri, H. Simple, fast and accurate two-diode model for photovoltaic modules. Solar Energy Materials and Solar Cells, (95), 2, 586-594. 2011

[79] Varshni, Y. P. Temperature dependence of the energy gap in semiconductors. Physica, (34), 1, 149-154.1967

[80] Villalva, M. G., Gazoli, J. R., & Filho, E. R. Comprehensive Approach to Modeling and Simulation of Photovoltaic Arrays. IEEE Transactions on Power Electronics, (24), 5, 1198-1208. 2009

[81] Hali, A., & Khlifi, Y. Photovoltaic panel parameters determination using two numerical methods. Materials Today: Proceedings, (45), 7377-7382. 2021

[82] Ibrahim, H., & Anani, N. Evaluation of Analytical Methods for Parameter Extraction of PV modules. Energy Procedia, (134), 69-78. 2017

[83] Lu, H., Zhang, Y., & Hao, P. An analytical method for parameter identification based on datasheet values. Journal of Physics: Conference Series, (2005), 1, 012006. 2021

[84] Petrone, G., Ramos-Paja, C. A., Spagnuolo G. Photovoltaic Sources Modeling, (1st Edition). Wiley-IEEE Press. 2017

[85] Perraki V., & Kounavis, P. Effect of temperature and radiation on the parameters of photovoltaic modules. Journal of Renewable and Sustainable Energy, (8), 1, 013102. 2016

[86] El Achouby, H., Zaimi, M., Ibral, A., & Assaid, E. M. New analytical approach for modelling effects of temperature and irradiance on physical parameters of photovoltaic solar module. Energy Conversion and Management, (177), 258-271. 2018

[87] Singh, P., & Ravindra, N. M. Temperature dependence of solar cell performance—an analysis. Solar Energy Materials and Solar Cells, (101), 36-45. 2012

[88] Chander, S., Purohit, A., Sharma, A., Arvind, Nehra, S. P., & Dhaka, M. S. A study on photovoltaic parameters of mono-crystalline silicon solar cell with cell temperature. Energy Reports, (1), 104-109. 2015

[89] Perraki V., & Kounavis, P. Effect of temperature and radiation on the parameters of photovoltaic modules. Journal of Renewable and Sustainable Energy, (8), 1, 013102. 2016

[90] Güneş Paneli 20cmx13cm 12 Volt 500 mAh + ve - Uç Kablolu Solar. (n.d.). Retrieved from https://urun.n11.com/arduino-urunleri-ve-setleri/gunes-paneli-20cmx13cm-12-volt-500-mah-ve-uc-kablolu-solar-P437382436

[91] TYPE K THERMOCOUPLE (Chromel / Alumel)200°C to +1260°C / -328°F to +2300°F. (n.d.). Retrieved from https://www.thermometricscorp.com/thertypk.html

[92] Tt Technic Tm 902 C Termometre. (n.d.). Retrieved from https://www.hepsiburada.com/tt-technic-tm-902-c-termometre-pm-HB00000JL5H0

[93] UT136B Digital Multimeter (Discontinued). (n.d.). Retrieved from https://www.uni-trend.com/meters/html/product/General_Meters/DigitalMultimeters/UT136/UT136B.html

[94] Lightning Levels. (n.d.). Retrieved from http://www.illumenate.com/Light-levels.htm

[95] Nayak, A., Parui, K., Sharma, S., & Ratha, S. Study and Analysis of Atomic Spectra. International Journal of Scientific and Research Publications (IJSRP), (10), 1, 946-955. 2020

[96] Operation Manual Digital Lux Meter. (n.d.). Retrieved from http://doc.diytrade.com/docdvr/1306637/21405093/1305869871.pdf

[97] LX1010B Handheld Digital LUX Meter Light Meter Photo Detector. (n.d.). Retrieved from https://www.amazon.com/LX1010B-Handheld-Digital-Meter-Detector/dp/B01FAGD96K

[98] Reference Air Mass 1.5 Spectra. (n.d.). Retrieved from https://www.nrel.gov /grid/solar-resource/spectra-am1.5.html

[99] 2000 ASTM Standard Extraterrestrial Spectrum Reference E-490-00. (n.d.). Retrieved from https://www.nrel.gov/grid/solar-resource/spectra-astm-e490.html

[100]Defining standard spectra for solar panels. (n.d.). Retrieved from http://www.greenrhinoenergy.com/solar/radiation/spectra.php

[101]Standard Solar Spectra. (n.d.). Retrieved from https://www.pveducation.org/pvcdrom/appendices/standard-solar-spectra

[102] Jeong, J. PHOTOVOLTAICS: Measuring the 'Sun'. Retrieved December 2, 2021, from https://www.laserfocusworld.com/lasers-sources/article/16566681/ photovoltaics-measuring-the-sun. 2009

[103] Michael, P.A CONVERSION GUIDE: SOLAR IRRADIANCE AND LUX ILLUMINANCE. Retrieved November 25, 2021, from https://ieee-dataport.org/open-access/conversion-guide-solar-irradiance-and-lux-illuminance. 2019

[104]Solar Power Meter Model SP505. (n.d.). Retrieved from http://www.extech.com/products/resources/SP505_UM-en.pdf

[105] DC Power Supply MT-303A MT-305B Kullanım Klavuzu. (n.d.). Retrieved from https://mervesanteknoloji.com/statics/file/MT-305B__YY2.jpg

[106] 1833: FIRST SEMICONDUCTOR EFFECT IS RECORDED. (n.d.). Retrieved from https://www.computerhistory.org/siliconengine/first-semiconductor-effect-is-recorded/

[107] Jones, D. Biomedical Sensors (Sensors Technology), (1st Edition). Momentum Press. 2010

[108] Lee, Y., Pan, J., Hathaway, R., Barkey, M. Fatigue Testing and Analysis: Theory and Practice, (1st Edition). Butterworth-Heinemann. 2011

[109] Morris A. S., Langari R. Measurement and Instrumentation: Theory and Application, (3rd Edition). Academic Press. 2020

[110] What is a Thermistor?. (n.d.). Retrieved from https://www.ei-sensor.com/what-is-a-thermistor/

[111] Carter, C., Mancini, R. Op Amps for Everyone, (5th Edition). Newnes. 2017